CIRFA Cruise 2022

22 April - 9 May 2022, *RV Kronprins Haakon*
IMR cruise ID 2022704

Cruise report

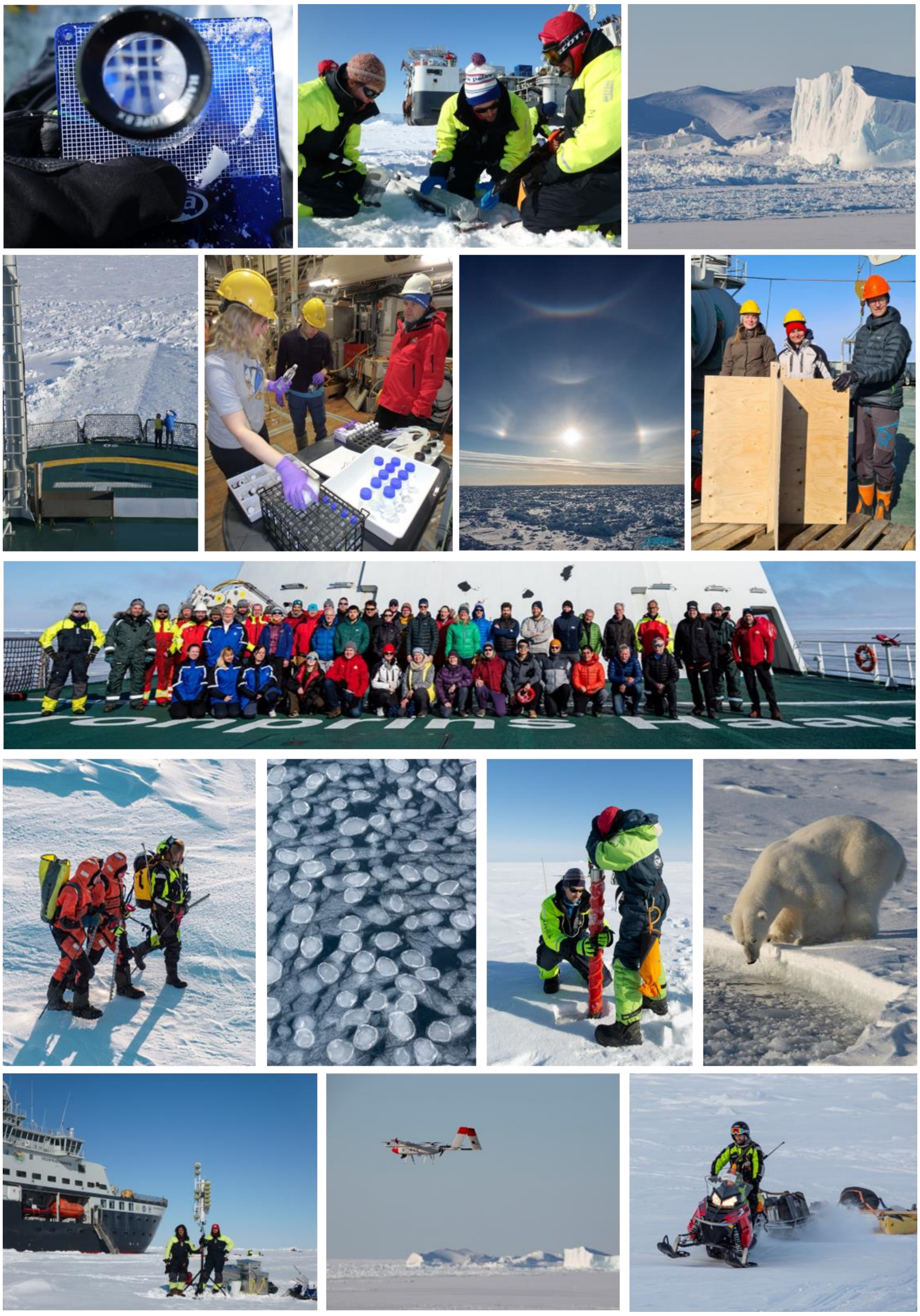

UiT The Arctic University of Norway

CIRFA
CENTRE FOR INTEGRATED REMOTE SENSING AND FORECASTING FOR ARCTIC OPERATIONS

Forskningsrådet
The Research Council of Norway

Acknowledgements

The CIRFA-cruise 2022 was funded by UiT the Arctic University of Norway, the European Space Agency (RFP Response No 3-17845), the Research Council of Norway (RCN project number 237906), and the CIRFA partners.

Additional funding and in-kind support came through the projects SIDRiFT (Research Council of Norway grant number 287871), and The Fram Strait Arctic Outflow Observatory project of the Norwegian Polar Institute.

Editors of this report

Wolfgang Dierking
Andrea Schneider
Torbjørn Eltoft
Sebastian Gerland

Contents

Introduction

Torbjørn Eltoft (UiT) and Sebastian Gerland (NPI)

The SFI *Centre for Integrated Remote Sensing for Arctic Operations* (CIRFA) has been active since September 1st, 2015. It was established to develop methods and technologies enabling improved remote sensing and monitoring capabilities for Arctic operations.

The CIRFA-Cruise 2022 with *RV Kronprins Haakon* to the north-eastern coast of Greenland in the period April 22nd to May 9th 2022 was organised to perform measurements and make observations which allow for validation of information and forecast products resulting from CIRFA´s work. Remote sensing monitoring of sea ice and icebergs are associated with many challenges, and a significant focus of the work in CIRFA has been devoted to analysis and interpretation of synthetic aperture radar (SAR) data for sea ice classification and iceberg detection. Through the years, CIRFA has developed several sea ice classification algorithms and investigated iceberg detection, both for icebergs floating in open water and when they are surrounded by sea ice. Additionally, CIRFA has contributed to advances in numerical modelling through the development of the Barents-2.5 ocean circulation and sea ice model for use in operational ocean forecasting.

The CIRFA-cruise 2022 with a scientific team of 33 from 17 nations and a crew of 19 persons reached the fast ice and embedded icebergs at Belgica Bank near the east coast of Greenland, as well as drifting sea ice with a variety of physical properties to work on.
In accordance with the predefined timetable and plans, most of the planned activities were realised. Data was collected at a number of longer ice stations, where snow and ice properties were thoroughly studied. The measurements were complimented by local drone surveys and ice mass balance buoy deployments, and at shorter ice stations with a smaller set of in-situ measurements. On the westward and eastward transits, the ship made stops to do oceanographic (CTD) stations as well as for sea ice and ocean drifter deployments.

Figure I1. displays a map of the ship track for the whole cruise, with symbols marking the locations of the various stations where data collection was performed, underlaid by a mosaic of selected SAR satellite scenes.

This report gives a complete record of all data sets that were collected by the team consisting of staff from UiT – The Arctic University of Norway, The Norwegian Polar Institute (NPI), the Norwegian Meteorological Institute (MET), NORCE, Maritime Robotics and ISAE-SUPAER.

For each of the activities, it gives an explanatory description of what was measured and how the various measurements were performed. The report also includes an overview of coincident satellite data covering the visited areas in the period, an overview over safety aspects and measures, outreach activities during the cruise, and the participant list.

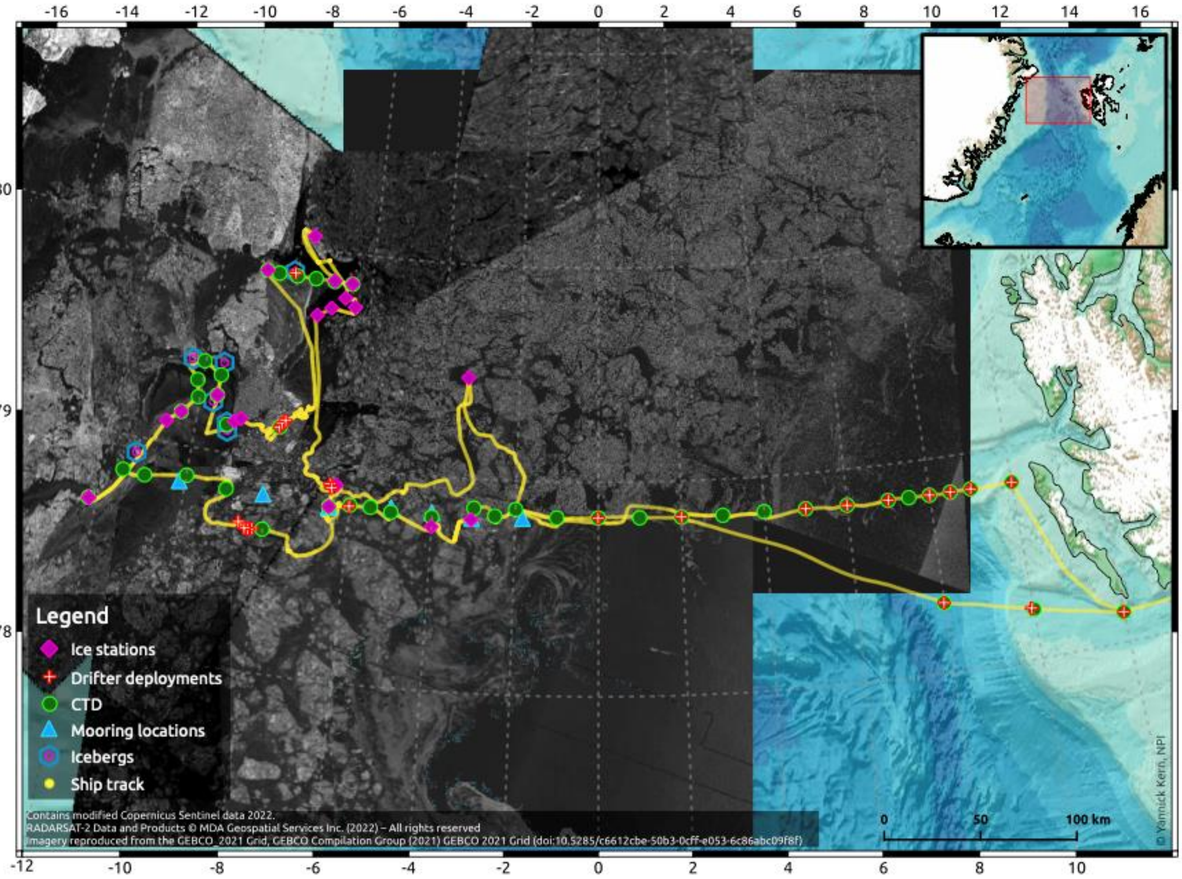

Figure I.1 *Map of Fram Strait showing the ship track along with markings of the various stations where data was collected during the cruise. The map was made by Yannick Kern (NPI), with underlying selected SAR sea ice remote sensing images.*

1 Region of interest: The overview

1.1 Sea ice and ocean conditions in the study area

Wolfgang Dierking (AWI/UiT) and Andrea Schneider (UiT)

The cruise track was planned along a profile at 78.5N, moving westwards from Svalbard towards Belgica Bank which is located between 78 – 80°N and 12 – 16°W in the western Fram Strait and offshore North East Greenland (Figure I1).

In its western part, Fram Strait is covered by an area of semi-permanent fast ice called the Norske Øer Ice Barrier (NØIB), which varies in extent annually. This ice barrier stretches 75–150 km from the coast toward the middle of the continental shelf. In its western part, the NØIB is bordered by East Greenland´s coastline with its fjords, marine terminating glaciers and a string of barrier islands. Coastal islands allow fast ice to form, and they keep it in place. In the east of NØIB, the cold East Greenland Current is moving sea ice southwards through Fram Strait, the only deep-water connection to the Arctic Ocean. Large grounded icebergs that originate from Greenland`s marine terminating glaciers, and sea ice ridge keels that reach down to 33m depth (Wadhams et al. 2006) hold the ice in place above about 200 metres deep banks or shoals as shallow as 20 – 80 metres (Arndt et al. 2015).

The NIØB has been a perennial feature during most of the 20th century with significant interannual variations in size and extent. It breaks up more frequently in the past 30 – 40 years and becomes a part of the drifting ice (Hughes et al. 2011). To the north of the NIØB is an open water area that is known as Northeast Water polynya and lasts from May/June until September (Böhm et al. 1997). During our expedition, an area of open water and very thin ice occurred between the landfast ice and dynamic drift ice of varying thickness.

This area has unique sea ice characteristics. Firstly, the NIØB is one of the most extensive areas of landfast ice on Earth (Schneider and Budeus, 1997; Hughes et al. 2011). Since landfast ice does not move horizontally, it is ideal for comparing different satellite data acquired at different times. Landfast ice, however, may move vertically by several centimetres due to tides, waves and swells.

Secondly, sea ice over Belgica Bank is a mixture of ice that has advected in from Fram Strait and ice which is formed locally during the freeze-up. As such the sea ice is present in all different stages of development. The interaction between the fast ice area and drift ice promotes itself to ice dynamics features including flaw leads, polynyas, and rafting and ridging zones. Icebergs reveal a variety of sizes and shapes. Since most of them are grounded, they are favoured for investigating their radar signatures at different frequencies, which requires the combination of SAR and optical images from different satellites, acquired with time gaps of a few to many hours.

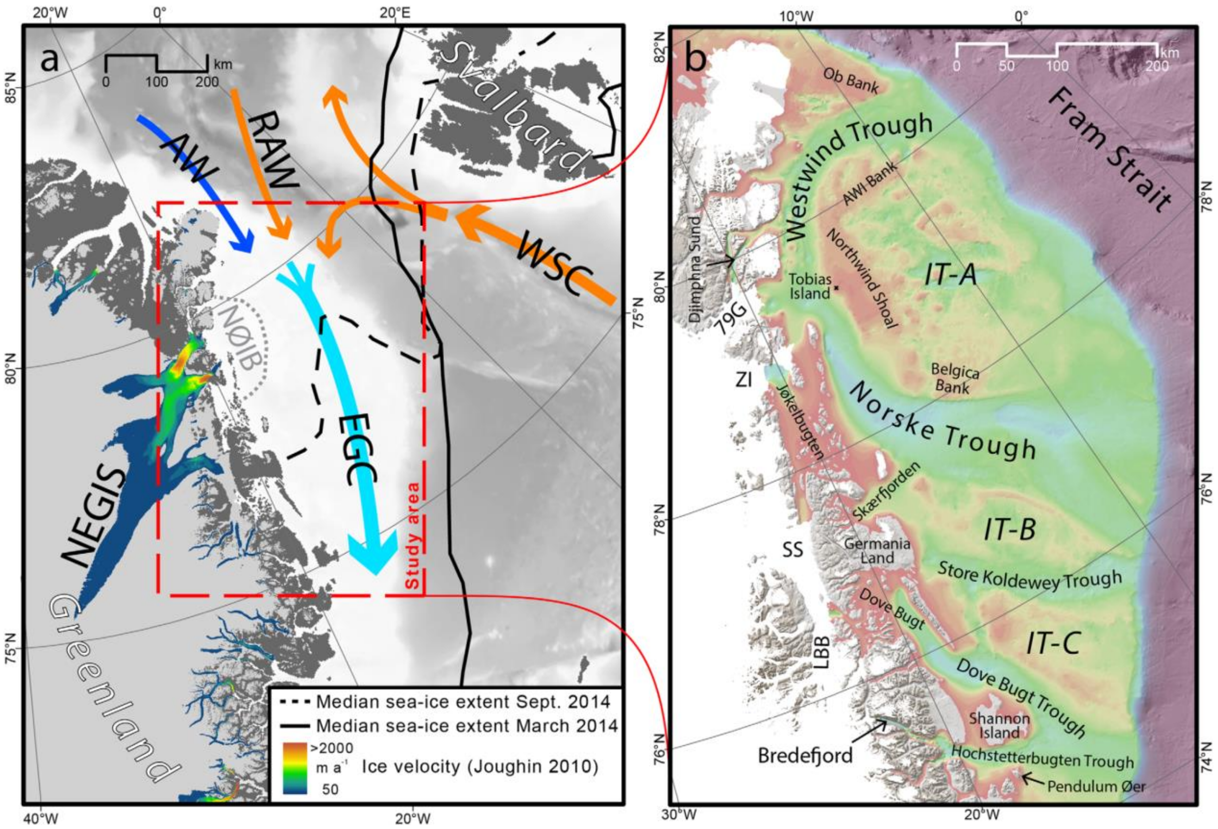

Figure 1.1 *Location map of the study area showing sea ice, glaciological, and oceanographic conditions. NEGIS = Northeast Greenland Ice Stream, NØIB = Norske Øer Ice Barrier, AW = Arctic Water, RAW = Return Atlantic Water, WSC = West Spitsbergen Current, and EGC = East Greenland Current. (b) Geographical names: 79G = 79 Glacier, ZI = Zachariae Isstrøm, SS = Storstrømmen, LBB = L. Bistrup Bræ, and IT = inter-trough areas. Map from Arndt et al. 2015.*

References

Arndt, J. E., W. Jokat, B. Dorschel, R. Myklebust, J. A. Dowdeswell, and J. Evans (2015), A new bathymetry of the Northeast Greenland continental shelf: Constraints on glacial and other processes, Geochem. Geophys. Geosyst., 16, 3733–3753, doi:10.1002/ 2015GC005931.

Böhm, E., T. S. Hopkins, and P. J. Minnett (1997). Passive microwave observations of the Northeast Water Polynya: 1978– 1994, J. Mar. Syst.,10, 85– 94.

Hughes, N., J. P. Wilkinson, and Wadhams, P. (2011), Multi-satellite sensor analysis of fast-ice development in the Norske Øer Ice Barrier, northeast Greenland. Annals of Glaciology, 57/10, 151 - 160. doi: https://doi.org/10.3189/172756411795931633

Schneider, W., and G. Budeus (1997), Summary of the Northeast Water Polynya formation and development (Greenland Sea), J. Mar. Syst., 10, 107– 122.

Wadhams, P., J. P. Wilkinson, and S. D. McPhail (2006). A new view of the underside of Arctic sea ice, Geophys. Res. Lett., 33, L04501, doi:10.1029/2005GL025131.

1.2 Ice Stations

Wolfgang Dierking (AWI/UiT)

The decision for Belgica Bank as target region for the CIRFA cruise was based on two motivations:
(1) the Norwegian Ice Service has been monitoring this region over several years, and it has been one of the test sites for an ESA-JAXA collaborative project since 2019, focusing on the complementary use of L- and C-band SAR imagery for sea ice charting; and
(2) the fast ice belt located along the north-east coast of Greenland in the region of Belgica Bank can be assumed to be stable in April and beginning of May (see Fig. 1.2.1), which makes it possible to fix positions of ice stations at the fast ice margin a few weeks ahead of the cruise and order satellite images for the days when the ship is expected to reach those stations (provided that ice conditions allow the transit through the drifting ice).

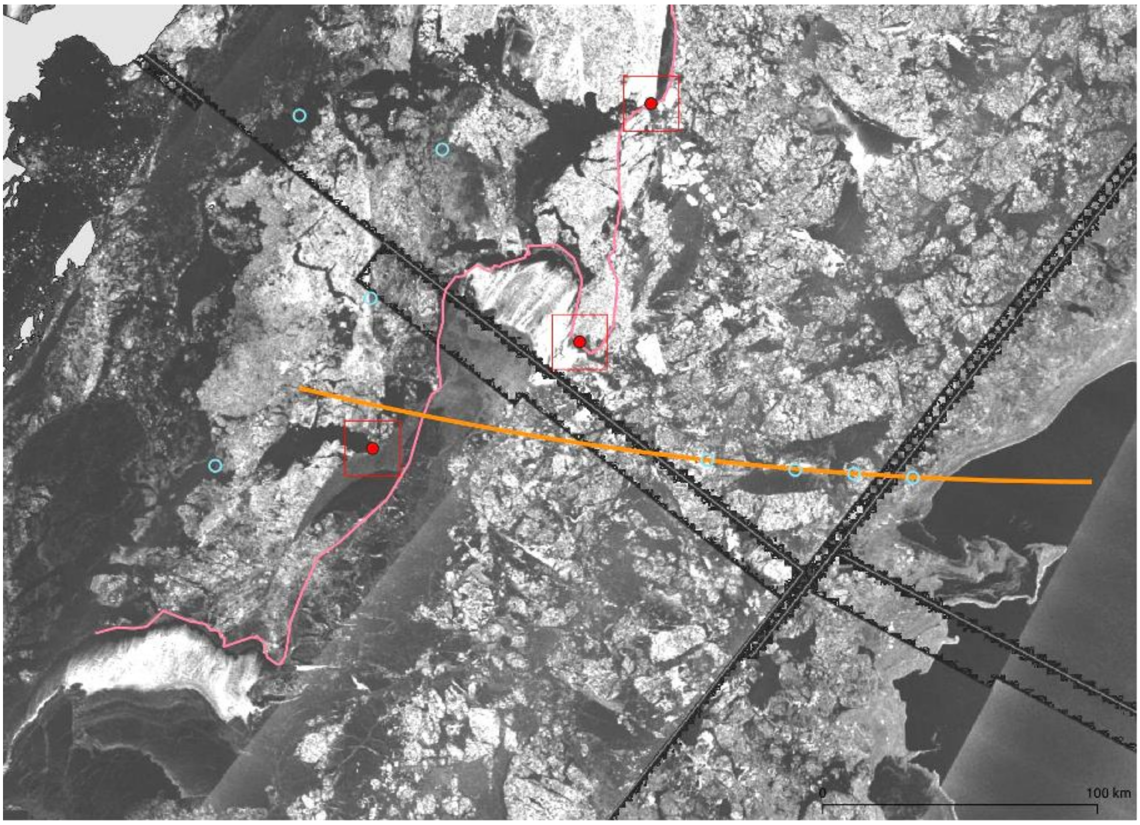

Figure 1.2.1 *Ice conditions in the region of Belgica Bank. This SAR image was acquired by Sentinel 1 (Extra Wide-Swath mode, C-band, HV-polarization) on April 21, 2022. The fast ice belt is located to the left of the pink line, drifting ice with patches of open water areas and new ice formation is visible to the right. The stations S(outh), M(idle), N(orth) are indicated by red dots (North is at the upper image boundary). The orange line is the oceanographic profile regularly monitored by NPI. Image provided by Nick Hughes, Norwegian Ice Service.*

Besides in-situ measurements at the fast ice stations, measurements on drifting ice and of thin ice properties are essential for understanding radar signatures at different frequencies and polarizations, and for validating and improving algorithms for ice classification and ice parameter retrieval such as thickness. During the CIRFA cruise, the three fast ice stations could be reached, and ice and snow data were also acquired for drifting ice and areas of new ice. Positions of icebergs and photographs of iceberg shapes were not only taken at stations but also when being in transit.

The final choice on-site for an ice station was made dependent on the following criteria: (a) safety, (b) satellite coverage and image acquisition times, (c) variability of ice conditions encountered during the cruise.
A full set of measurements consisted of ice coring, snow pit measurements, snow and ice surface roughness data acquisitions, transect data collection of snow and ice thickness both on ground and by a drone equipped with radar, tomographic ground radar measurements, deployments of sea ice mass balance buoys (SIMBAs) and drifters, and acquisitions of optical and infrared imagery from drones.
However, dependent on ice conditions and available time, only selected components of the full measurement set were carried out at some stations (see Sect. 2). The station time varied between more than 48 hours and one hour. Short time periods were typical for drifter deployments. Data gathering was always carried out at the starboard side of the ship. The SIMBAs were deployed on fast ice at larger distances from the ship (see Sect. 2.7).

Figure 1.2a *Bringing the ship into position for work at ice station S. The thicker level ice is located behind the field of rubble. A small section of the thinner level ice can be seen at the lower left of the photo. In the distance, two icebergs are visible. Photo: Wolfgang Dierking (AWI/UiT).*

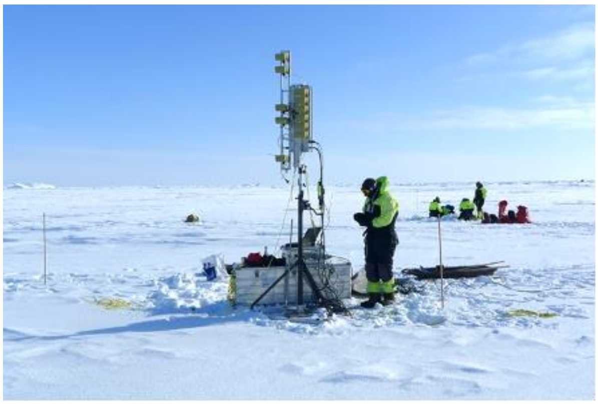

Figure 1.2b *Radar measurements on level ice (left) and snow data sampling in the rubble field (right) at station S. Photo: Wolfgang Dierking (AWI/UiT).*

Measurements at the first fast ice station (**Station S**) at 78°40.7’N 12°12.05’W were carried out from 27th to 29th of April. The site consisted of first-year ice, separated into three different zones (Fig. 1.2): level ice of about 0.9 and 1 m thickness with a snow coverage between 15 and 35 cm, a narrow rubble field, where the ice was compressed to partly more than 4 m thickness with a variable snow layer of up to half a metre, and another level ice zone approximately 0.6 – 0.7 m thick and a snow layer between a few and about 20 cm. Note that the approximate numbers of ice and snow thickness are based on point measurements close to the ship (see Sect. 2), a more detailed picture of thickness variations will be available after processing of the transect data.

Figure 1.3 *Station M, view on measurement sites at the ship’s starboard side. Photo: Wolfgang Dierking (AWI/UiT).*

The second fast ice station (**station M**, Fig. 1.3) at 79°10.2'N 008°54.2'W was examined on May 1st and was characterised by level multi-year ice. The ship was parked between two icebergs. Ice coring revealed thicknesses around two meters, the snow depth was between 15 and 30 cm.

Due to severe ice conditions on the transit towards the third fast ice station (**station N**) at 79°52.6'N 008°48.2'W (Fig. 1.4), only a limited measurement program could be realised at the station on May 3rd (Fig. 1.5) The level ice revealed a thickness of 84 cm, snow depth was between 15 and 25 cm.

Figure 1.4 *Ice conditions during transit towards fast ice station N. This photo was taken on May 2, 18:37 UTC, at 79°16.1'N 007°7.9'W. Photo: Wolfgang Dierking (AWI/UiT).*

Measurements on drifting ice were carried out at four stations, see Table 1.1 below, partly with the full set of measurements except deployment of SIMBAs.

Table 1.1 *Measurement sites on drifting ice.*

Position	Date	Ice type	Ice thickness	Snow thickness
80°03.7'N 007° 41.5'W	May 4	heavily deformed multi-year ice	4.4 m	89 cm
79°47.6'N. 006°39.9'W	May 4	heavily deformed multi-year ice	0.55 m	70 cm

79°45.0’N 006°23.2’W	May 5	not specified	2.2 m	15.5 – 41 cm
79°28.1’N 003°18.8’W	May 7	not specified	1,95 m	27 – 37 cm

Figure 1.5 *Snow sampling at station N. Photo: Wolfgang Dierking (AWI/UiT).*

Figure 1.6 *Broken thin ice examined from the transfer basket on May 4. See Table 2.4.1 for further information. Photo: Wolfgang Dierking (AWI/UiT).*

Thin ice was examined at eight stations between April 29th and May 5th. In this case, two persons in a transfer basket were placed over the ice. If possible, the basket was put on the ice surface (see section 2.4 and Table 2.4.1 for positions and dates). Different forms were probed: smooth ice partly covered with frost flowers of different areal densities, ice roughened due to rafting or compressive breaking (Fig. 1.6), and pancakes at different stages of development. The ice thickness varied between 4 and 14 cm, the size of pancakes ranged between a few cm and up to 60 cm. Various thin ice structures (rafting, ridging, cracks, different stages of pancakes) and surface characteristics (frost flowers, roughness patterns) were documented with photos while on transit between stations. An example is shown in Fig. 1.7.

Figure 1.7 *New ice and pancake formation at the edge of a lead. The photo was taken on May 3rd at 79°38.8'N 007°41.9'W. Photo: Wolfgang Dierking (AWI/UiT).*

Fifteen short ship stops were carried out for the deployment of sea ice drifters between April 24th and May 6. Additional stops were necessary for the deployments of drifters by a drone, two were placed on sea ice and three on icebergs. During three deployments on May 6, ice thickness measurements were taken, amounting to 1.65, 3.49, and 4.83 m (Sect. 2.1). Also, three surface velocity profilers were deployed on 1st, 2nd, and 3rd of May.

1.3 Oceanography

Paul A. Dodd (NPI), Mats Granskog (NPI), Yannick Kern (NPI)

The Fram Strait is the largest and deepest gateway that connects the Arctic Ocean to the world ocean. It is characterised by the northward inflow of relatively warm Atlantic waters into the Arctic Ocean on the eastern side along Spitsbergen with the West Spitsbergen Current (WSC), and by southward outflow of fresher and cold Arctic waters with the East Greenland Current (EGC), see Figure 1.3.1.

The Norwegian Polar Institute maintains a monitoring effort of the water exchange through the Fram Strait for several decades. Annual oceanographic cruises across the strait (at about 79N) and an array of ocean moorings across the western part of the strait, monitor sea ice and ocean outflow with the EGC. Find a summary of The Fram Strait Arctic Outflow Observatory online (https://www.npolar.no/prosjekter/fram-strait-arctic-outflow-observatory/).

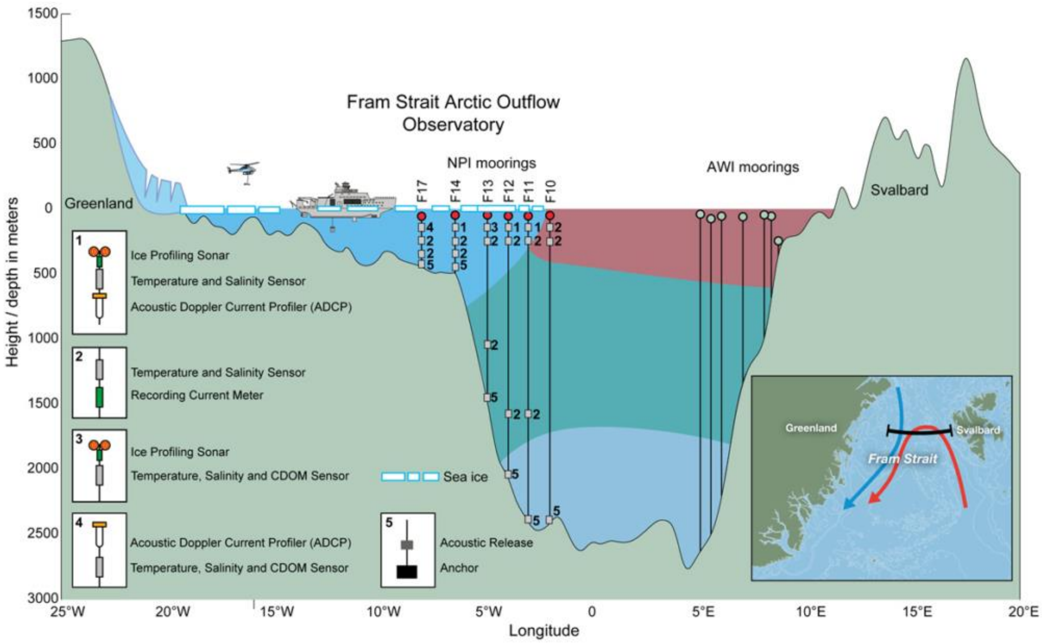

Figure 1.3.1 *An array of moorings is maintained across Fram Strait since the 1990s by NPI (western Fram Strait) and AWI (eastern Fram Strait).*

Winter observations on the east Greenland shelf are rare, and the CIRFA 2022 cruise gave an opportunity to collect data supporting the long-term observations. The primary aim was to collect a hydrographic section across the western half of the strait, in the EGC. And to deploy one shallow mooring on the shelf.

In the end, despite challenging sea ice conditions, a nearly complete set of stations was collected across the whole strait (Fig. I.1), and in addition a number of CTD casts were done opportunistically in polynya-like openings in the ice north of the main section when in transit between ice stations (Fig. I.1). In total 45 CTD casts were made, some of them associated with drifter deployments. From a subset of casts water samples were collected for oceanographic tracers to detect the presence of different water masses and freshwater sources.

2 Measurements

2.1. Ice Coring

Team: Johannes Lohse (UiT), Eduard Khachatrian (UiT), Wenkai Guo (UiT), Martina Idzanovic (MET), Jack Landy (UiT), Catherine Taelman (UiT), Edel Rikardsen (MET), Marina Duran Moro (MET), Knut-Frode Dagestad (MET), Yannick Kern (NPI), Mats Granskog (NPI), Paul Dodd (NPI) and Polona Itkin (UiT)

Ice cores were drilled at 14 main coring sites, distributed over 12 different sea ice stations. At most sea ice stations only one coring site was selected, two stations have multiple core sites (CIRFA22-024C and CIRFA22-034A, see Table 2.1.1). Additional ice cores were drilled at the IMB deployment sites. The ice cores were immediately bagged and transported to the freezer lab of the ship for later analysis in the lab at NPI. For details about the IMB deployment sites and the corresponding ice cores, see Sect. 2.7 in this report.

The 14 main ice core sites were located next to either the snow pits site and/or next to the ground-based radar system (Section 2.6). A complete set of ice cores from one site includes the following cores:

Temperature core (T):

- Temperature was measured immediately after core retrieval using a Testo 720 with robust stainless steel food probe PT100. Measurement intervals are 5 cm in the upper part of the core (0-50cm) and 10 cm in the lower part (below 50cm).
- The cores were kept for further analysis in the freezer lab at NPI.

Salinity core (S):

- On the ice and directly after drilling, the core was cut into sections with a length of 5 cm (upper part, 0-50cm) or 10 cm (lower part, below 50cm). The precise length of the individual pieces was measured to allow for a rough estimation of ice density. The pieces were stored in melting cups and taken to the ship.
- After melting, the salinity and weight of each sample was measured in one ship lab. For measurements of salinity, the WTW LF340 probe was used. The weight of the empty melting cups was determined afterwards.
- Samples for oxygen isotope analysis were taken and stored in bottles for later analysis at NPI.

Density core (D):

- The core was bagged and labelled in a core sleeve directly after retrieval and taken on board the ship.
- The entire core was stored in the freezer lab of the ship at -20 deg C and taken to NPI for density analysis.

Archive core (A):

- The core was bagged and labelled in a core sleeve directly after retrieval and taken on board the ship.

- The entire core was stored in the freezer lab at -20 deg C and taken to NPI for archiving.

Chemistry cores (C):

- Up to three cores were taken at each site for chemistry analysis.
- A bulk snow sample was taken at the same location.

Photographs of the cores were taken for additional documentation. At some core sites, the number of cores was reduced because of time constraints. Hence, not all cores listed above could be drilled at every core site. A summary of the work at each core site is given in Table 2.1.1. Table 2.1.2 gives an overview over the cores that were shipped back to Tromsø for processing in the freezer lab at NPI.

Table 2.1.1 *Overview of ice core sites.*

Station # Site #	Date (dd/mm/yyyy)	Time (UTC)	Lat Lon	Cores taken	SIT [cm]	Comments
CIRFA22-024A 1	27/04/2022	11:20	78.67905 N 12.20053 W	T, S, D, A, C	97	level ice, fast ice (FYI), station S
CIRFA22-024B 2	28/04/2022	08:42	78.67908 N 12.20185 W	T, S, D, C	94	level ice, fast ice (FYI), station S
CIRFA22-024C 3	29/04/2022	10:46	78.67680 N 12.18372 W	T, S, D, A, C	67	level ice, fast ice (FYI), station S
CIRFA22-024C 4	29/04/2022	12:45	78.67736 N 12.18046 W	T, S	~400	rubble field, fast ice, station S
CIRFA22-034A 5	01/05/2022	08:00	79.16945 N 08.90408 W	T, S, D, A, C	190	level ice, fast ice (MYI) station M
CIRFA22-034A 6	01/05/2022	12:15	79.16900 N 08.90388 W	S	205	level ice, fast ice (MYI) station M
CIRFA22-038A 7	03/05/2022	11:15	79.87372 N 08.81355 W	T, S, D, A, C	84	level ice, fast ice, station N
CIRFA22-045 8	04/05/2022	08:15	80.06083 N 07.69177 W	S	440	short drift ice station
CIRFA22-046 9	04/05/2022	14:55	79.79328 N 06.65868 W	S	55	short drift ice station
CIRFA22-047 10	05/05/2022	06:50	79.75414 N 06.39042 W	T, S, D, A, C	220	drift ice station
CIRFA22-051 11	06/05/2022	11:28	78.92011 N 06.53986 W	S	165	during drifter deployment
CIRFA22-052 12	06/05/2022	13:05	78.90400 N 06.48533 W	S	349	during drifter deployment
CIRFA22-053 13	06/05/2022	14:42	78.91953 N 06.36737 W	S	483	during drifter deployment
CIRFA22-054 14	07/05/2022	6:55	79.47111 N 03.30817 W	T, S, D, A, C	195	drift ice station

The observed ice thickness values at the core sites varied between 67 and 483 cm, including two sites with relatively young first-year ice (FYI) as well as sites with presumably old second- or multi-year ice (MYI). Besides the difference in salinity (saline FYI, fresher MYI), FYI and MYI could often be distinguished by the presence of clearly visible air bubbles, in particular in the top layers of MYI cores (Figure 2.1.1). The freeboard at all sites was positive, with the exception of Site 11 (freeboard of -4 cm).

Table 2.1.2 *Ice core inventory for processing in the lab at NPI. In some cases, the ice core was separated into different pieces.*

Station # Site #	**Date dd/mm/yyyy**	**Lat Lon**	**Use**	**Pieces and lengths**
CIRFA22-024A 1	27/04/2022	78.67905 N 12.20053 W	D	1: 96cm
CIRFA22-024A 1	27/04/2022	78.67905 N 12.20053 W	A	1: 97.5cm
CIRFA22-024A 1	27/04/2022	78.67905 N 12.20053 W	T/other	1: 100cm
CIRFA22-024B 2	28/04/2022	78.67908 N 12.20185 W	D	1: 94.5cm
CIRFA22-024C 3	29/04/2022	78.67680 N 12.18372 W	D	1: 66cm
CIRFA22-024C 3	29/04/2022	78.67680 N 12.18372 W	A	1: 64cm
CIRFA22-024C 3	29/04/2022	78.67680 N 12.18372 W	T/other	1: 67cm
CIRFA22-024C 4	29/04/2022	78.67736 N 12.18046 W	T/other	1: 100cm
CIRFA22-034A 5	01/05/2022	79.16945 N 08.90408 W	D	1: 92.5cm 2: 102cm
CIRFA22-034A 5	01/05/2022	79.16945 N 08.90408 W	T/other	1: 11cm 2:100cm 3: 106cm
CIRFA22-038A 7	03/05/2022	79.87372 N 08.81355 W	A	1: 82cm
CIRFA22-038A 7	03/05/2022	79.87372 N 08.81355 W	D	1: 86cm
CIRFA22-038A 7	03/05/2022	79.87372 N 08.81355 W	T	1:89cm
CIRFA22-045 8	04/05/2022	80.06083 N 07.69177 W	tbd	5 pcs, total: 440cm
CIRFA22-047 10	05/05/2022	79.75414 N 06.39042 W	D	1: 102cm 2: 101cm 3: 21cm
CIRFA22-047 10	05/05/2022	79.75414 N 06.39042 W	A	1: 68cm 2: 101cm 3: 66.5cm
CIRFA22-047 10	05/05/2022	79.75414 N 06.39042 W	T	1: 100cm 2: 74cm

				3: 54cm
CIRFA22-054 14	07/05/2022	79.47111 N 03.30817 W	T	1: 103cm 2: 80cm 3: 31cm
CIRFA22-054 14	07/05/2022	79.47111 N 03.30817 W	D	1: 102cm 2: 71cm

Figure 2.1.1 *Top section (16 – 28 cm) of a core taken at Site 6. Air bubbles are clearly visible. Photo: Johannes Lohse (UiT*

Figure 2.1.2 *Temperature measurements in the field. The core is kept in the shade during processing in the field. Photo: Johannes Lohse (UiT).*

Figure 2.1.3 *Ice core at Site 7 after retrieval, ready for processing. Algae are visible at the bottom (left side). Photo: Johanne Lohse (UiT).*

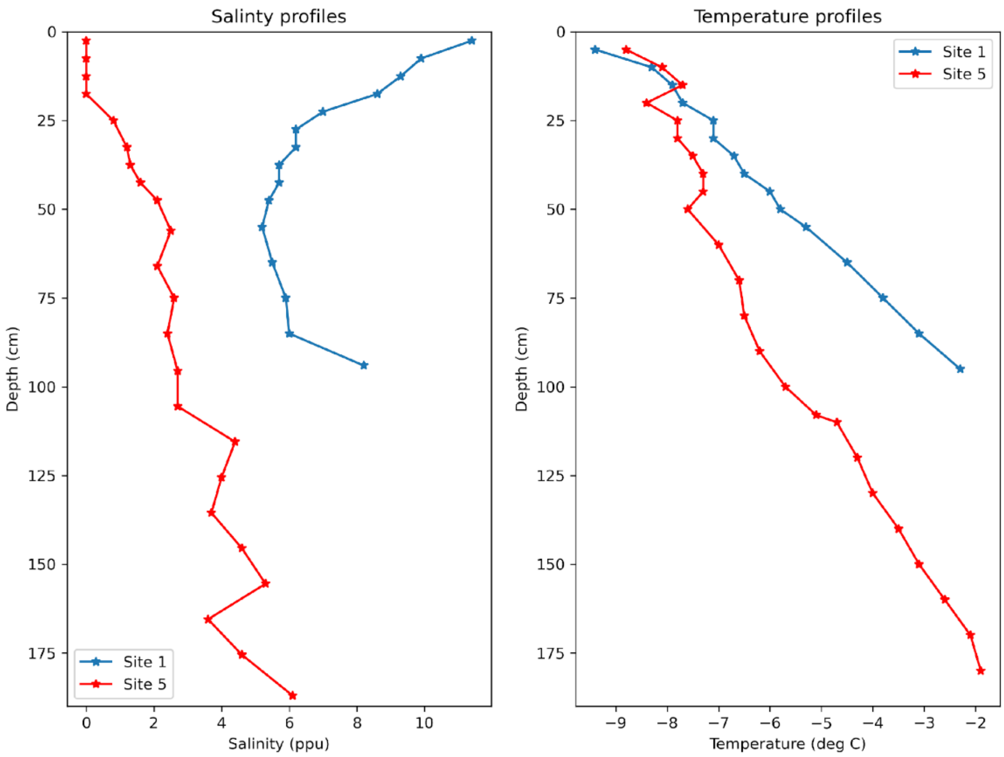

Figure 2.1.4 *Salinity and temperature profiles of cores taken at Site 1 (blue) and Site 5 (red). Depth scale in cm is on the left.*

2.2. Surface roughness profiling

Team: Jack Landy (UiT), Catherine Taelman (UiT) and Wolfgang Dierking (AWI/UiT)

In total 25 sets of surface roughness profiles, with a total number of 156 individual profiles, were collected over snow and sea ice surfaces from 7 sites at sea ice stations, see Table 2.2.1 below.

The surface roughness profiler consists of a ~1.8 m long frame mounted on two feet, with a rail-mounted motor on a rubber belt transporting a nadir-looking laser up and down the rail (Fig. 2.2.1). The laser is a SICK model, with a wavelength of 658 nm (red) and a maximum range of approximately 150 mm. The motor travels at a speed of 50 mm/s acquiring measurements of the relative range to the surface from the rail position along profiles of ~1400 mm. The sample resolution is therefore ~0.1 mm. The motor and laser are connected by cable to a control box (see below) into which a laptop must also be connected to operate the system. After connecting the system, the full control box was enclosed in a watertight plastic bag to protect it from moisture.

Pairs of height profiles are acquired automatically as the motor moves up and down the rail, so although we acquired 156 profiles here only 78 can be considered independent.

Figure 2.2.1 *The roughness profiler set up in the office, showing the control box on the left and the profiling frame on the right. Photos: Anca Cristea (NPI).*

Initially the system was operated inside a 2 x 2 m ice fishing tent to protect the sensor, but in stable weather when the wind speed was lower and in the absence of snowfall/blowing snow, the system could be operated outside (Fig. 2.2.2). We used a Honda 1000W generator to power both the 8W laser and ~65W laptop simultaneously.

First tests with the profiler showed strong backscattering of the red laser from snow and white ice (i.e., scattering) surfaces, but strong penetration of the laser into more transparent sea ice surfaces after clearing snow. Examples of these penetration ‘spikes’ can be seen in the example profile from 29/04/22 below (Fig. 2.2.3). Only following additional careful analysis can we decide which of the acquired profiles should be used for sea ice roughness measurements. Some profiles may have to be discarded if all penetration/multi-path reflection spikes cannot be reliably removed. *We recommend a near infrared (NIR) laser should be used with the system in future*, as absorption is higher at NIR wavelengths than at red, meaning penetration into sea ice should be limited.

Surface roughness profiles were acquired over untouched snow surfaces, over deeper layers of the snowpack and from the snow-sea ice interface by invasively removing snow (see below). Shovels were used to remove the upper snow layers away from the interface of interest. A plastic broom was then used to clear snow crystals at the interface, with a smaller snow crystal brush used to carefully clear remaining crystals over complex ice surfaces. It is not clear how much invasive snow removal affected the roughness measurements, with some snow layers being removed from ice surfaces more easily than others. For each set of measurements, a tape measure was laid across the profiler feet and photos were taken of the measured surface (Fig. 2.2.3), with the camera time stamp matching the laptop time stamp used for the roughness profiles.

Figure 2.2.2 *The surface roughness team measuring a profile over sea ice exposed with a shovel and brush. Photo: Andrea Schneider (UiT).*

Figure 2.2.3 *(Left) snow surface roughness from surface hoar over thin FYI at the sea ice station on 29/04/22, and (right) sea ice surface roughness from 'suncups' exposed at the interface between snow and sea ice at the MYI station on 01/05/22. Photos: Catherine Taelman (UiT).*

After acquisition, a small amount of pre-processing was performed on the raw surface roughness profiles. Initial tests showed that paired profiles from the motor up and down transits were not identical in length and did not collect observations at exactly the same location. Although the paired profiles were very similar, they could not be directly compared without further steps to match samples (interpolation, etc.). Thus, the similarities between pairs have not yet been analysed.

For each profile the following preprocessing was carried out:

1. A median filter with a span of 301 samples (30 mm) is used to obtain a downsampled version of the profile. All 'spikes' with a range greater than 150 mm or height difference greater than 20 mm from the median downsampled profile are removed.
2. A finite impulse response (FIR) high-pass filter is then used to extract only the relevant scales of the roughness for radar backscattering. At typical radar wavelengths, the 'small scale roughness' (mm-cm) is important for understanding how the backscattering varies with incidence angle (Fig. 2.2.3). Larger scales of roughness modulate the backscattering response by tilting the small-scale facets towards or away from the sensor. With these short profiles we are interested in only the small-scale roughness, so we use a band limit of 150 mm, i.e. signal components with a characteristic horizontal scale >150 mm are removed. An example is given between the blue and red profiles below. (A stopband attenuation of 60 dB and filter 'steepness' of 0.9 are used).
3. NOTE the band limit of 150 mm is arbitrary and impacts of the cutoff scale and shape of the high-pass filter on the derived roughness parameters need to be investigated.
4. The standard deviation of the spike-removed and filtered profile height distribution is used to derived an estimate for the root-mean square (RMS) height.
5. The autocorrelation of the spike-removed and filtered profile is calculated for lag distances between zero and the maximum length of the profile (1400 mm). A generalised correlation function $C(\rho) = e^{-\left(\frac{\rho}{l}\right)^n}$, where ρ is the lag distance, is fit to the observed autocorrelation function to minimise the free parameters l and n. l is the correlation length (where the correlation drops below $1/e$), and n is the exponent where n = 1 is equal to the exponential correlation function and n = 2 is equal to the gaussian correlation function.

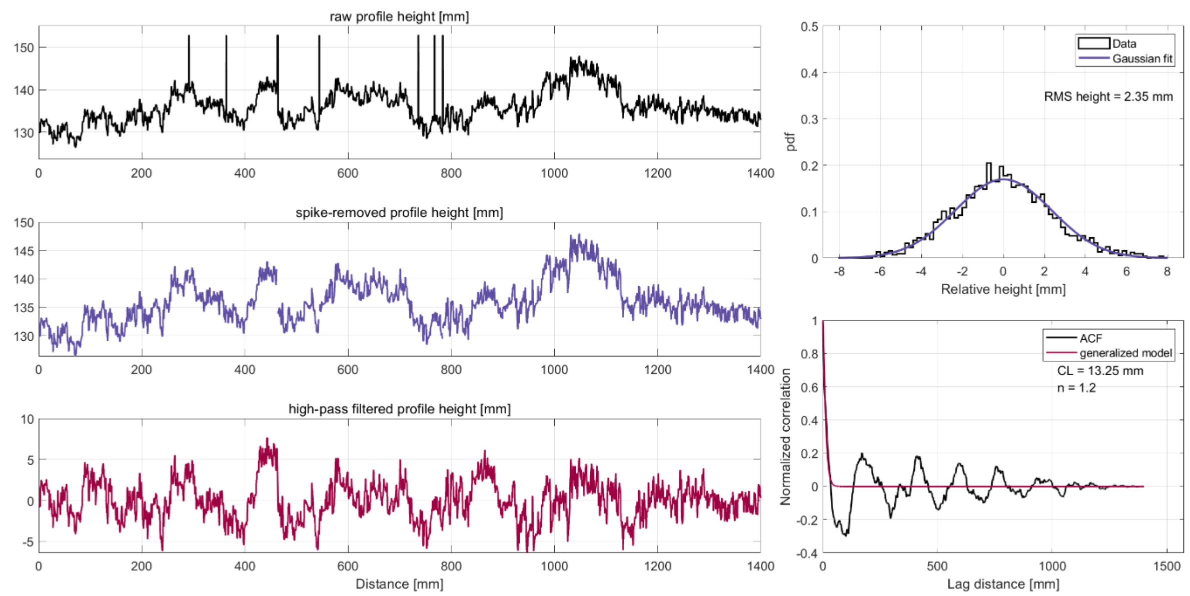

***Figure 2.2.4** Processing steps for quantitative roughness characterization. Upper left: original profile with spikes. Middle left: Profile after spike removal. Bottom left: high-pass filtered profile. Upper right: distribution of height values. Bottom right: Autocorrelation function.*

Fig. 2.2.4 shows an example roughness profile from the snow-ice interface on thin FYI at the sea ice station on 29/04/22 (for dataset “MERIS Data 29-04-2022 141904.txt”). Anomalous spikes are removed from the raw roughness profile, before larger scale undulations with a horizontal scale >15 cm in the surface are removed through FIR high-pass filtering. Surface roughness parameters are derived from the height distribution and autocorrelation function shown on the right.

For the example profile of snow-ice interface roughness above, the RMS height is 2.35 mm, correlation length is 13.3 mm and exponent is 1.2 (i.e., close to exponential). Some evidence for remaining larger scale surface undulations is clear from the oscillations of the autocorrelation function around the model fit. These undulations are also evident in the filtered red profile.

***Table 2.2.1** Surface roughness measurement sites (# = number of profiles).*

Station #	Site	Date	Start Time (UTC)	Surface Type	#
CIRFA22-024A	1	27/04/2022	11:51	snow_and_ice_surface_inside_tent	4
CIRFA22-024A	1	27/04/2022	12:26	snow_and_ice_surface_inside_tent	6
CIRFA22-024A	1	27/04/2022	13:00	ice_surface_1_gently_brushed	10
CIRFA22-024A	1	27/04/2022	13:26	ice_surface_1_heavily_brushed	6
CIRFA22-024A	1	27/04/2022	13:41	snow_ripples_perpendicular	8
CIRFA22-024A	1	27/04/2022	13:59	snow_ripples_parallel	6
CIRFA22-024A	1	27/04/2022	14:11	ice_surface_2_gently_brushed	6
CIRFA22-024C	2	29/04/2022	11:21	ice_surface	6
CIRFA22-024C	2	29/04/2022	11:39	snow_surface	8
CIRFA22-024C	3	29/04/2022	12:04	snow_surface	6
CIRFA22-024C	3	29/04/2022	12:17	ice_ripples	8
CIRFA22-034A	4	01/05/2022	07:41	snow_surface	6
CIRFA22-034A	4	01/05/2022	07:49	snow_surface_perpendicular	6
CIRFA22-034A	4	01/05/2022	08:04	snow_midlayer	6
CIRFA22-034A	4	01/05/2022	08:12	ice_surface	6
CIRFA22-034A	5	01/05/2022	08:51	ice_surface_suncups	10
CIRFA22-047	6	05/05/2022	07:04	snow_ripples_1	6
CIRFA22-047	6	05/05/2022	07:11	snow_ripples_2	6
CIRFA22-047	6	05/05/2022	07:37	snow_midlayer	6
CIRFA22-047	6	05/05/2022	10:00	superimposed_ice	6
CIRFA22-047	6	05/05/2022	08:43	sea_ice_surface	6
CIRFA22-054	7	07/05/2022	07:07	snow_ripples	6
CIRFA22-054	7	07/05/2022	07:15	flat_snow	6
CIRFA22-054	7	07/05/2022	07:47	snow_under_surface_ppt_layer	6
CIRFA22-054	7	07/05/2022	08:02	depth_hoar_crust	6

2.3. Snow pits

Team: Malin Johansson (UiT), Anna Telegina (UiT), Laust Færch (UiT), Jozef Rusin (MET) and Polona Itkin (UiT)

In total 18 snow pits were analysed on 8 ice stations (Figs. 2.3.2 – 2.3.4), plus additional measurements of snow properties during deployment of SMBs (Section 2.7) and drifters (Section 2.8).

Snow pits were dug next to either the sea ice cores and/or next to the ground radar system (positions and other details see Table 2.3.1 at the end of this section). When possible were multiple pits dug on the same ice floe to give a wider aerial coverage and some statistical measure. At all the stations the following parameters were measured:

- Snow thickness
- Number and thickness of snow layers
- Snow grain sizes within the respective layers
- Salinity of the layers
- Density of the layers
- Temperature
- Snow water equivalent (SWE)

Thickness and layer extent were measured using a ruler. Each layer was analysed for grain type, grain size, and hardness. The hardness of each layer was measured based on the levels, fist, fingers, finger, pencil, and knife. Snow grain size within each layer was analysed using a blue plastic crystal card with 2mm grid pattern. The snow grains were categorised into one or two of 5 categories: depth hoar, surface hoar, rounded grains, faceted crystals and defragmented.

Snow salinity samples were collected in 3 cm increments starting from the bottom (0-3, 3-6, 6-9, 9-12, 12-15) and one surface sample (surface - 3cm). They were collected in melting cups and later analysed for salinity using a WTW LF340-A. One set of density measurement was collected for every layer that was thick enough to allow for this. The density cutter used has a volume of 100 cm^3 and the scale used for the weighing was a digital scale with an accuracy of 0.1 g. The temperature was measured every 5 cm in the snowpack using a Hanna HI98501 thermometer. In addition, were air/snow interface and snow/ice interface temperatures measured. SWE was measured using an ETH Standard SWE probe. The snow thickness was measured, the sample weighted (mm SWE) and finally the sample were saved for salinity analysis.

In addition, a Toikka snow fork was used to measure snow density and wetness every 3 cm throughout the snowpack. Frequency, bandwidth and attenuation were also measured. No snow fork measurements were carried out at CIRFA22-045 and CIRFA22-046. SWE and salinity were also measured at the IMB deployment sites, for these stations the snow fork was not used. For details about the IMB see section 2.7 in this report.

Between 4 to 11 different snow layers were observed in the snow pits. An illustration of the layer structure, temperature, salinity and density from CIRFA22-024B site two is shown in Fig. 2.3.1 below. On most of the snow pit stations, at least one bottom depth hoar layer was observed, though for many stations multiple such layers were present. Multiple stations on the fast ice also had surface hoar layers. In addition, faceted crystals and rounded grain layers were also observed frequently. At station CIRFA22-047 an ice lens was observed at the first attempted snow pit (Fig. 2.3.5), and this area was later also measured with the roughness scanner. For the other 3 stations were a hard snow/ice layer of 7 cm thickness observed that could be broken using a shovel with quite some force or an ice axe.

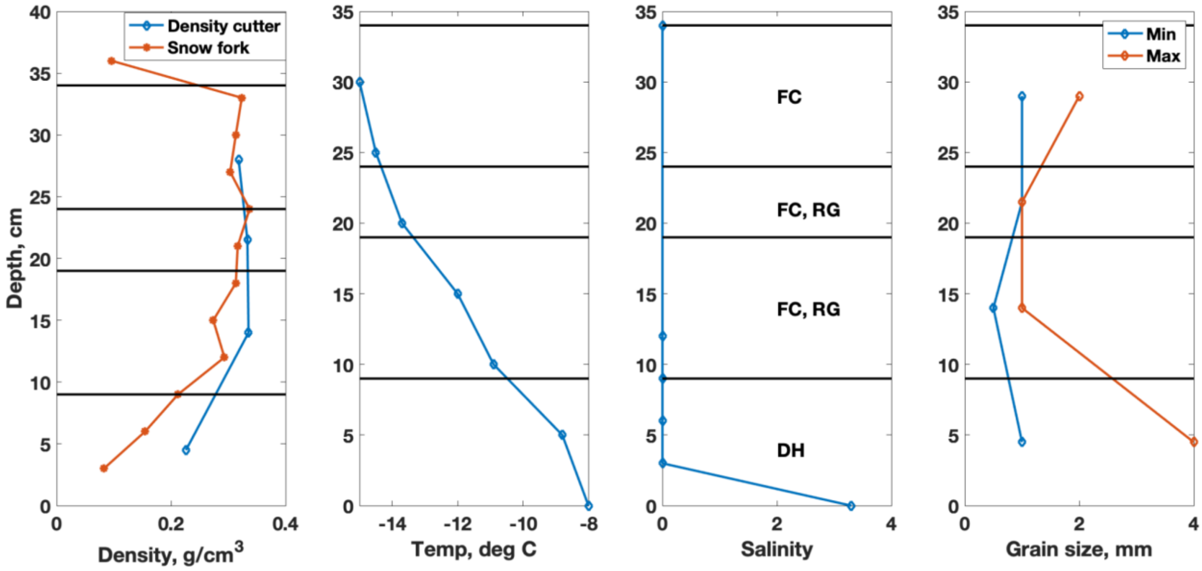

Figure 2.3.1 *Illustration of observations from snow pit CIRFA22-024B site two. DH = Depth hoar, FC = faceted crystals, RG = Rounded grains. Depth is measured from the bottom of the pit.*

Figure 2.3.2 *The snow pit team at the final snow pit (CIRFA22-054). Photo: Paul Dodd (NPI).*

Figure 2.3.3 *Snow pit from CIRFA22-034A showing Laust analysing snow grain sizes and Malin taking notes. Photo: Jozef Rusin (MET).*

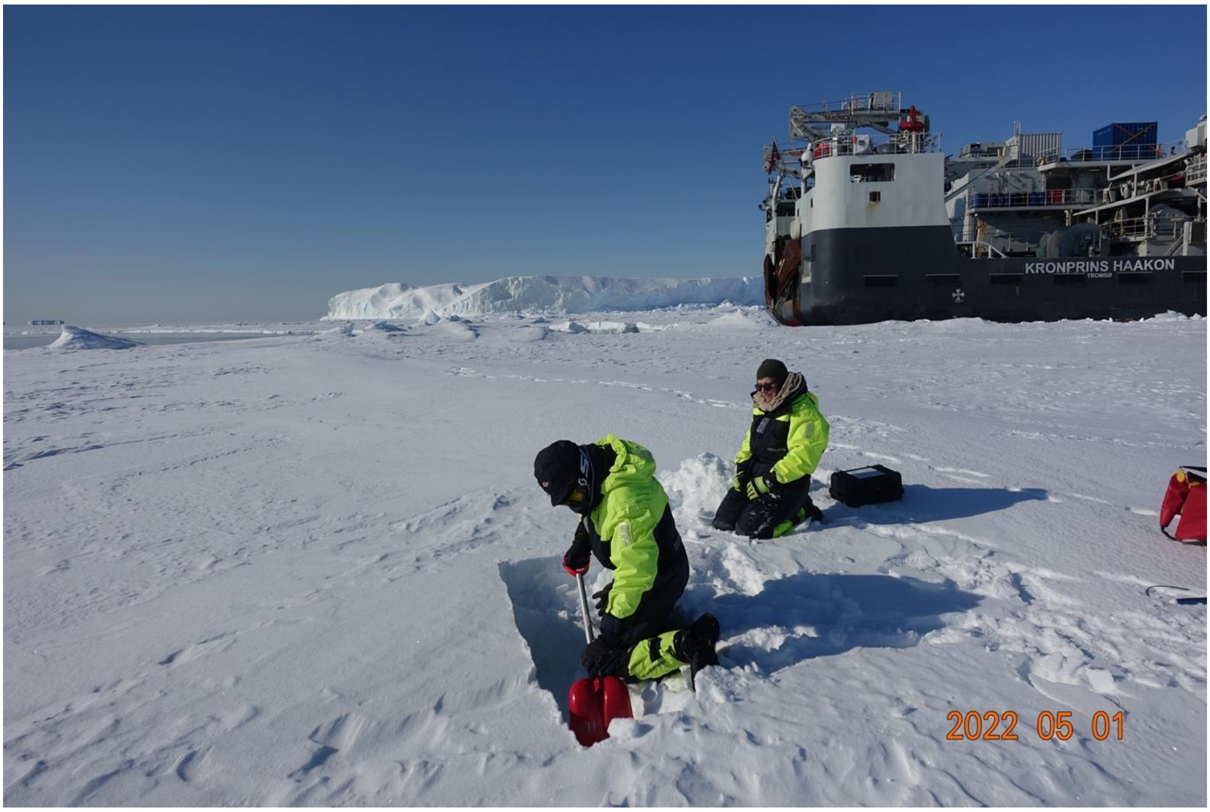

Figure 2.3.4 *Snow pit from CIRFA22-034A showing Jozef and Anna digging a snow pit and setting up the work. Photo: Malin Johansson (UiT).*

Figure 2.3.5 *Left: The ice lens from CIRFA22-047 with beautiful crystals underneath (note the bottom of the ice lence is facing towards Malin). Photo: Anna Telegina (UiT). Right: Depth hoar layer crystals seen through magnifying lens. Photo: Jozef Rusin (MET).*

Table 2.3.1 *Snow pit sites.*

Station #	Date dd/mm/yyyy	Time (UTC)	Latitude	Longitude	Comments
CIRFA22-024A 1	27/04/2022	11:12	78 40.743'N	012 12.032'W	17 cm snow, Pit 1/4 CIRFA22-024A, fast ice (FYI)
CIRFA22-024A 2	27/04/2022	13:17	78 40.734'N	012 12.034'W	34.5 cm snow, Pit 2/4 CIRFA22-024A, fast ice (FYI)
CIRFA22-024B 3	28/04/2022	08:20	78 40.745'N	012 12.095'W	16.5 cm snow, Pit 3/4 CIRFA22-024A, next to the ground radar system, fast ice (FYI)
CIRFA22-024B 4	28/04/2022	11:20	78 40.745'N	012 12.135'W	19 cm snow, Pit 4/4 CIRFA22-024A, next to the ground radar system, fast ice (FYI)
CIRFA22-024C 5	29/04/2022	10:45	78 40.608'N	012 11.023'W	10 cm snow, Pit 1/2 2nd Station CIRFA22-024C, fast ice (FYI)
CIRFA22-024C 6	29/04/2022	11:55	78 40.642'N	012 10.824' W	42 cm snow, Pit 2/2 2nd Station CIRFA22-024C, next to the ground radar system in

					rubble field, fast ice (FYI)
CIRFA22-034A 7	01/05/2022	07:15	79 10.167'N	008 54.245'W	18 cm snow, Pit 1/3 CIRFA22-034A, fast ice (MYI)
CIRFA22-034A 8	01/05/2022	10: 05	79 10.180'N	008 54.215'W	27.5 cm snow, Pit 2/3 CIRFA22-034A, next to the ground radar system, fast ice (MYI)
CIRFA22-034A 9	01/05/2022	12:35	79 10.138'N	008 54.232'W	26 cm snow, Pit 3/3 CIRFA22-034A, fast ice (MYI)
CIRFA22-038A 10	03/05/2022	11:10	79 52.423'N	008 48.813'W	17 cm snow, Pit 1/2 CIRFA22-038A, fast ice
CIRFA22-038A 11	03/05/2022	12:05	79 52.851'N	008 47.680'W	24 cm snow, Pit 2/2 CIRFA22-038A, fast ice
CIRFA22-045 12	04/05/2022	08:15	80 3.650'N	007 41.506'W	89 cm snow, express station, heavily deformed MYI, drift ice
CIRFA22-046 13	04/05/2022	14:44	79 47.578'N	006 39.93'W	70 cm snow, express station, heavily deformed MYI, drift ice
CIRFA22-047 14	05/05/2022	06:50	79 45.248'N	006 23.425'W	15.5 cm snow, Pit 1/3 CIRFA22-047, close to 1st ground radar system site, drift ice
CIRFA22-047 15	05/05/2022	08:15	79 45.004'N	006 23.205'W	26 cm snow, Pit 2/3 CIRFA22-047, close to 1st ground radar system site, drift ice
CIRFA22-047 16	05/05/2022	11:00	79 44.483'N	006 23.008'W	41 cm snow, Pit 3/3 CIRFA22-047, close to 2nd ground radar system site, drift ice
CIRFA22-054 17	07/05/2022	06:50	79 28.249'N	003 18.477'W	27-33 cm snow, Pit 1/2 CIRFA22-054 drift ice.
CIRFA22-054 18	07/05/2022	08:17	79 27.908'N	003 19.094'W	37 cm snow, Pit 2/2 CIRFA22-054 drift ice.

2.4. Thin ice basket stations

Team: Wolfgang Dierking (AWI/UiT), Johannes Lohse (UiT), Malin Johansson (UiT), Jack Landy (UiT), Laust Færch (UiT) and Jozef Rusin (MET)

In total 8 thin ice basket stations were carried out (Table 2.4.1). The measurements were done from the ship basket next to the boat (see Figs. 2.4.1 and 2.4.2 below). Care was taken to perform basket stations within areas that were representative of the wider area around the ship. Sentinel-1 images and drone footage were used to identify areas of interest for the thin ice basket stations as they represented different backscatter regions.

At all the stations the following parameters were measured:

- Sea ice thickness
- Salinity

At all stations a piece of the sea ice was collected, and its thickness and salinity measured. When frost flowers were present, a sample was scraped off and collected, and the salinity measured. In the case of pancakes, the rims were collected separately and analysed for salinity. For the so-called "dragon skin" site (see figures below) a pancake was dislodged and sampled individually for salinity. All salinity samples were collected in melting cups and later analysed for salinity using a WTW LF340-A.

In the case of pancakes or similar structures the diameter and rim height were measured over as many samples that could be reached from the edge of the basket.

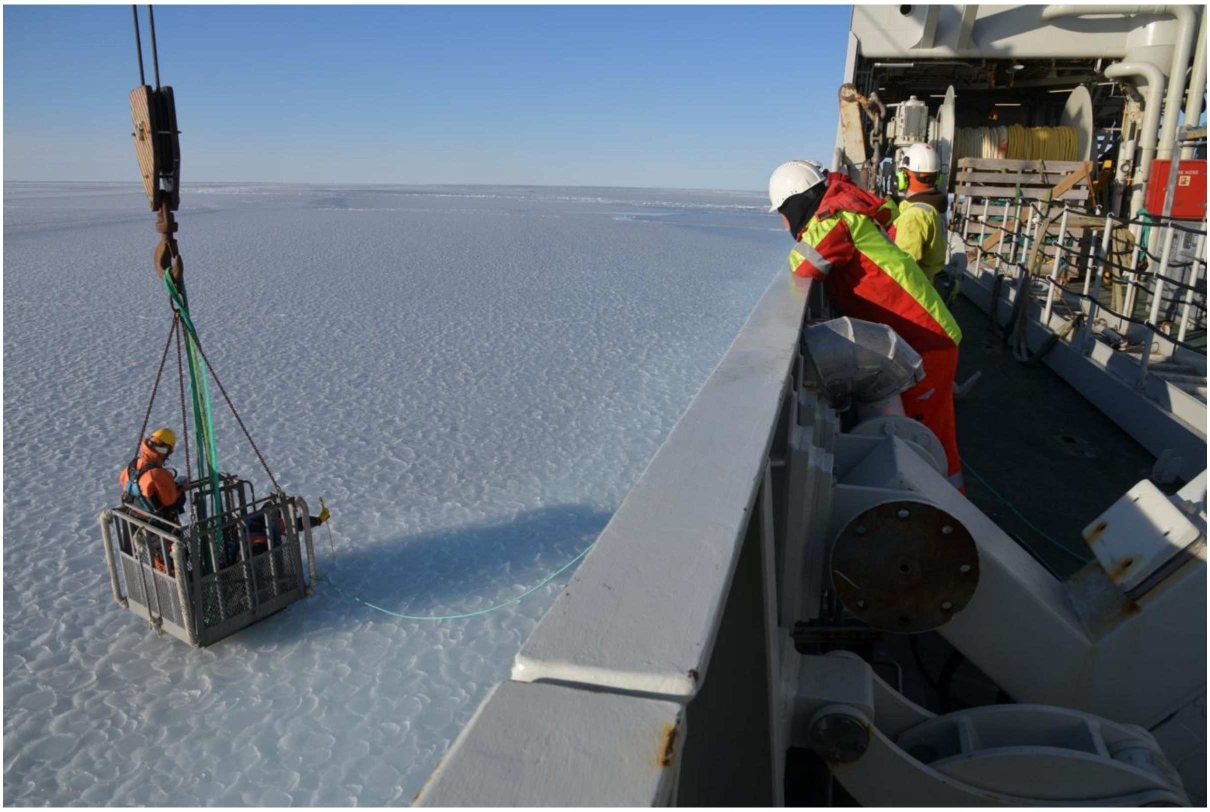

Figure 2.4.1 *"Dragon's skin" sea ice from CIRFA22-049, on 05/05/2022 showing Jozef Rusin and Malin Johansson in the basket next to the ship. Photo: Wolfgang Dierking (AWI/UiT).*

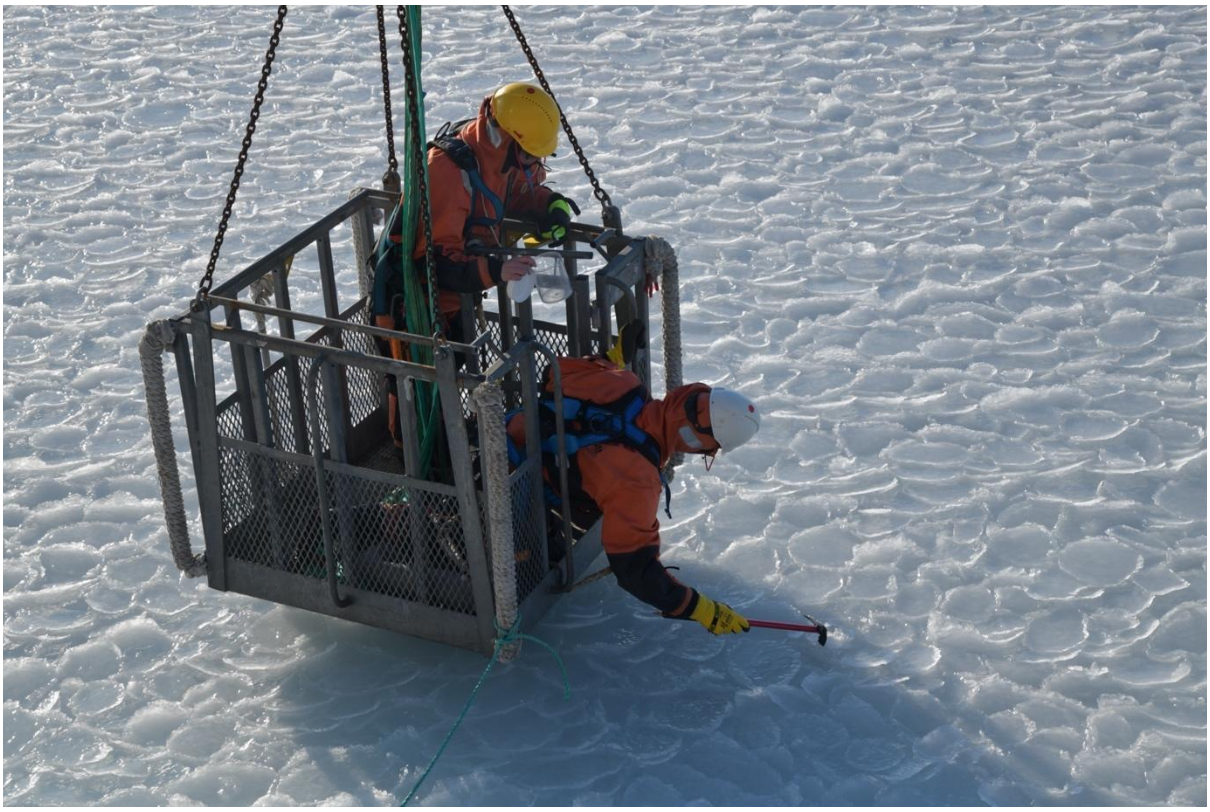

Figure 2.4.2 *"Dragon's skin" sea ice from CIRFA22-049, on 05/05/2022 showing Jozef Rusin removing a sample from the ice surface. Photo: Wolfgang Dierking (AWI/UiT).*

Table 2.4.1 *Thin ice sites.*

Station #	Date dd/mm/yyyy	Time (UTC)	Lat	Long	Comments
CIRFA22-025	29/04/2022	22:05	79 06.096' N	010 43.102' W	11cm ice with frost flowers
CIRFA22-026	29/04/2022	23:20	79 09.326' N	010 23.875' W	14 cm ice with frost flowers
CIRFA22-031	30/04/2022	07:30	79 15.654' N	009 34. 870' W	8 cm ice with sparse frost flowers, brine skin
CIRFA22-033	30/04/2022	14:30	79 09.122' N	009 03.537' W	4.5 cm ice with frost flowers
CIRFA22-043	03/05/2022	20:15	79 51.829'N	007 00.297' W	5 cm thick pancakes, size 40-60cm in diameter. Rims 1.5-4 cm
CIRFA22-044	03/05/2022	21:45	79 51.500' N	006 32.133' W	4 cm smooth ice, rafted in places
CIRFA22-048	05/05/2022	17:00	79 44.3' N	006 58.0' W	10 cm thick, rough surface, some rafting
CIRFA22-049	05/05/2022	19:00	79 41.837' N	007 20.919' W	10 cm thick, dragons' skin, wet surface

2.5. Transects

Team: Polona Itkin (UiT)

The main goals of the transects were:

1. Characterization of snow depth and ice thickness variations along profiles on the floe where the ice station was taking place. If possible, also sections of neighbouring floes, refrozen leads, rubble fields and ridges were sampled

2. Co-location with the SnowRadar mounted on drone (NORCE) for validation of their snow depth product

The instruments used in transect surveys were (Fig. 2.5.1):

1. **GEM-2** to estimate total sea ice thickness by electromagnetic induction. Sea ice thickness can be derived if snow depth is subtracted. GEM-2 is sensitive to conductivity (including environmental temperature) and was calibrated after every transect or at least for every ice type.

2. **Magnaprobe** which is an automated and GPS enabled snow probe that logs the snow depth and position by manual operation (pushing a button after penetrating the snow).

3. **Snow Micropenetrometer (SMP)** which has a force sensor that is driven at a constant speed through the snow. The penetration stops as soon as the sensor detects a certain threshold typical for snow-ice interface. This force recording is directly related to snow hardness, but it can also be correlated to other snow properties such as density and grain size with additional information from snow pits.

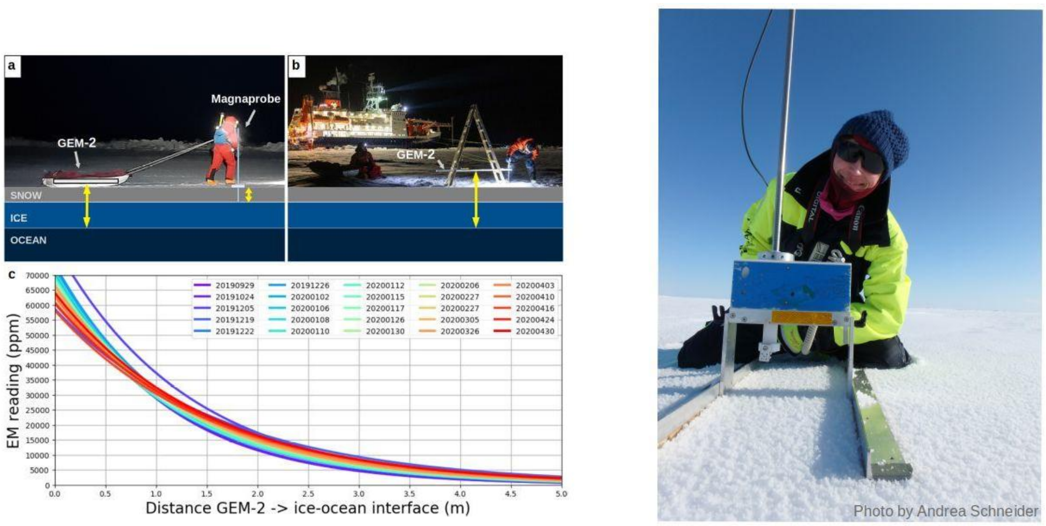

Figure 2.5.1 Methods used in transects: GEM-2 (requires calibration) and Magnaprobe on the left side, Polona using the SMP on the right side.

In total 8 combined magnaprobe and GEM-2 transect surveys were carried out during the cruise. The transects all started at the ship gangway and passed the other teams working on the ice. Where possible parts of the transect were overflown by the SnowRadar (NORCE, Rolf-Ole Jenssen).

Some short (up to 100m-long) transects were measured by the SMP at two stations. In addition, snow depth was collected with a snow probe on short stations: about 30 measurements were made on level ice. Finally, whenever possible data were collected over longer transects by towing GEM-2 in a pulk behind a skidoo. A summary of transects is given in the table below.

Table 2.5.1 *Transect surveys.*

Station #	**Date dd/mm/yyyy**	**Comments**
CIRFA22-024A	27/04/2022	Transect between the flags, overflown by SnowRadar, SMP transect in parts
CIRFA22-024B	28/04/2022	Long GEM-2 transect with the IMB deployments
CIRFA22-024C	29/04/2022	Short transect of irregular shape
CIRFA22-034A	01/05/2022	Station transect. Short SMP transect – SMP failure here
CIRFA22-034A	01/05/2022	Long GEM-2 transect for IMB deployment
CIRFA22-038A	03/05/2022	Long GEM-2 transect for IMB deployment
CIRFA22-047	05/05/2022	Station transect and short GEM-2 transect on skidoo.
CIRFA22-054	07/05/2022	Station transect and short GEM-2 transect on skidoo.

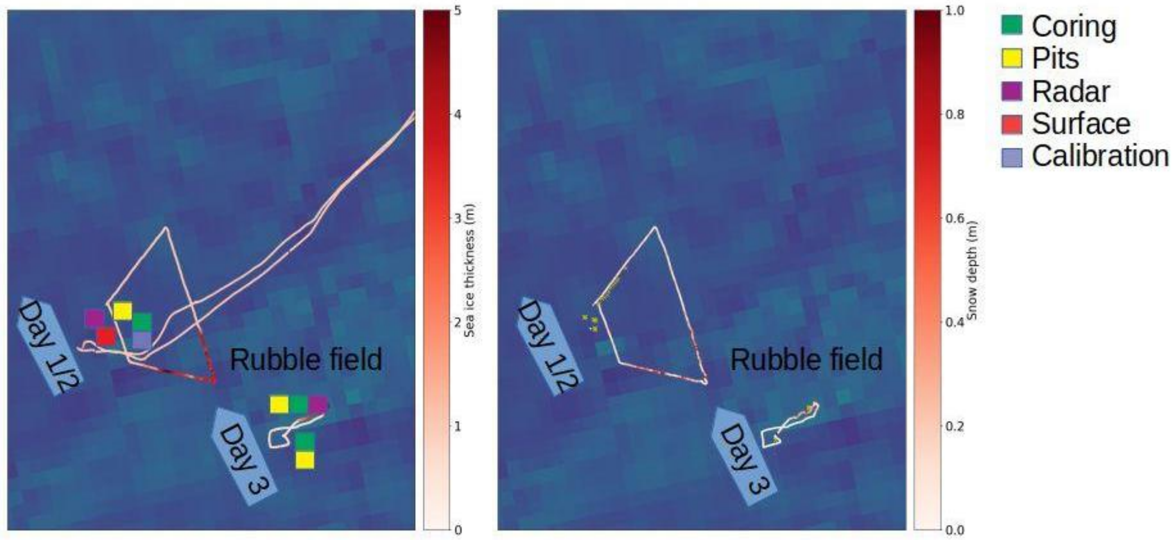

Figure 2.5.2 *Transects at landfast ice station S, CIRFA22-024A-B-C.*

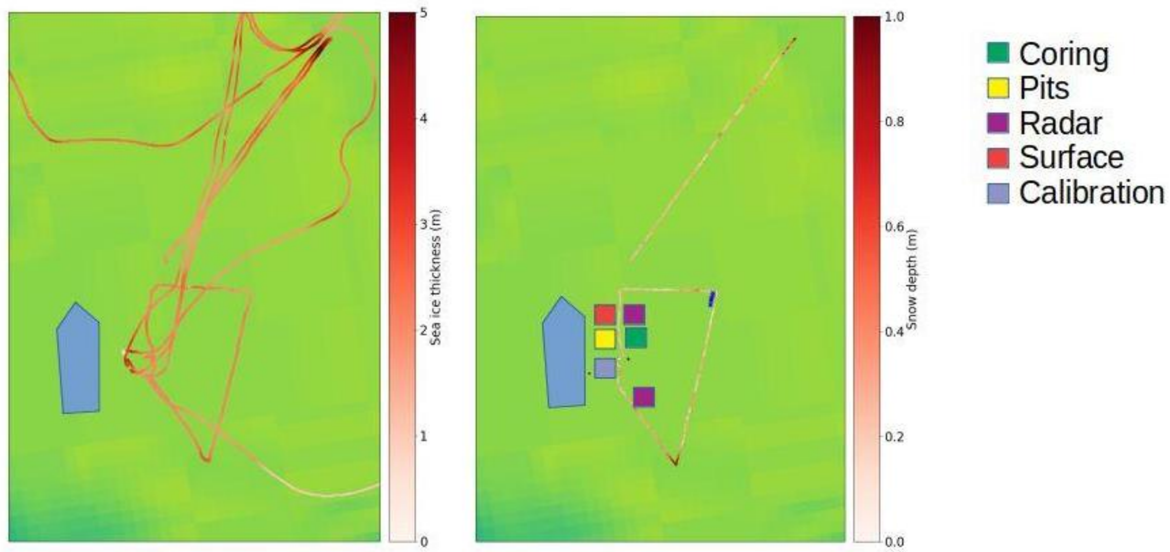

Figure 2.5.3 *Transects at landfast ice station M, CIRFA22-034A.*

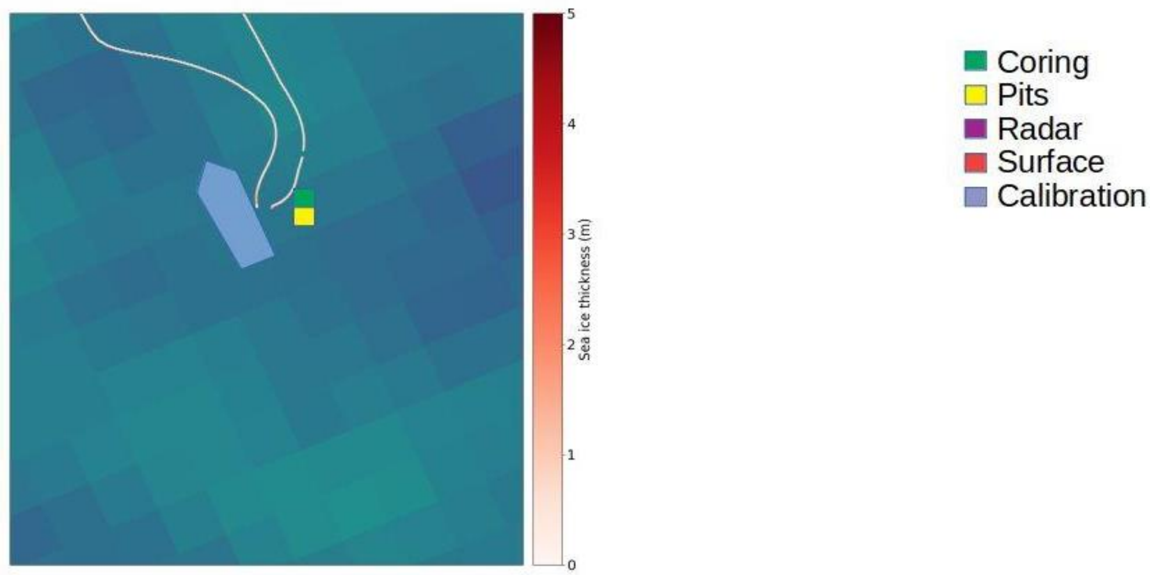

Figure 2.5.4 *Layout of station N, CIRFA22-038A. Transect measurements were not carried out on the station - only skidoo transect for buoy deployments.*

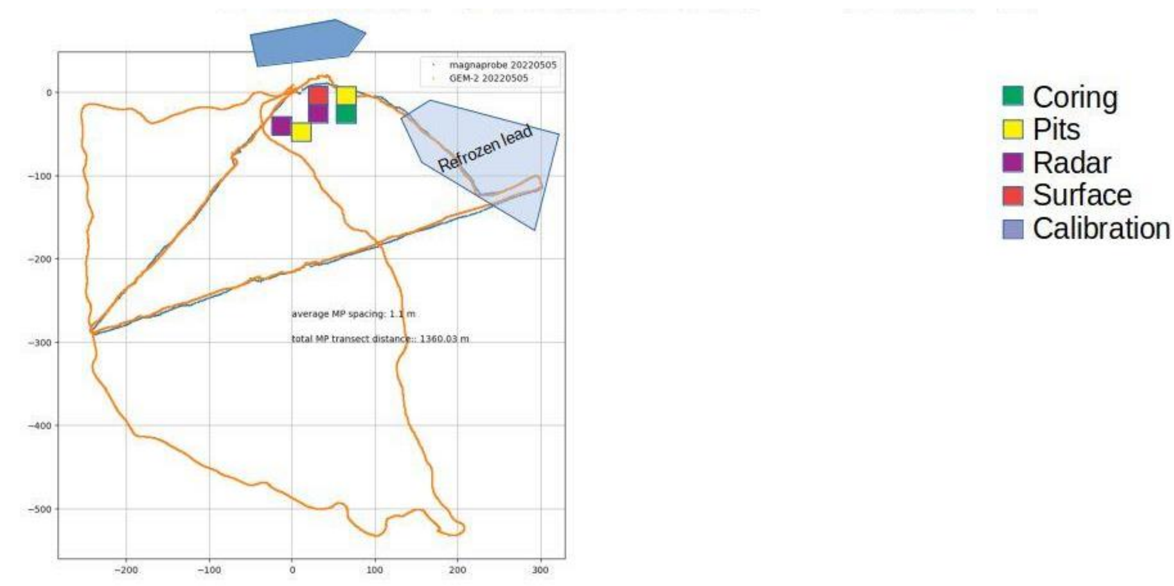

Figure 2.5.5 *Layout of drift station 1, CIRFA22-047.*

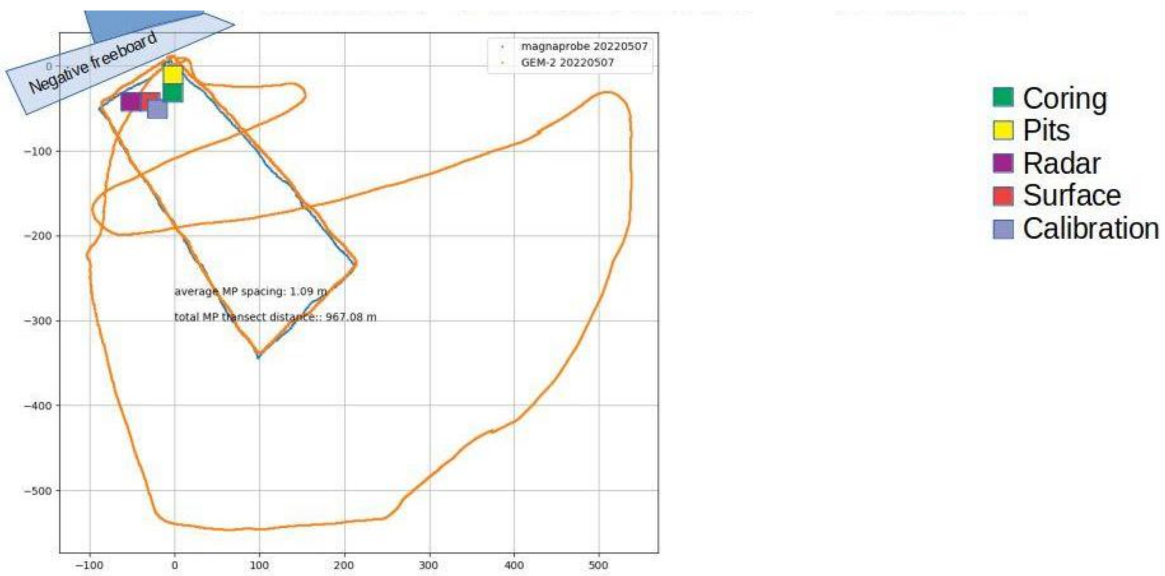

Figure 2.5.6 *Layout of drift station 2, CIRFA22-054.*

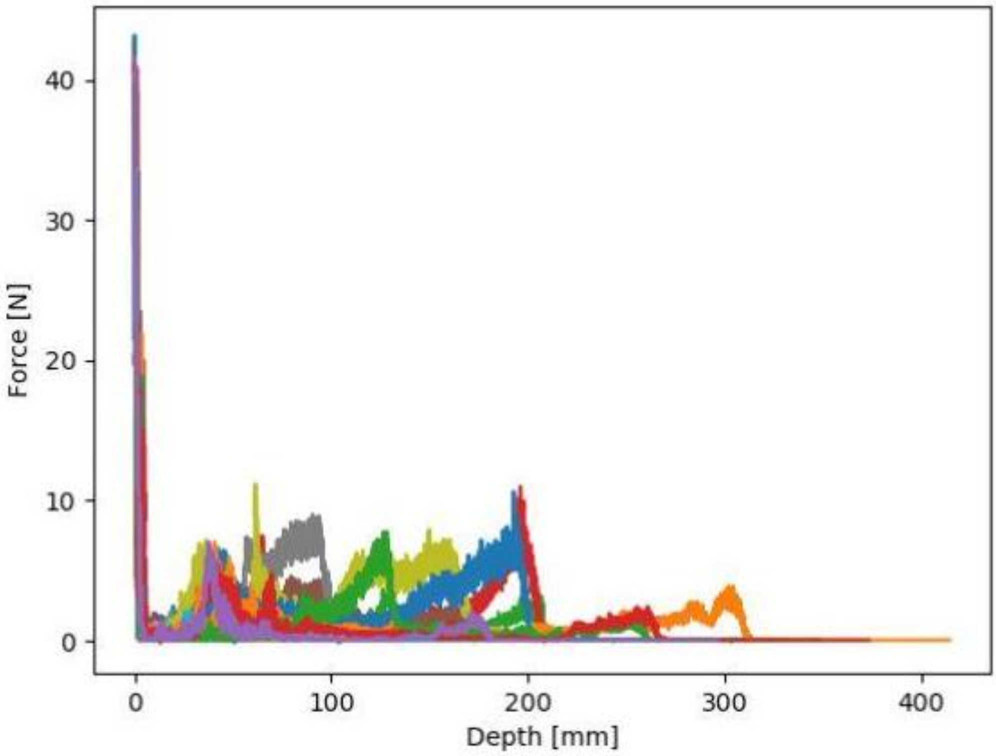

Figure 2.5.7 *Sample data from SMP on the snow radar transect for station CIRFA22-024A. The different colours represent different measurements along the SMP transects (about 0.5m apart). Spikes in the curves represent higher force that was required to penetrate the snow, ie. representing harder snow layers or crusts.*

2.6. Ground-based radar measurements

Team: Laurent Ferro-Famil (ISAE-SUPAERO), Frédéric Boutet (Universite Rennes 1) and Andrea Schneider (UiT)

High-resolution and very local coverage radar measurements were performed at C band using a portable radar system directly deployed on the ice during long stations. The main objectives of this series of acquisitions may be summarised as follows:

- Provide electromagnetic (EM) wave scattering patterns equivalent to those measured by the spaceborne SAR sensor Sentinel-1 (S1), at much higher resolution and with associated ground measurements,
- Assess usual assumptions and principles associated to the radar response of sea-ice at C band (S1),
- Discriminate sources of scattering within a volumetric medium consisting of sea ice and snow, explain the associated EM mechanisms and evaluate their importance in the global returned echo for different kinds of sea-ice.

The analysis performed in this task relies on the use of a multi-channel (MIMO) radar prototype developed and the U. Rennes 1, and whose operating principle is sketched in Fig. 2.6.1. Several acquisitions performed at different positions are combined into a synthetic aperture in order to image the observed volume in range and elevation.

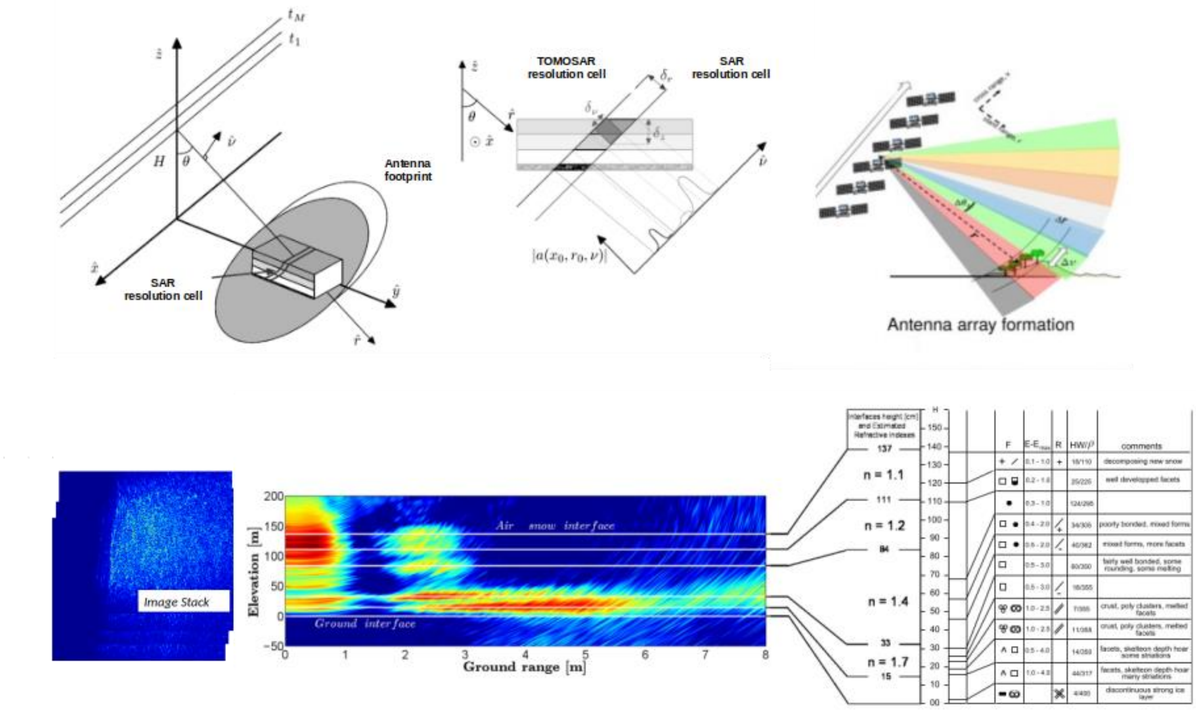

Figure 2.6.1 *Principles of classical 2-D SAR imaging and 3-D SAR imaging using tomographic multi-antenna processing.*

The radar system depicted in Fig. 2.6.2 allows to synthesise images in the range-elevation plane for both quasi-monostatic (with emitters and receivers located on the same side of the medium) and bistatic (with a deported receiver positioned on the opposite side of the illuminated scene and facing the emitters, in the so-called Bizona mode) configurations. These configurations provide very complementary kinds of EM information and help to further characterise complex volumes.

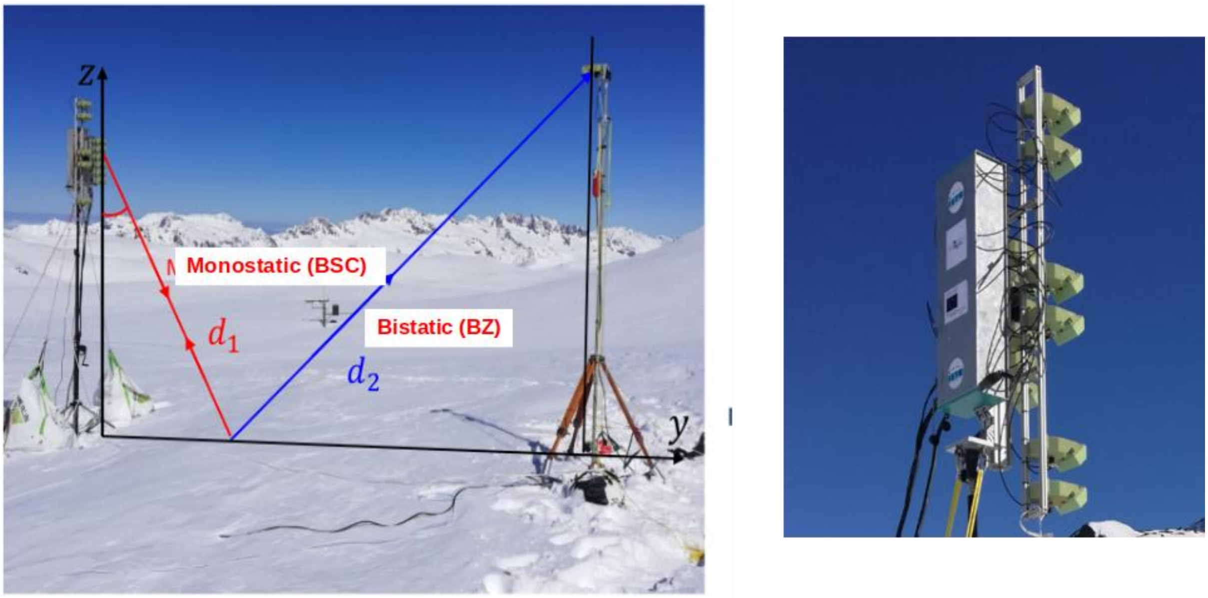

Figure 2.6.2 *Portable tomographic radar system operating in both BSC and BZ configurations. Photos: L. Harkati.*

Tomographic data, that may be used to create range elevation profiles, were acquired at 11 positions and for different types of sea-ice and snow conditions, for both back-scattering at dual pol VV & HV monostatic (BSC) and bistatic VV (BZ) modes. Several profiles were acquired at each location. The synthesised images have a resolution of approx. 9 cm in slant range, 15 cm in elevation in both BSC and BZ modes. The date, location and specific sea-ice conditions corresponding to the different acquisitions performed during this campaign are summarised in Table 2.6.1.

Table 2.6.1 *Ground-based radar stations.* ***!! Confirm GPS locations with Laurent.***

Station #	Date	Latitude	Longitude	Comments
CIRFA22-024A 1	27/04/2022	78 40.745'N	012 12.095'W	Snow-covered small roughness FYI, no penetration. BSC & BZ.
CIRFA22-024A 2	27/04/2022	78 40.745'N	012 12.095'W	Snow-free (shovelling) small roughness FYI, no penetration. BSC.
CIRFA22-024B 1	28/04/2022	78 40.745'N	012 12.095'W	Snow-covered small roughness FYI, no penetration. BSC & BZ.
CIRFA22-024B 2	28/04/2022	78 40.745'N	012 12.135'W	Snow-free (shovelling) small roughness FYI, no penetration. BSC & BZ.
CIRFA22-024C 1	29/04/2022	78 40.642'N	012 11.835'W	Flat disk-like area embedded in rubble field. Penetration through a

				layer of low salinity ice. BSC & BZ
CIRFA22-024C 2	29/04/2022	78 40.642'N	012 11.835'W	Profile located inside rubble field, flat area and high salinity ice chunks, BSC & BZ
CIRFA22-034A 1	01/05/2022	79.16945 N	08.90408 W	MYI, rough ice surface, penetration, BSC & BZ
CIRFA22-034A	01/05/2022	79.16900 N	08.90388 W	MYI, very rough and dense dry layer at the snow-ice interface, large penetration, BSC & BZ
CIRFA22-047 1	05/05/2022	79 45.248'N	006 23.425'W	MYI, rough ice surface, penetration, BSC & BZ
CIRFA22-047 2	05/05/2022	79 44.483'N	006 23.008'W	MYI, very rough and dense dry layer at the snow-ice interface, large penetration, BSC.
CIRFA22-054	07/05/2022	79.47111 N	03.30817 W	MYI, very rough and dense dry layer at the snow-ice interface, large penetration, BSC.

Examples of tomograms obtained over FYI with and without snow cover are given in Fig. 2.6.3. From these reflectivity profiles, one can observe that, in agreement with results published in the literature, at C band, dry snow has a negligible reflectivity and salty sea ice may be considered as an excellent conductor, and hence cannot be penetrated by EM waves. Nevertheless, this experiment shows that the presence of a snow layer, which may be assimilated to a lossless dielectric layer at such a carrier frequency, significantly modifies the dielectric contrast and effective roughness of the upper ice interface, and may strongly modify its reflectivity features.

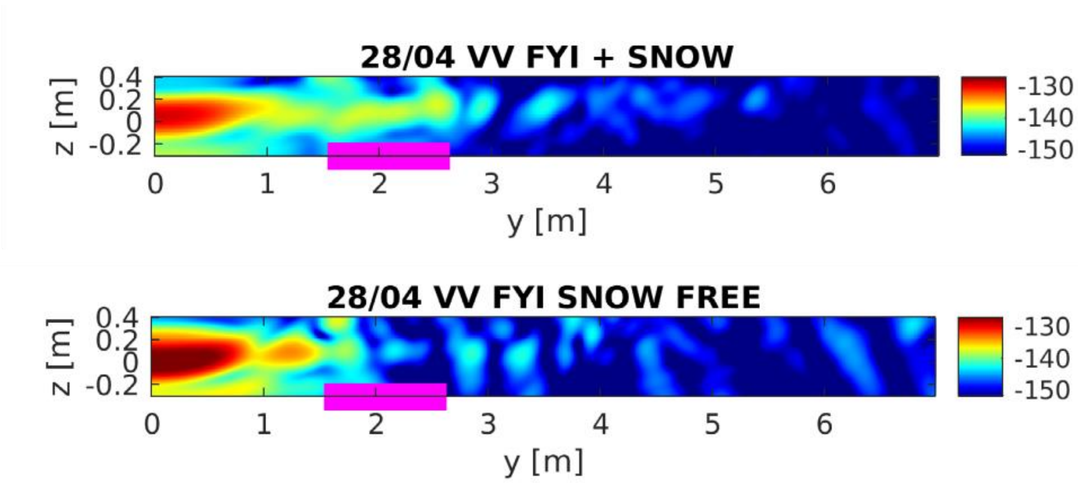

Figure 2.6.3 *Tomograms of FYI before and after the removal (shovelling) of the overlying snow cover. The magenta segment indicates the range domain corresponding to incidence angles covered by the S1 spaceborne sensor.*

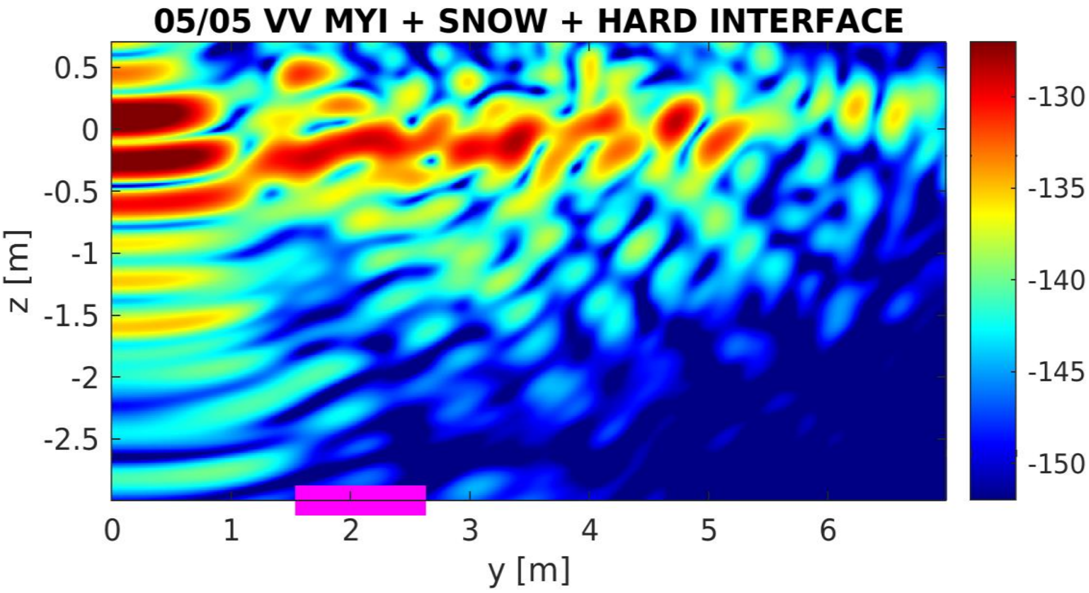

Figure 2.6.4 *Tomogram of MYI covered by a dense and hard ice/snow layer The magenta segment indicates the range domain corresponding to incidence angles covered by the S1 spaceborne sensor.*

A second case study, illustrated in Fig. 2.6.4 concerns MYI, with a thin layer (approx. 5 – 10 cm thick) of very dense and hard ice and snow particles located between the upper snow volume and the bottom sea ice. The tomogram of Fig. 2.6.4 clearly demonstrates the preponderant contribution of the rough layer to the global response, as well as the deep penetration of C-band EM waves in the ice volume, leading to significant scattering levels related to the presence of air bubbles.

2.7. Sea ice mass balance buoys

Team: Polona Itkin (UiT), Jack Landy (UiT) and Christian Zoelly (NPI)

Five sea ice mass balance buoys (SIMBAs) from SAMS Enterprise and three surface velocity profilers (SVPs) from MetOcean were deployed on landfast sea ice floes within 5 km of the three main (south, middle, and north) fast ice stations. Ancillary observations were collected at ice floes alongside the deployments, including: snow depth and properties, sea ice freeboard and thickness, and sea ice cores for archive at NPI. Transects of total thickness (snow depth + ice thickness) were made using the GEM system (see Section 2.5) along snowmobile routes too and at the deployment sites.

2.7.1 SIMBAs

Each SIMBA unit consists of a control box, mounted inside a Pelican Case, connected to an Iridium modem and a Lithium-Ion battery pack. A 4.8 m length chain of thermistors, spaced at 2 cm intervals, is attached to the control box through the wall of the case and lowered into a 2” auger hole made through the snow and sea ice cover (see Fig. 2.7.1 below). A weight is attached to the lower end of the chain to keep the chain vertical. The case is fixed onto a PVC platform frozen ~50 cm into the sea ice. The upper end of the chain is fixed to the platform so that 10-20 thermistors remain above the snow to give observations of air temperature or snow temperature after new snowfall. An air temperature sensor on a separate cable is attached to a pole drilled into the sea ice and sits ~50-80 cm above the snow surface.

Figure 2.7.1 *SIMBA deployments. (Left) drilling the 2” hole for fixing the thermistor chain in the sea ice, and (right) the final SIMBA unit sitting on a platform frozen into the ice with an air temperature sensor fixed onto a pole next to the unit. Photos: Christian Zoelly (NPI).*

The SIMBA was initially programmed to acquire a full profile of temperature readings every 6 hours, a heating cycle every 24 hours and a GPS position every 12 hours. *The sampling interval is likely to be shortened after returning from the cruise to produce higher temporal resolution data, for a shorter (3-6 month) buoy lifetime.* In the heating cycle, thermistors are heated slightly and the unit monitors how long temperatures take to return to levels prior to heating. Since the thermal conductivities of air, snow, sea ice and ocean water are very different, the conductivities measured during the heating cycle provide estimates for the upper and lower interfaces of the sea ice profile, thereby monitoring the ice mass balance over time.

An example for the temperature profiles recorded at one SIMBA (AWI-09-01, deployed at the lower (S) fast ice station) in the eight days following deployment is shown below in Fig. 2.7.2. It is clear from the temperature profile that the thermistor chain froze into the ice within two days of deployment and that air temperature fluctuations were transmitted through the upper 20-40 cm of the ice cover.

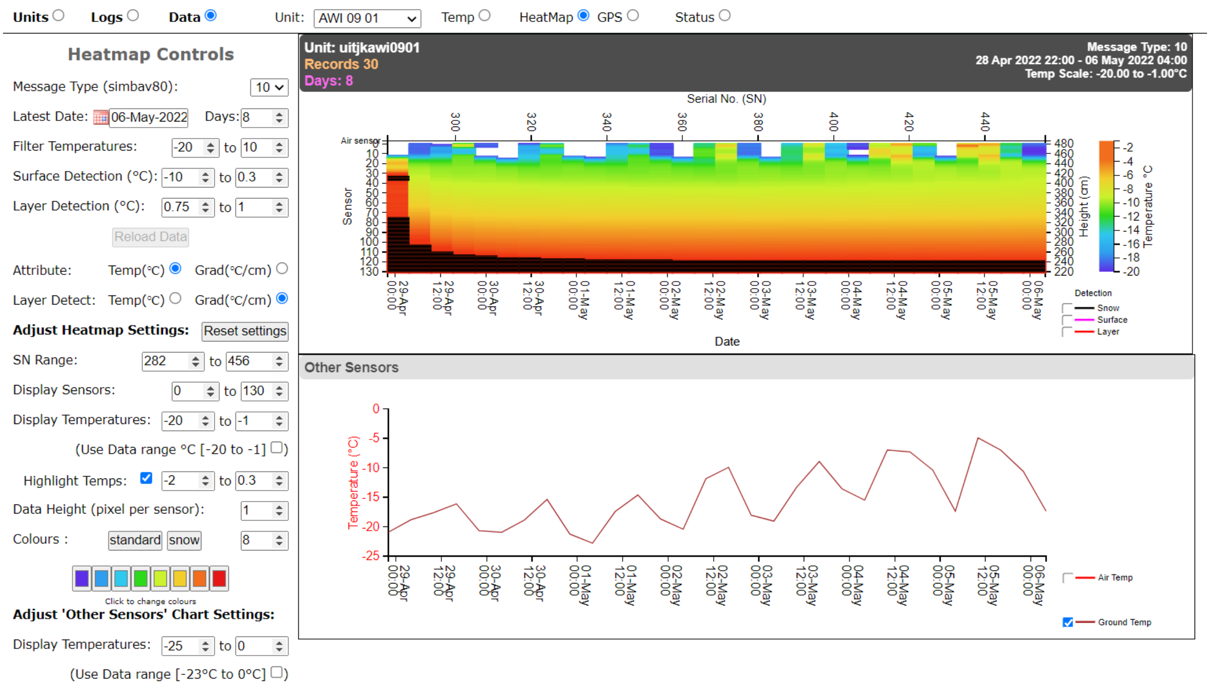

__Figure 2.7.2__ Example readout from the SAMS Web Interface for SIMBA AWI-09-01, showing in the upper plot the sea ice temperatures logged over 8 days following deployment and in the lower plot the air temperature. The black region of the heatmap highlights the interface between sea ice and ocean, illustrating the freeze up of the thermistor chain after deployment. All data from the SIMBA are transmitted via Iridium.

2.7.2 SVPs

Each SVP includes a GPS and temperature sensor connected to an Iridium modem and mounted inside a waterproof ruggedized buoy. The SVPs transmit GPS recordings every 60 minutes. The SVPs were all deployed on landfast sea ice floes within 2 km of SIMBA locations to provide more information on the sea ice drift and deformation after fast ice breakup. Battery life in the SVPs is expected to be much longer than the regular drifters (see Section 2.8) so by deploying them on the fast ice we could monitor breakup and drift patterns for months after the cruise.

2.7.3 Additional observations at buoy locations

A set of ancillary snow and sea ice parameters were collected alongside buoy deployments; however, the exact set varied with each deployment, as listed in the table below.
Spot measurements of sea ice thickness (SIT), sea ice freeboard (FB), and snow depth (SD), were collected at 2” auger drill holes close to and/or at the buoy deployment locations. These measurements were taken with an ice thickness measuring tape and snow probe. Further observations of the local snow depth distribution (SDD) were collected with a snow probe from 25-25 sample points within ~50 m of the buoy.

Snow properties including density profiles (DENS), salinity observations from the bulk snowpack and 3 cm layer above the snow-ice interface (SAL), and snow water equivalent (SWE) were also acquired within ~10 m of buoy deployment locations. Full details of the instruments and methods used to acquire snow observations are provided in Section 2.3. Here, a short summary is presented: Snow layer-wise density estimates were collected with a 3 cm deep, 100 cm^3 density cutter and weighed onsite. Bulk and interface snow samples were bagged onsite, melted back at the ship and measured for salinity with a conductivity meter. A SWE corer was used to collect bulk snow cores, with the volume and weight of the sample measured onsite.

Sea ice cores (CORE) were collected at some buoy deployment sites for later analysis. Only a single full sea ice core was collected at each location, principally for analysing ice salinity, oxygen isotope content and potentially ice density. Full details of the instruments and methods used to acquire sea ice cores are provided in Section 2.1. Sea ice cores from buoy deployment sites were immediately bagged and transported frozen to the ship for archive. Archived cores were labelled with information on the deployment site, sea ice type and extraction details, and then shipped to NPI for future analysis.

2.7.4 Sea ice thickness transects from the GEM-2 system

Total snow plus ice thickness transects were made using the GEM-2 system (see Section 2.5) towed behind a snowmobile on the way to and from buoy deployment locations.

Table 2.7.1 *SIMBA and SVP deployment locations. Codes for instruments deployed/data collected: SIMBA = sea ice mass balance buoy, SVP = surface velocity profiler, SIT = sea ice thickness, FB = freeboard, SD = snow depth, SDD = snow depth distribution, SWE = bulk snow water equivalent estimate, SAL = snow salinity measurements, DENS = snow density measurements, CORE = sea ice core.*

Station #	**Date dd/mm/yyyy**	**Latitude**	**Longitude**	**Time (UTC)**	**Comments**
CIRFA22-024B	28/04/22	78.72041	-12.14769	16:45	SIMBA #1 (NPI0801). SIT, FB, SD. SDD. SWE. DENS. SAL. FYI CORE.
CIRFA22-024B	28/04/22	78.6916	-12.0771		SIMBA #2 (AWI0901). SIT, FB, SD. SAL. MYI CORE
CIRFA22-034A	01/05/22	79.17252	-8.90594		SIMBA #3 (FMI0705). SIT, FB, SD. SDD. SWE. SAL. MYI CORE.
CIRFA22-034A	01/05/22	79.173139	-8.855991	22:38	SWE. SIT, FB, SD. SAL. FYI CORE.
CIRFA22-034A	01/05/22	79.186604	-8.83009	23:45	SVP #1. SDD.
CIRFA22-034A	02/05/22	79.196115	-8.832709	00:42	SVP #2. SDD.
CIRFA22-038A	03/05/22	79.90455	-8.94553		SIMBA #4 (FMI0501). SIT, FB, SD. SDD. SWE. SAL.
CIRFA22-038A	03/05/22	79.89833	-8.917		SIMBA #5 (AWI0902). SIT, FB, SD. SDD. SWE. SAL.
CIRFA22-038A	03/05/22	79.91313	-8.88268	13:02	SVP #3. SDD. SWE. SAL.

2.8. Sea-Ice and Iceberg Drifters

Team: Catherine Taelman (UiT), Malin Johansson (UiT), Johannes Lohse (UiT), Jack Landy (UiT), Polona Itkin (UiT), Anna Telegina (UiT), Eduard Khachatrian (UiT), Edel Rikardsen (MET), Wolfgang Dierking (AWI/UiT) and Laust Færch (UiT)

A total of 20 drifters were built for the cruise. Of these, 17 were deployed on sea-ice, while the remaining 3 were deployed on icebergs. The sea-ice drifters collect position data via GNSS every 30 minutes and record the wave spectrum for a duration of 20 minutes every 3 hours.

For the 3 iceberg drifters deployed on icebergs, a distinction was made between 'grounded iceberg drifters' and 'floating iceberg drifters'. Their hardware design is identical, but the software differs. The grounded iceberg drifters (2 drifters) collect position data via GNSS every 12 hours, while the floating iceberg drifter (1 drifter) collects position every 30 minutes. The reasoning behind this different position sampling rate is that the grounded icebergs might only start moving weeks after deployment, and hence a lower sampling rate is preferred in order to extend the battery lifetime. None of the iceberg drifters is recording wave spectra due to weight restrictions related to the deployment by drone.

All information collected by the drifters is sent out via Iridium and retrieved on our user account on the Rock7 website (https://rockblock.rock7.com/Operations).

Instrument description

The instruments were built after the open-source buoy design proposed by Jean Rabault et al.: "OpenMetBuoy-V2021: an easy-to-build, affordable, customizable, open-source instrument for oceanographic measurements of drift and waves in sea ice and the open ocean." Geosciences (2022). The components list and assembly manual is openly available on GitHub: https://github.com/jerabaul29/OpenMetBuoy-v2021a. The 20 drifters for this cruise were built at UiT in Tromsø by Sveinung Olsen and Catherine Taelman (Fig. 2.8.1).

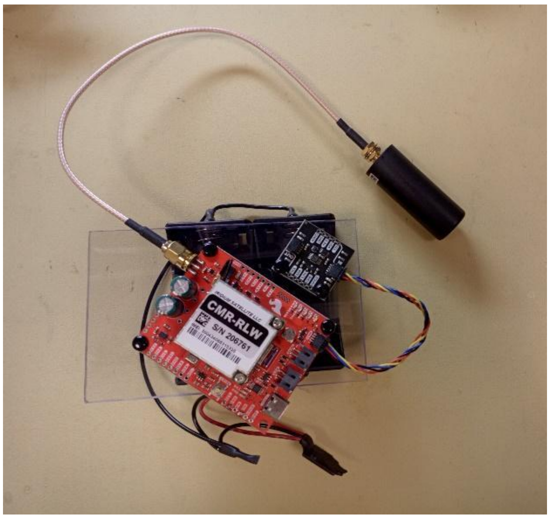

Figure 2.8.1 *Hardware assembly in progress: Arduino board with built-in Iridium modem, switch for wave sensor, antenna and battery casing. Note that the wave sensor is not connected yet in this picture. Photo: Catherine Taelman (UiT).*

The hardware components, antenna and battery pack (2 Lithium batteries) are fitted into a plastic box of size 12x12x9 cm. The iceberg drifters have slightly smaller boxes and no wave sensor, due to the (initial) weight restrictions for flying them by drone.

<u>Deployment modes</u>
Two deployment modes were used: manual deployment and deployment by drone.
15 out of 17 sea-ice drifters were deployed manually, the remaining 2 out of 17 by drone. All 3 iceberg drifters were deployed by drone. Sites of deployment are provided in Table 2.8.1 below.

Manual deployment
Most manual deployments took place around 50 m away from ship, by two scientists who were craned down onto the ice and walked a short distance off the ship to avoid positioning the drifter too close to the crack made by the ship. For the manual deployment, a setup was designed to fix the drifter into the sea-ice. A 50 cm long PVC pipe was attached underneath the drifter via metal hooks. This pipe was frozen into the sea-ice by putting it into a drilled hole that is filled up with water (Figs. 2.8.2 and 2.8.3).

Figure 2.8.2 *A sea-ice drifter frozen into the ice at the starboard side of the ship. Photo: Johannes Lohse (UiT).*

Figure 2.8.3 *PVC pipe setup to freeze the drifter into the ice: materials (left) and prototype (right). Photos: Catherine Taelman (UiT).*

Drone deployment
Five drifters were deployed by drone (Fig. 2.8.4). A setup with fishing wire and a key ring was designed such that the drifter hangs approx. 5 m underneath the drone during the flight. To avoid the drifter from sinking into deep snow and/or sliding on icy surfaces at the deployment site, a styrofoam base ring with metal spikes and screws underneath was attached around the drifter using tape (Fig. 2.8.5).

Figure 2.8.4 *Drone deployment of an iceberg drifter. Photos: William Copeland (MET).*

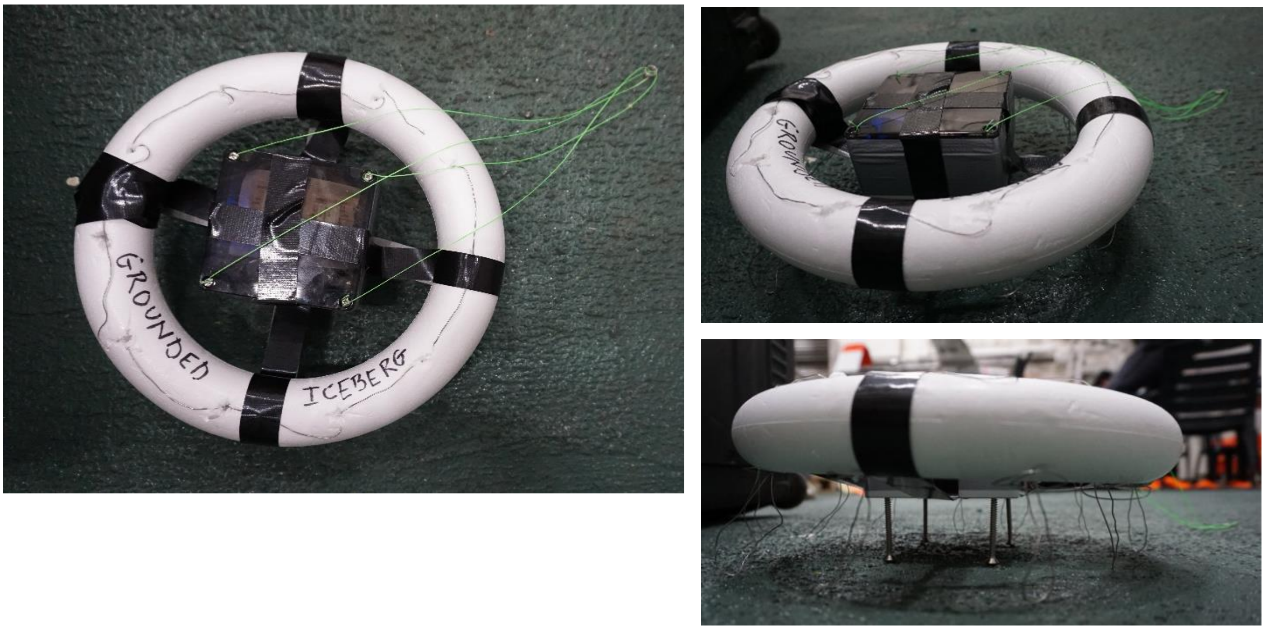

***Figure 2.8.5** Iceberg drifter setup in top view: ring around drifter box and wires to attach it to the drone. Iceberg drifter setup in side view: metal 'spikes' and screws underneath the ring and drifter box. Photos: Catherine Taelman (UiT).*

***Table 2.8.1** Sites of deployment.*

Station #	Drifter S\N	Date dd/mm/yyyy	Time (UTC)	Lat	Long	Comments
CIRFA22-010	206794	24/04/2022	20:30	N 78˚48.258'	W 03˚04.532'	
CIRFA22-011	206809	25/04/2022	08:47	N 78˚45.612'	W 03˚59.701'	Stopped data transmission
CIRFA22-014	206764	25/04/2022	17:00	N 78˚49.611'	W 06˚01.070'	
CIRFA22-016	206770	26/04/2022	10:07	N 78˚40.210'	W 08˚15.752'	
CIRFA22-017	206810	26/04/2022	12:28	N 78˚39.908'	W 08˚20.115'	
CIRFA22-018	206759	26/04/2022	13:33	N 78˚39.949'	W 08˚25.785'	
CIRFA22-019	206754	26/04/2022	14:43	N 78˚41.495'	W 08˚35.656'	
CIRFA22-032	206800	30/04/2022	13:00	N 79˚08.350'	W 09˚13.150'	Grounded iceberg drifter, deployed by drone
CIRFA22-032	206801	30/04/2022	13:15	N 79˚08.400'	W 09˚15.630'	Grounded iceberg drifter, deployed by drone
CIRFA22-035	206812	02/05/2022	11:25	N 79˚09.219'	W 07˚55.493'	
CIRFA22-036	206771	02/05/2022	14:04	N 79˚10.462'	W 07˚52.284'	
CIRFA22-037	206822	02/05/2022	15:30	N 79˚11.309'	W 07˚47.899'	
CIRFA22-037	206761	02/05/2022	15:10	N 79˚12.317'	W 07˚45.230'	Deployed by drone on ice floe
CIRFA22-040	206804	03/05/2022	17:30	N 79˚10.171'	W 08˚54.349'	Floating iceberg drifter,

						deployed by drone
CIRFA22-046	206769	04/05/2022	14:41	N 79˚47.583’	W 06˚40.060'	
CIRFA22-046	206811	04/05/2022	17:00	N 79˚47.397’	W 06˚38.706'	Deployed by drone on ice floe. Stopped transmitting.
CIRFA22-047	206766	05/05/2022	11:23	N 79˚44.495'	W 06˚21.867'	
CIRFA22-051	206755	06/05/2022	11:28	N 78˚55.207’	W06˚32.392’	
CIRFA22-052	206799	06/05/2022	13:05	N 78˚54.240’	W06˚29.120’	
CIRFA22-053	206797	06/05/2022	14:42	N 78˚55.172'	W06˚22.042'	

Auxiliary data: snow and ice measurements at sea-ice deployment sites

The following parameters were recorded at deployment sites:

- Ice thickness
- Snow depth (30 stake measurements)
- Salinity of snow-ice interface samples (0-3 cm and 3-6 cm)
- Snow water equivalent (SWE)
- Salinity ice core (only at stations CIRFA22-051, CIRFA22-052, CIRFA22-053)

Preliminary example of drift data

Figure 2.8.6 below shows a screenshot of QGIS showing the path of 5 sea-ice drifters deployed with small spatial gaps:

Figure 2.8.6 *Examples of drift patterns. The four drifters deployed in array configuration were spaced 2-3 km apart from each other at the start.*

2.9. Icebergs

Team: Laust Færch (UiT) and Wolfgang Dierking (AWI/UiT)

The iceberg observations that were performed as part of the CIRFA Cruise 2022 will be used to clarify how different types of icebergs appear in satellite images, especially in Synthetic Aperture Radar (SAR) imagery, and might help to explain some artefacts that are observed for some icebergs when imaged at a specific wavelength.
A catalogue was established that relates photographs of icebergs along the ship track (an example is shown in Fig. 2.9.1) to Sentinel-2 imagery (Figure 2.9.3). In total, the catalogue contains 114 individual icebergs and 208 photographs. Each iceberg observation listed in the catalogue includes geographical coordinate, photograph(s), and iceberg type according to Table 2.9.1 and Fig. 2.9.2 below.

Figure 2.9.1 *Photograph ('DSC_1070') of iceberg with the ID '56'. This iceberg was classified as 'pinnacled'.* Photo: Laust Færch (UiT).

Only stationary icebergs are considered in the dataset. This includes icebergs that are grounded but surrounded by open water, and icebergs that are grounded or otherwise stuck in the fast ice. By knowing the location and approximate heading of the ship it was possible to match icebergs observed from the observation deck with icebergs that could be identified in Sentinel-2 images acquired prior to the cruise. Icebergs that were not visible in the Sentinel-2 image and icebergs that could not accurately be matched to the Sentinel-2 image were ignored. This means that only icebergs that remained stationary between satellite data acquisition and observation from the ship and were close to the ship route are included in the dataset. Additionally, in some areas with a high density of icebergs, larger icebergs close to the ship shadowed smaller icebergs hiding behind them, hence making observations impossible.

To ensure an accurate dataset, the optical satellite images were carefully inspected to aid the iceberg identification. Here, the approximate size, shape, and orientation of the icebergs in the satellite images were considered, when trying to match icebergs in the images with the icebergs observed from the ship. The optical satellite images used were from Sentinel-2 with timestamps ‘20220326T145831’, and ‘20220416T142751’.

If possible, iceberg observations were accompanied by one or more photographs. In some cases, it was possible to acquire photographs from different angles, while in others it was not possible to acquire any photograph at all. All photographs were taken from the observation room and surrounding outdoor platform on deck 9 of the ship. The height of deck 9 is approximately 20.5 meters above sea level.

The camera used was a NIKON D850. Two different optics were used for close distance and far distance, respectively. The close distance optic was of the type AF-S Nikkor 24-120 mm 1:4G (zoomable). The far distance optic was of the type AF Nikkor 300 mm 1:4 (not zoomable). For each image the focal length and F-stop of the camera is saved in the image metadata, and can be accessed later for post-processing purposes.

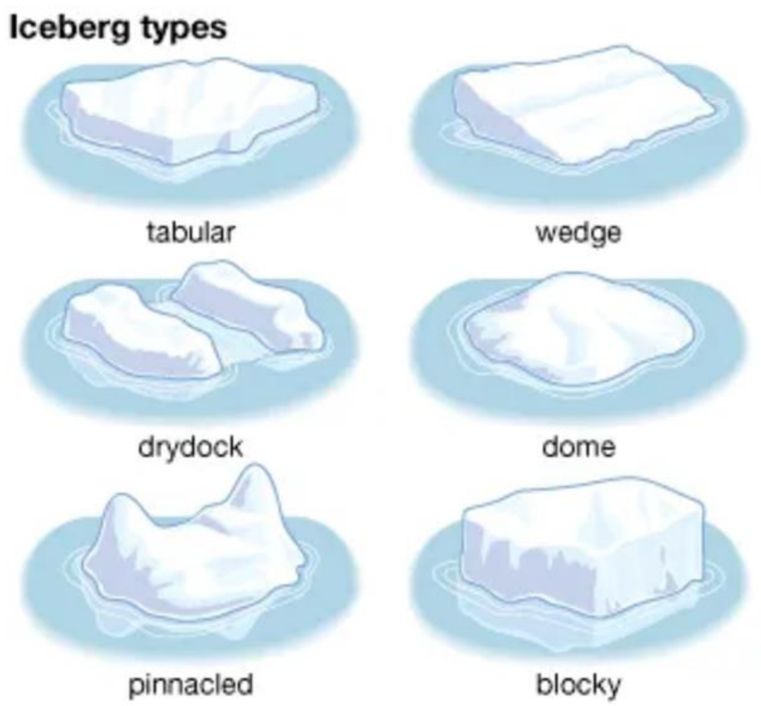

Figure 2.9.2 *Iceberg types according to* the WMO Sea Ice Nomenclature*. From Encyclopædia Britannica (https://www.britannica.com/science/iceberg/Iceberg-size-and-shape).*

Table 2.9.1 *Iceberg types and their corresponding ID in the shapefile.*

Iceberg Type	ID
Tabular	1
Wedge	2
Drydock	3
Dome	4
Pinnacled	5
Blocky	6
Irregular	7
Unknown	0

Each observed iceberg was categorised into one of the types listed in Table 2.9.1, which correspond to the iceberg types found in the WMO Sea Ice Nomenclature (see Figure 2.9.2). Additional to the six iceberg types outlined here, two additional classes were considered. The 'irregular' class exhibited a mixture of the different iceberg classes and 'unknown' indicates that a classification was not possible. The type classification is inherently subjective and might be erroneous, especially when considering the observations were done through binoculars, over long distances, and from a moving vessel. For this reason, photographs were included in the dataset whenever possible.

Table 2.9.2 *Contents of the shapefile.*

ID	**Type**	**DSC_id**	**Centroid**	**Comments**
Number	Number	Number(s)	Point	String
Unique ID for each iceberg	Iceberg Type	Unique ID for each image of the iceberg	Geometry centroid coordinate of the iceberg	Additional comments made during observation

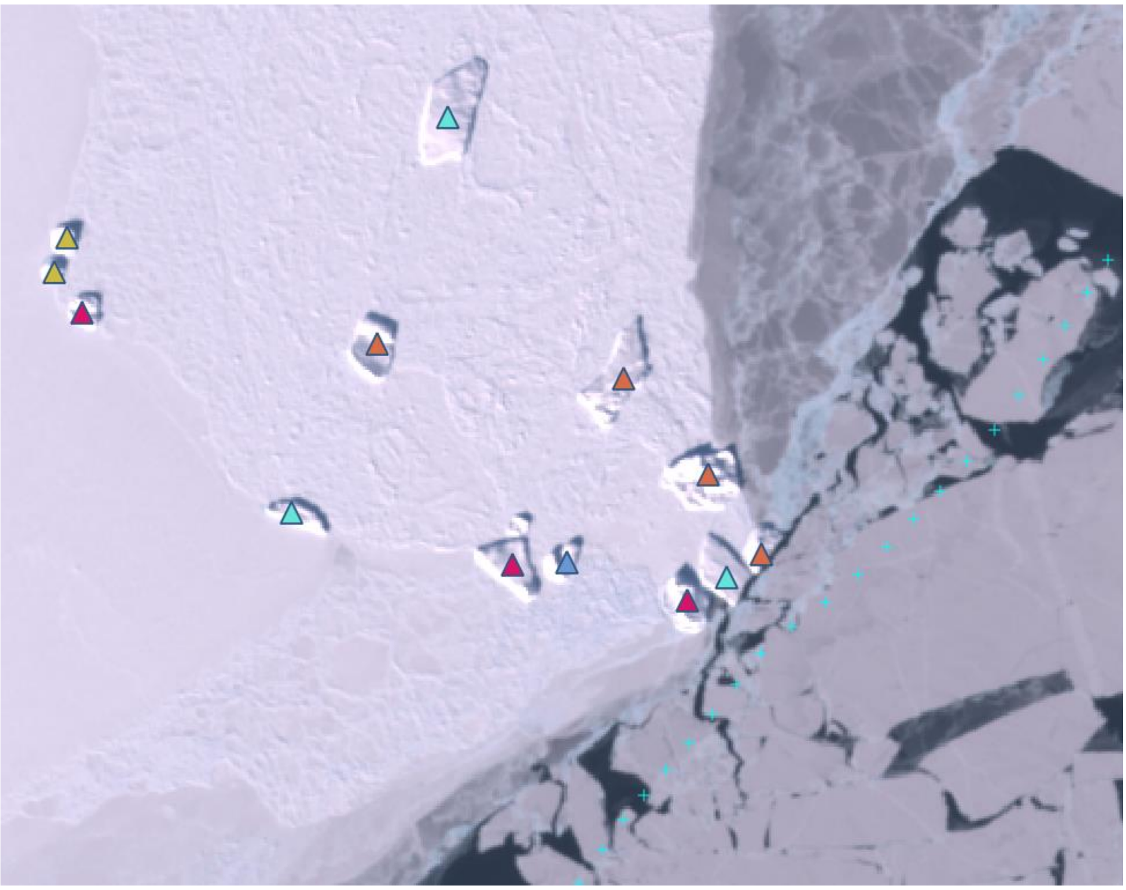

Figure 2.9.3 *Visualisation of the dataset. Each triangle represents a single iceberg observed from the observation deck. The colour of the triangle represents the iceberg type. The cyan crosses represent the ship track. Background layer from Sentinel-2.*

The GPS track of the ship, together with the timestamp of the images, offers the possibility to later geolocate each image acquired. The timestamps of the photographs and the timestamps of the GPS track are both in UTC format.
Each iceberg was given a unique ID. The ID and corresponding iceberg type, coordinate and image ids are all stored in a shapefile. Individual photographs are stored in an accompanied folder. The photographs have yet to be sorted and catalogued for the individual icebergs, and as such, more than 208 images are included in the folder currently. Comments made during observations are also included in the shapefile. A visualisation of the dataset over a small subset of the area covered in the data is shown in Fig. 2.9.3. A description of the shapefile is provided in Table 2.9.2

2.10a. Satellite images

Team: Malin Johansson (UiT), Nick Hughes (MET) and Wolfgang Dierking (AWI/UiT)

In total 86 satellite images were ordered or are freely available to cover the area traversed during the cruise. Only one acquisition was cancelled, all other images were acquired. For the cruise, images were ordered from the following satellites:

- Sentinel-1 (EW)
- ALOS-2 (ScanSAR, SM2, SM3 and Fully polarimetric)
- Radarsat-2 (ScanSAR and Fully polarimetric)
- Iceye-X (Stripmap)
- TerraSAR-X (ScanSAR)
- Cosmo Skymed (Hugeregion and Himage)

An overview of each of the different sensors is given below. UiT placed the orders for the ALOS-2, Radarsat-2 and TerraSAR-X images, and Met.Norge the ones for Iceye-X and Cosmo Skymed.

Satellite type	**Satellite mode**	**Polarization**
Sentinel-1	Extra Wide (EW)	HH + HV
ALOS-2	High sensitive [6m] Quadpol (HBQ)	HH+HV+VH+VV
ALOS-2	StripMap (Fine [10m]) (SM)	HH + HV
ALOS-2	ScanSAR	HH + HV
Radarsat-2	ScanSAR	HH + HV
Radarsat-2	Fine Quadpol (FQ)	HH+HV+VH+VV
Iceye-X	Stripmap	VV
TerraSAR-X	ScanSAR	HH
Cosmo Skymed	Hugeregion	HH
Cosmo Skymed	Himage	HH

Sentinel-1 – 15 EW

Date	**Time (UTC)**	**Mode**	**Comment**
23/04/2022	08:10	EW	
24/04/2022	07:12	EW	Drift ice
25/04/2022	07:53	EW	
26/04/2022	06:56	EW	Drift ice

27/04/2022	07:37	EW	Fast ice, S station just included
28/04/2022	08:18	EW	Fast ice
29/04/2022	07:21	EW	Drift ice
30/04/2022	08:01	EW	Fast ice
30/04/2022	17:47	EW	Fast ice, only southern part
02/05/2022	07:45	EW	
03/05/2022	08:26	EW	
04/05/2022	07:29	EW	
05/05/2022	08:10	EW	
07/05/2022	07:53	EW	
08/05/2022	06:56	EW	

ALOS-2 – 10 HBQ, 7 SM, 3 ScanSAR. ScanSAR images cover the whole Belgica Bank area.

Date	Time (UTC)	Mode	IA	Comment
18/04/2022	23:16	HBQ	28	South
24/04/2022	14:06	ScanSAR	35	
25/04/2022	14:26	ScanSAR	35	
26/04/2022	13:10	SM3	48	Belgica Bank
26/04/2022	22:49	HBQ	35	Belgica Bank
28/04/2022	13:52	SM2	28	
29/04/2022	14:13	SM3	33	
30/04/2022	14:34	SM3	28	
01/05/2022	13:17	SM3	46	
01/05/2022	22:56	HBQ	28	Station M
02/05/2022	23:17	HBQ	30	
03/05/2022	13:59	SM3	36	
04/05/2022	22:22	HBQ	30	
05/05/2022	22:43	HBQ	30	Drift station CIRFA22-047 and basket station CIRFA22-048.
06/05/2022	23:03	HBQ	30	Station M
07/05/2022	13:45	ScanSAR	35	
07/05/2022	23:24	HBQ	30	Station S
08/05/2022	14:06	SM3	34	
09/05/2022	22:28	HBQ	30	Drift ice
10/05/2022	22:49	HBQ	30	Station N

Radarsat-2 – 9 ScanSAR, 20 Fully polarimetric. ScanSAR images cover the whole Belgica Bank area and specifics are given for the fully polarimetric images

Date	Time (UTC)	Mode	IA	Beam	Comment
11/04/2022	07:33	QP	43	FQ24	Station N
11/04/2022	07:34	QP	42	FQ23	Station M
11/04/2022	17:32	QP	36.60	FQ17	Station S
25/04/2022	17:25	ScanSAR			

27/04/2022	08:07	ScanSAR			
27/04/2022	16:26	QP	25.91	FQ7	Station N old
28/04/2022	07:38	QP	43.79	FQ25	Station S
28/04/2022	17:37	ScanSAR			
29/04/2022	08:48	ScanSAR			
29/04/2022	17:07	QP	29.32	FQ10	Station S
30/04/2022	08:20	ScanSAR			
30/04/2022	16:38	QP	24.73	FQ6	Station M
01/05/2022	07:48	ScanSAR			
01/05/2022	17:49	QP	41.23	FQ22	Station S
02/05/2022	17:20	QP	32.56	FQ13	Station S
03/05/2022	08:32	ScanSAR			
03/05/2022	16:50	QP	29.32	FQ10	Station M
04/05/2022	08:03	QP	34.62	FQ15	Station M
04/05/2022	08:03	QP	36.60	FQ17	Station S
05/05/2022	07:34	ScanSAR			
05/05/2022	17:32	QP x 2	43.79	FQ25	Station N
06/05/2022	07:04	QP	48.46	FQ31	Station N
06/05/2022	08:44	QP	23.54	FQ5	Station N
06/05/2022	17:01	QP	36.2	FQ16	
06/05/2022	17:01	QP	36.60	FQ17	Station N
07/05/2022	08:16	QP	31.50	FQ12	Station N
07/05/2022	08:16	QP	27.06	FQ8	Mooring site
08/05/2022	07:46	ScanSAR			

Iceye-X – ordered by Met – 6 Stripmap

Date	**Time (UTC)**	**Mode**	**IA**	**Comment**
26/04/2022	00:42	Stripmap	23	Station M
26/04/2022	00:54	Stripmap	19	Station N old
26/04/2022	14:57	Stripmap	15	Station S
07/05/2022	06:58	Stripmap	25	Station S
07/05/2022	19:08	Stripmap	29	Station N old
07/05/2022	22:16	Stripmap	29	Station M

TerraSAR-X -12 ScanSAR. ScanSAR images cover the whole Belgica Bank area.

Date	**Time (UTC)**	**Beam**	**IA**	**Comment**
01/04/2022	16:59	Scan_009R	38	
27/04/2022	17:25	Scan_011R	42	
28/04/2022	17:07	Scan_010R	40	
29/04/2022	16:50	Scan_008R	35	
01/05/2022	08:27	Scan_006R	31	
02/05/2022	08:09	Scan_009R	36	
02/05/2022	17:33	Scan_011R	42	

03/05/2022	07:52	Scan_011R	42	
04/05/2022	07:35	Scan_011R	42	
04/05/2022	16:59	Scan_010R	38	
05/05/2022	16:42	Scan_008R	35	
08/05/2022	08:01	Scan_008R	35	

Cosmo Skymed. Hugeregion images cover the whole Belgica Bank area.

Date	Time (UTC)	Mode	IA	Comment
25/04/2022	04:44	Himage		Fast ice south
25/04/2022	20:18	Himage		Fast ice middle
25/04/2022	20:42	Himage		Fast ice north
26/04/2022	05:32	Hugeregion	18	18.4 - 59.9 incidence angle
27/04/2022	06:14	Hugeregion	18	
28/04/2022	04:32	Hugeregion	18	
29/04/2022	04:50	Hugeregion	18	
30/04/2022	04:38	Hugeregion	18	
01/05/2022	04:38	Hugeregion	18	
02/05/2022	05:14	Hugeregion	18	
03/05/2022	06:02	Hugeregion	18	
04/05/2022	04:44	Hugeregion	18	
06/05/2022	04:50	Himage		Fast ice south
06/05/2022	19:12	Hugeregion	18	
06/05/2022	20:00	Himage		Fast ice middle
07/05/2022	05:08	Hugeregion	18	
08/05/2022	04:20	Himage		Fast ice north

There was no satellite altimetry data ordered/tasked during the CIRFA cruise. However, there are radar altimeter (CryoSat-2, Sentinel-3A, Sentinel-3B) and laser altimeter (ICESat-2) tracks available covering the region, over the period of the cruise.

2.10b. Satellite Data Transfer

Team: Johannes Lohse (UiT), Alistair Everett (MET) and Nick Hughes (MET)

During the cruise, satellite imagery was transferred to the ship in order to help with both route planning and navigation as well as the identification of interesting research areas for in-situ measurements.

The data transfer was organized and set up in collaboration with the Norwegian Ice Service at the Meteorological Institute (Met Norway). Images acquired in wide-swath mode were cropped to three regions of interest, centered around the planned positions of the fast ice stations south, middle, and north, respectively. Images with a smaller footprint were geo-coded and made available at full coverage.

In addition to the original imagery, results of automated ice type classification from Sentinel-1 were transferred to the ship for direct validation. To make images and results available as fast as possible, the classification algorithm was set up directly at Met Norway.

Both the original imagery as well as the classification results were made available on an ftp server at different spatial resolutions. Image compression was applied in order to keep file sizes at a maximum of 5 Mb, but ideally below 1Mb for coarse resolution. The ftp server could be accessed from the ship and, depending on the internet access at the current location, the appropriate resolution could be chosen and downloaded. A schematic of the sharing of code for classification and the data transfer to the ship for validation is shown in Figure 2.10b.1.

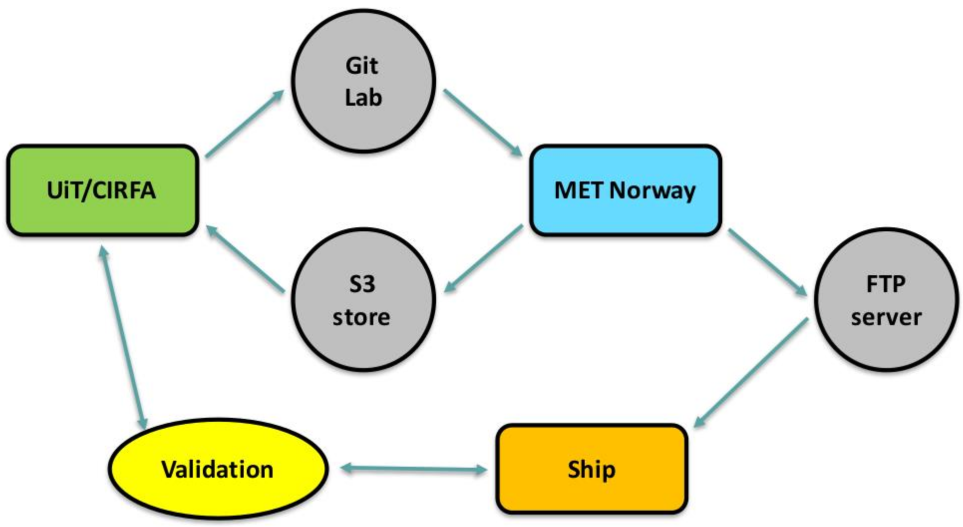

2.10b.1 *Schematic illustrating the sharing of classification code between UiT and Met Norway, as well as data transfer to the ship for validation.*

2.11. Ocean Drifters

Team: Knut-Frode Dagestad (MET), Martina Idžanović (MET), Edel Rikardsen (MET), Marina Durán Moro (MET), Jean Rabault Førland (MET) and Johannes Röhrs (MET)

A total of 15 drifters with custom design were built by Martina Idžanović and Jean Rabault Førland (MET). These are similar to the drifters built by Catherine Taelman (UiT) for sea ice and icebergs.

One drifter was equipped with a 1m large drogue anchor at 15m depth. A drogue extending to 1m was built for 14 of the drifters, but not used for deployment because the shipment of drogues did not arrive in Longyearbyen. Due to the lack of drouge, the drifters are more affected by wind (rule of thumb: ocean current + 3.5% of wind) as compared to drogued drifters (ocean current + 1% of the wind). For the purpose of validating the Barents EPS ocean model, this yields a lower signal to noise ratio. However, for the purpose of studying drift of objects in the ocean (e.g., person-in-water), the lack of drogues is not a drawback but provides more realistic drift properties.

The sea-ice drifters collect position data via GNSS every 30 minutes and record the wave spectrum for a duration of 20 minutes every 3 hours. All information collected by the drifters is transmitted via Iridium every 2 hours, but is stored onboard for later submission in case contact with a satellite cannot be established at the given time.

The goal of the deployment was to spread the drifters as much as possible in time and space with the model domain of the Barents-2.5 EPS, trying to avoid drifters stranding on land (e.g. on Svalbard) or drifting into the ice. Drift simulations prior and during the cruise were used to aid the selection of deployment locations.

Six drifters were deployed on the way from Longyearbyen (April 22 and 23), at longitudes of 12°E, 10°E, and 8°E, as well as at the first 3 planned CTD stations (2°E, 1°E, and 0°E). A CTD profile to at least 200m was recorded at each of the deployment locations. All six drifters were successfully transmitting their positions after deployment. The drifters deployed at 2°E and 0°E stopped transmitting after 63 and 37 hours, respectively. As these were the two westernmost drifters (the drifter deployed at 2°E had crossed the track of the drifter deployed at 1°E), one theory is that ice accretion (icing) may have occurred on the drifters (northerly wind 10m/s and -15°C). Another theory is that the drifters might have encountered an area of ice floes and had been crushed. Sea-ice concentration was less than 5% at the time of deployment (only a few smaller floes were observed).

On the way back from Belgica Bank, based on updated drift simulations, the plan was to deploy drifters each full degree of longitude from 3°E to 10°E, with an additional drifter with sail at 15m depth at 8°E. However, at 3°E and 4°E, sea-ice concentration was still around 90% due to prevailing north-westerly winds. These two drifters were therefore re-scheduled for deployments at 7.5°E and 8.5°E, along with planned CTD stations. The nine drifters were deployed on May 8 and were transmitting their positions successfully, as of the end of cruise (May 9).

The additional drifter deployed at 8°E was attached to a floating buoy, which again was attached with a line of 15m to a 1x1m cross-sail built by chipboard. Two bricks with weight of 5kg were attached to the sail to keep the cross-sail at (or close to) 15m depth. The aim was to measure the current/drift at 15m depth instead of the combination of currents, waves, and wind drift at the surface. During deployment, a strong shear in the upper ocean (about 2m significant wave height and 15m/s winds) tilted the sail sideways. It was observed to float horizontally instead of sinking to 15m depth as planned. The weight of the bricks is sufficient to keep the drifter at depth as long as it is upright (cross-shape as visible from above), but not sufficient to tilt the sail to upright position as long as it was lying horizontally in water, with one of the arcs of the crosses acting as a keel.

At the end of the cruise, it is however interesting to observe that the drift of this construction (sail+buoy+drifter+ropes) is nearly identical to the additional drifter deployed at the same time and location. This is an indication that the shape and size of a drifting object is of less importance than believed. This identical drift is clear evidence that the sail has not yet sunk, but a potential future sudden change in behaviour (clear inertial current motions and less correlation with wind) will be an indicator that the sail has sunk to its planned position.

Figure 2.11.1 shows the track of all drifters until the end of cruise (May 9). Table 2.11.1 gives an overview of drifter deployments.

Table 2.11.1 *Ocean-drifter deployments.*

Drifter ID	Deployment time	Deployment longitude	Deployment latitude
2022_CIRFA_JR_drifter_9_waves_ISM Serial no. 206763	2022-04-22 23:53:20	11.9815854	78.1378185
2022_CIRFA_JR_drifter_4 Serial no. 206663	2022-04-23 03:39:58	9.9322273	78.2291449
2022_CIRFA_JR_drifter_10_waves_ISM Serial no. 206671	2022-04-23 06:50:32	7.8959036	78.350701
2022_CIRFA_JR_drifter_14_waves_LSM Serial no. 207757	2022-04-23 16:04:24	2.0017341	78.8326382
2022_CIRFA_JR_drifter_11_waves_ISM Serial no. 206660	2022-04-23 19:55:29	0.9976129	78.8338178
2022_CIRFA_JR_drifter_6 Serial no. 206741	2022-04-24 01:43:21	0.1084796	78.8388671
2022_CIRFA_JR_drifter_8	2022-05-08 11:41:31	4.9900446	78.8387979
2022_CIRFA_JR_drifter_7	2022-05-08 13:50:49	6.1441467	78.8104722
2022_CIRFA_JR_drifter_13_waves_ISM Serial no. 203812	2022-05-08 14:32:50	6.9977633	78.8342176
2022_CIRFA_JR_drifter_2	2022-05-08 16:02:49	7.5585916	78.8350575
2022_CIRFA_JR_drifter_3	2022-05-08 17:28:25	7.9972335	78.8326891
2022_CIRFA_JR_drifter_15_waves_LSM	2022-05-08 17:28:28	7.9973702	78.8324469
2022_CIRFA_JR_drifter_1 Serial no. 203787	2022-05-08 19:13:29	8.5040078	78.8324251
2022_CIRFA_JR_drifter_5 Serial no. 206751	2022-05-08 21:53:20	10.0054384	78.8331541
2022_CIRFA_JR_drifter_12_waves_ISM	2022-05-08 22:08:22	9.0530851	78.8118567

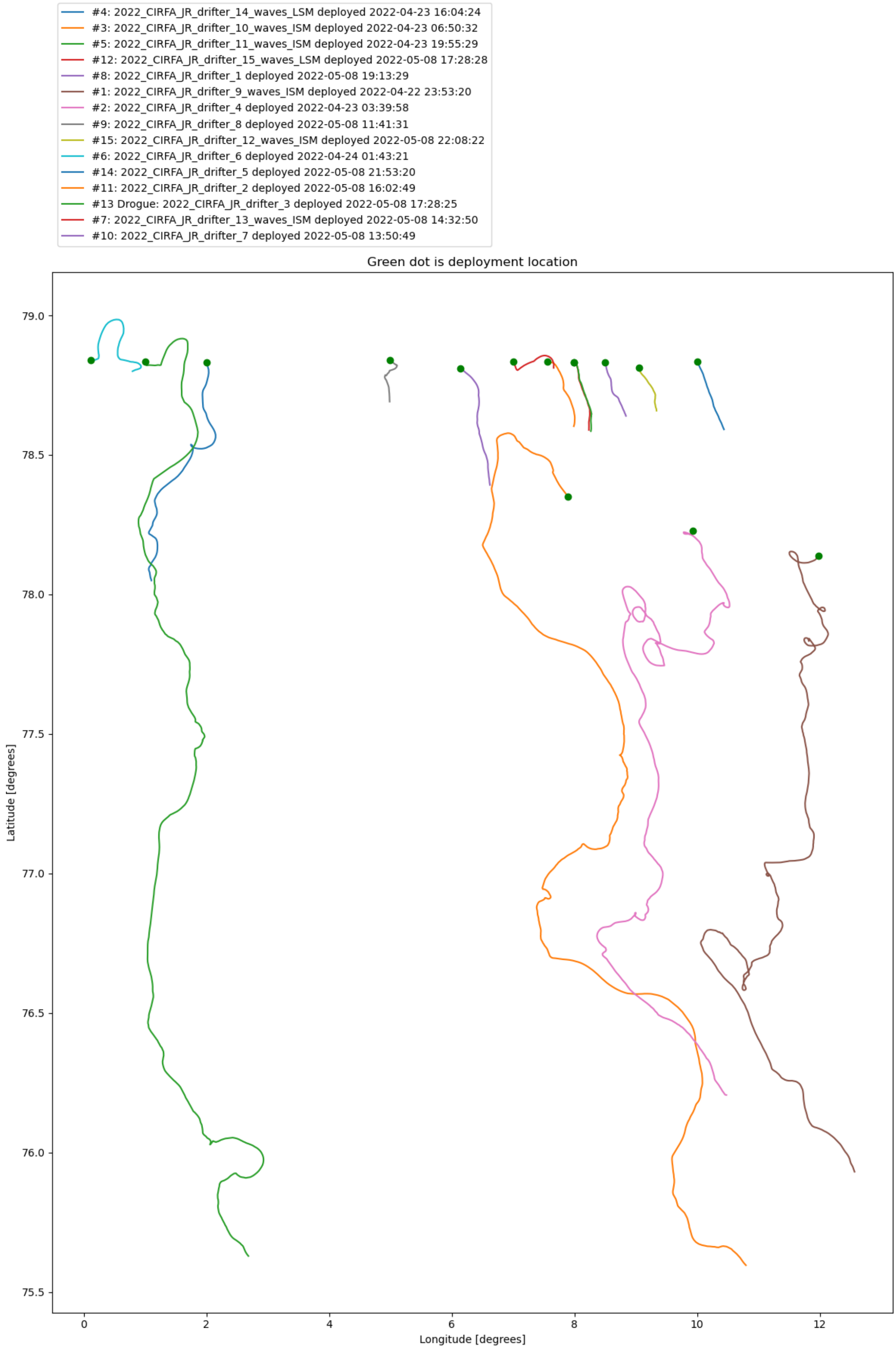

***Figure 2.11.1** Tracks of deployed ocean drifters on May 9. The green dots are deployment locations.*

2.12. Drone Operations

NORCE' Drone Operations

Team: Tom Rune Lauknes (NORCE), Agnar Sivertsen (NORCE), Rolf Ole Rydeng Jenssen (NORCE) and Tore Riise (NORCE)

The main objective of NORCEs part of the cruise was to collect observations of sea ice drift and ice coverage and type, at different positions both in drift ice and fast ice. Another goal of NORCE during this cruise was to demonstrate a real-time operational sea-ice navigation support system combining, sea-ice data from drones with ship-based radar and satellite SAR data. NORCE operated a suite of different unmanned aerial vehicle (UAV) systems, including multirotor, fixed wing, and vertical take-off and landing (VTOL) systems.

The main payload onboard the UAS systems were optical sensors, providing optical imagery, which is very valuable for validation purposes by providing information about ice morphology. One multirotor system was used to deploy ice drift buoys on icebergs. In addition, NORCE operated an ultra-wideband radar system on a multirotor UAS platform. The radar, can detect layers in the snow and ice and was operated along selected profiles where also snow and ice samples were collected. NORCE operated an imaging Ku-band (17 GHz) radar system. This radar was mainly operated during the periods where the vessel was stationary in the ice, providing valuable information about ice drift and ice conditions.

During the cruise, CIRFA tasked high-resolution satellite SAR scenes (Radarsat-2, Cosmo-SkyMed, IceEye) which were used during the cruise for navigation. The satellite SAR imagery was used to task and plan the daily UAS operations, and the NLive visualisation tool was used for both planning operation but also allowed cruise participants and crew on bridge to follow and interact with ongoing UAS operations.

1. Data Collection Systems

As part of the CIRFA cruise, NORCE operated six different Unmanned Aircraft Systems (UAS) and radar systems. All are described in this section. Data examples can be found in the next section.

Shark VTOL

The baby Shark VTOL drone is a fixed wing UAV manufactured by Foxtech (Figure 2.12.1). The UAV has a wing span of 2.5 m, a maximum takeoff weight of 13 kg with a payload capacity of 2.5 kg. The aircraft has been modified by NORCE with an improved GNSS system (simpleRTK3B Heading from Ardusimple), a 5.8GHz broadband radio (CRE2-144 by Radionor) and an optical payload developed by NORCE described below. The two antenna GNSS system provides accurate heading information to the autopilot, eliminating the need of a magnetometer and improving the overall accuracy of the direct georeferencing. The broadband radio has a range of 50 km with a bandwidth of up to 15 Mbit/s. The optical payload consists of one USB3.1 5 Mpix nadir camera with 8.5 mm lens (Flir Blackfly BFS51S5c) and one USB3.1 5 Mpix forward looking camera with 8.5 mm lens (Ximea, MX050CG_SY_X2G2). The forward-looking camera sees approximately 5 degrees above the horizon while the aircraft flies straight and level. Each camera is controlled by a Raspberry pi 4 compute module mounted on a custom carrier card (Figure 2.12.2), providing automatic exposure control and georeferencing the images in real time before sharing the images with the ground station and the Nlive server.

Figure 2.12.1 *Left: The baby shark photographed at the helicopter deck of Kronprins Håkon during the CIRFA 2022 cruise. Right: The Dji matrice 210 RTK and the DroMight Talon drop kit used for buoy deployment.*

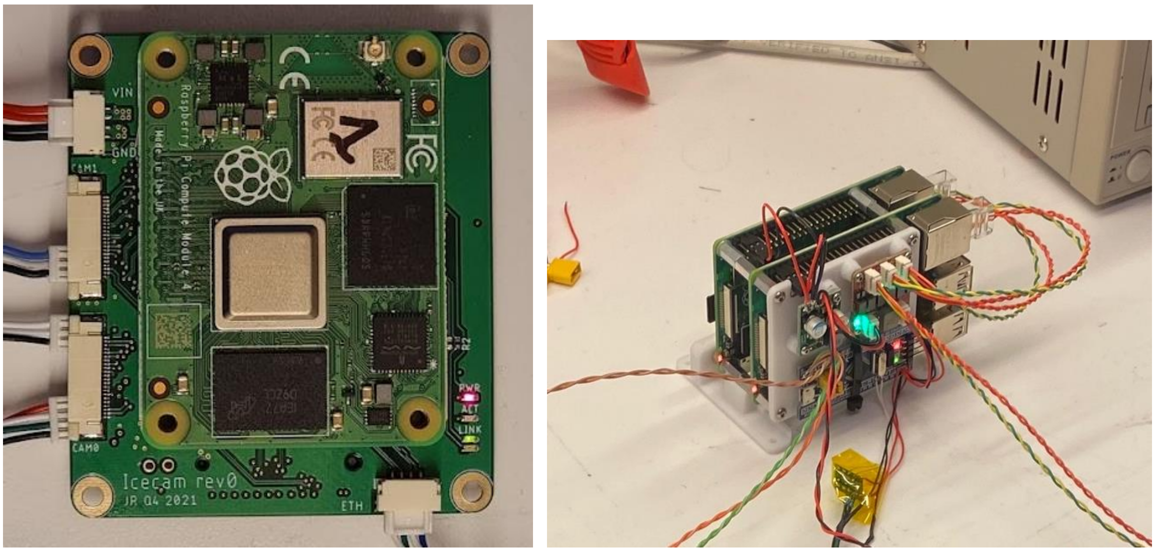

Figure 2.12.2 *Left: One of two carrier cards used in the optical payload on the Shark VTOL drone. Right: The complete payload computer stack before mounting into the UAV.*

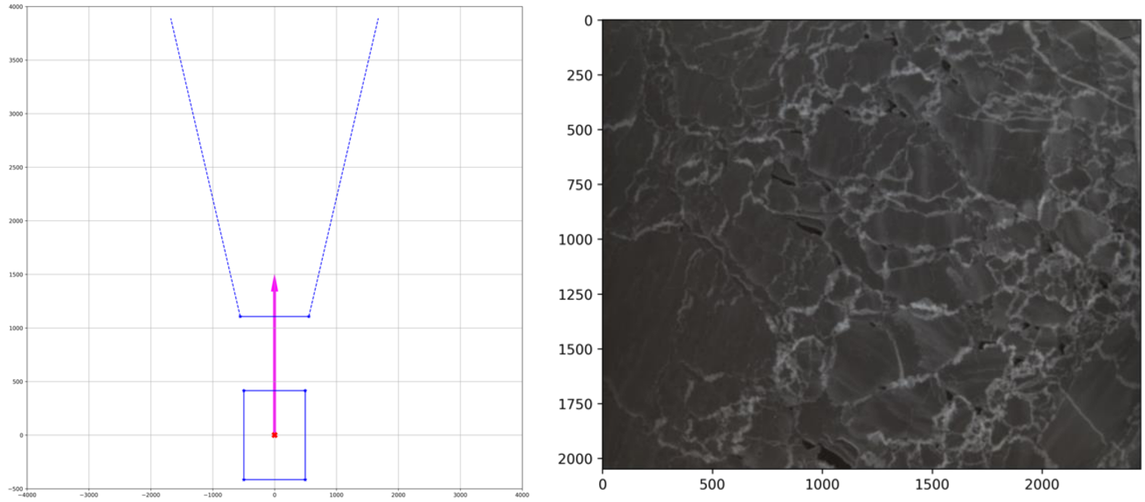

Figure 2.12.3 *Left: Footprint of the optical cameras from 1000 m altitude where the arrow indicates direction of travel. Right: Image from the nadir camera taken at 1000m altitude, with approximately 35cm ground resolution. The phenomenon, referred to as finger rafting, is clearly visible in the image.*

DJI Matrice 210 RTK

The DJI Matrice was modified with the Talon dropkit from DroMight (Figure 2.12.1) and used for deploying drift buoys on ice bergs. In addition the drone is also equipped with a thermal and an optical camera.

Parrot Disco fixed-wing drone

The Parrot Disco has a wingspan of 1.15 m and the low weight of 750 gram provides an endurance up to 45 minutes. The system has auto takeoff and landing, and the system carries a nadir-looking optical camera with an onboard GPS receiver, including a forward-looking camera for navigational purposes.

Figure 2.12.4 *Left: Parrot Disco fixed-wing drone. Right: NORCE Fox multirotor drone.*

NORCE 'Fox' multi rotor drone

The unmanned aerial vehicle (UAV) used to carry the ultra-wideband snow sounder (UWiBaSS) is a purpose-built X8 multicopter called 'Fox'. The 'Fox' can lift a maximum payload of 25 kg. Each of the eight motors (U11, 120KV) has a maximum rated thrust of 12.3 kg using 27" propellers. For navigation and control, a 'Cube Black' running ArduCopter is used. An SF11 laser rangefinder, accurately measures the distance to the ground. It is set up with a 'Here+' real-time kinematic (RTK) global positioning system (GPS) providing much more accurate position estimates than regular GPS. The positioning system has relative and absolute accuracy below 10 cm and 1 m respectively, in single-channel mode, given the distance to the base station is less than 20 km. This also provides autonomous flights that have been tested at above ground altitudes as low as 1 m.

Gamma Portable Radar Interferometer (GPRI)

The Gamma Portable Radar Interferometer (GPRI) is a frequency-modulated continuous-wave (FM-CW) interferometric real aperture radar operating in the frequency range of 17.1–17.3 GHz (Werner et al., 2012). The three real aperture antennas are mounted on a rigid 1-metre-high tower mounted on a precision rotational scanner (Figure 2.12.2). The radar image is built up line by line by azimuthally rotating the antennas about the vertical axis. The two receiving antennas are separated vertically forming a spatial interferometer useful for measurement of height information. The spatial resolution is 0.75 m in range and 7 m in azimuth at 1 km (12.6 m at 1 NM) distance. By rotating the antenna tower, images are formed at second to minute intervals.

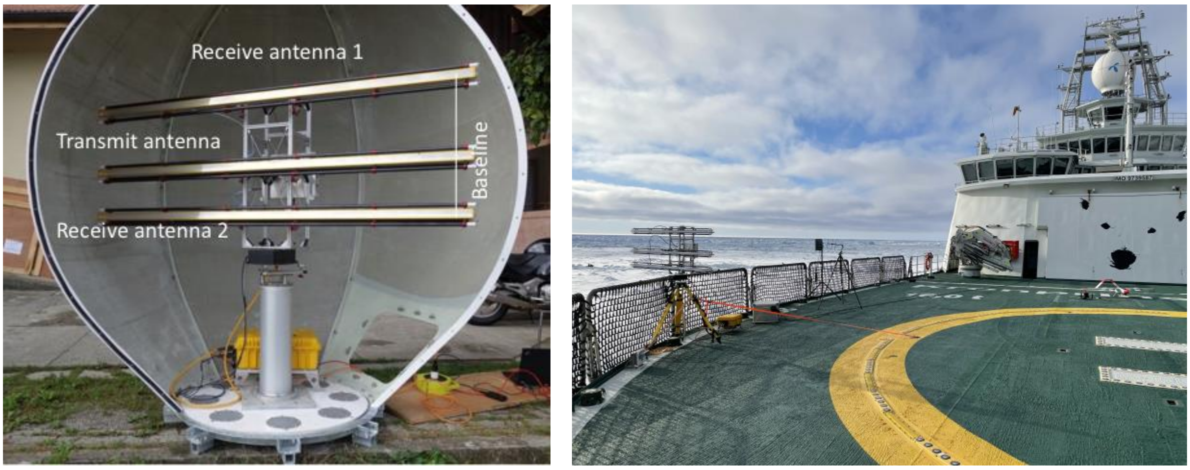

Figure 2.12.5 *Left: The GPRI radar system consists of three rotating antennas. The spatial baseline between the antennas provides sensitivity to topography. Right: The radar was mounted on the helicopter deck on the starboard side.*

UWiBaSS drone mounted radar

The ultra-wide band snow sounder (UWiBaSS) is a ground penetrating radar system developed for drone mounted operations. The radar system was designed with focus on low payload weight to fulfil UAV mounting and high range resolution requirements for snow measurements, contributing to the relatively new field of UAV mounted instrumentation. The UWiBaSS will enable autonomous, drone-based measurements of snow-cover over large and hard-to-reach regions. The radar transmits a wideband pseudo noise signal that can penetrate dry and wet snow as well as resolving thin layers in the snow stratigraphy.

Preliminary results from the UWiBaSS measurements show reliable snow depth measurements across different ice regimes. Future work includes investigation in scattering properties from rubble fields and snow density estimation. The dataset will also be compared with satellite SAR products to better understand the effects of snow cover.

Figure 2.12.6 *UWiBaSS mounted under CryoCopter FOX.*

Table 2.12.1 *Summary of the UWiBaSS key characteristics*

Attribute	Value
Waveform	UWB Pseudo noise
System bandwidth	3.8 GHz (0.7 – 4.5 GHz)
Range resolution	≈ 5 cm
Measurement rate	52 Hz (max 1 kHz)
Nominal output power	2.4 dBm
Unambiguous range in air	5.98 m
Average power consumption	9 W
Total weight	≈ 3 kg

Table 2.12.2 *Overview of UwiBaSS data collection during CIRFA cruise.*

Station	Date	Number of flights	Start Time (UTC)	Notes
CIRFA22-024A	27/04/2022	1	15:05	Flag survey

CIRFA22-024A	28/04/2022	2	10:40 12:37	Flag survey, 1.5 km line, zig-zag survey
CIRFA22-034A	01/05/2022	2	10:54 13:30	Flag survey, zig-zag survey, long transects over different ice regimes

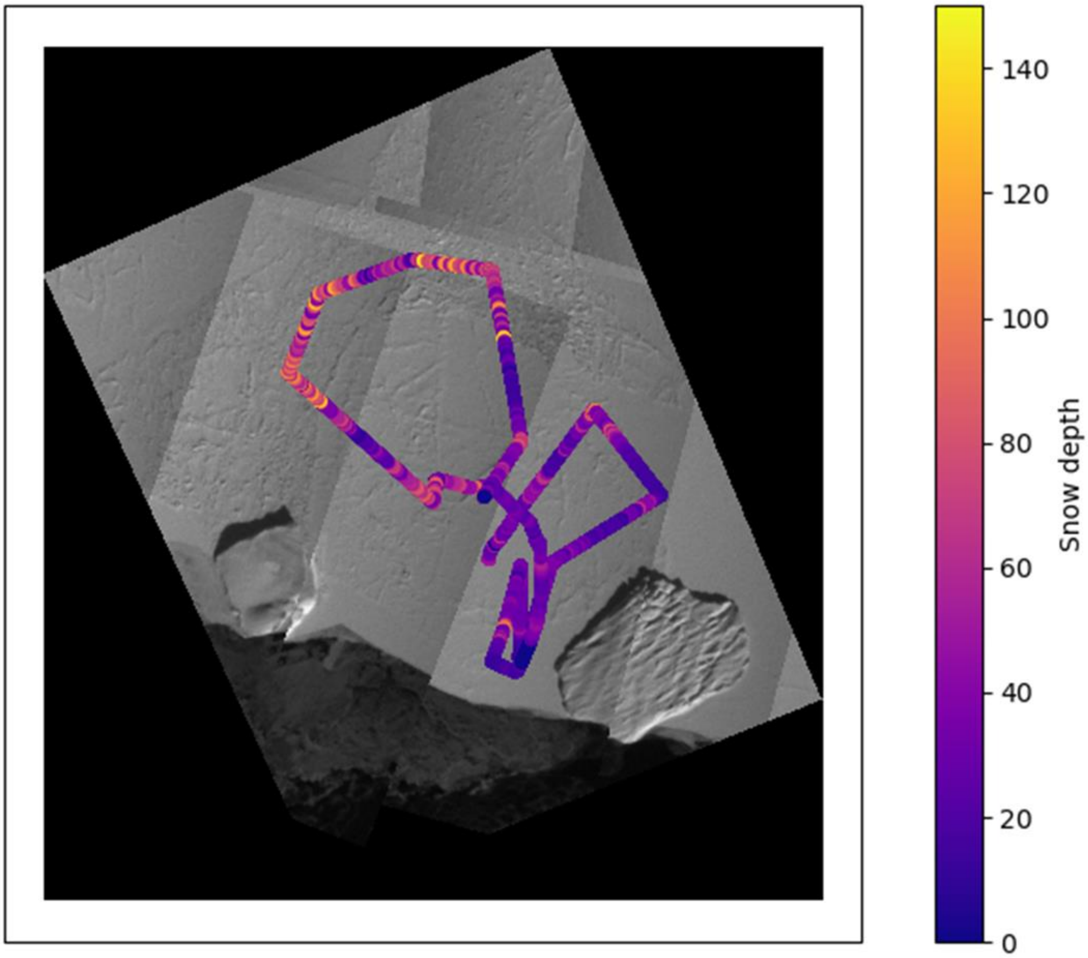

Figure 2.12.7 *Example snow depth dataset from Ice station CIRFA22-034A.*

2. Experiments carried out during CIRFA cruise

All drone operations were carried out from the helicopter deck on the vessel, coordinated with bridge personnel.

Shark VTOL

A total of 9 flights were conducted using the Shark VTOL drone (Table 2.13.3). The images captured from the two cameras were synchronised using the hardware trigger feature on the cameras. The hardware trigger was also connected to the Pixhawk flight controller. Every time a set of images were captured an accurate flight state was calculated by the flight controller and shared with the onboard computers over serial interface. The flight state was then used for direct georeferencing the images before they were shared with the ground station over the 5.8GHz broadband link. After the flight a quick view mosaic was generated, consisting of every 10th direct georeferenced image projected on the sea surface (Figure 2.12.8). The Shark flights had multiple objectives, in addition to capture images of sea ice, and several overlapping tests were carried out:

1. Robust navigation solution during takeoff and landing on helidecks.
2. Multiple synchronised cameras for increased situational awareness
3. Real time georeferencing and sharing of data via NLive portal
4. Moving base station to allow for flights when ship is moving
5. Dynamic and autonomous route planning to account for sea ice
6. Sea ice drift estimation from overlapping flight paths

Table 2.12.3 *Shark VTOL flights.*

Position (ca.)	**Date**	**Number of images**
78.6992, -12.1849	27/04/2022	370
78.7252, -12.0136	28/04/2022	2420
78.6789, -12.2039	28/04/2022	2320
78.91432, -11.1855	29/04/2022	2710
79.12190, -9.52000	30/04/2022	4250
80.0643, -7.6894	04/05/2022	1280
79.7936, -6.6129	04/05/2022	1700
79.7584, -6.0965	05/05/2022	1740
79.7235, -7.1635	05/05/2022	2190

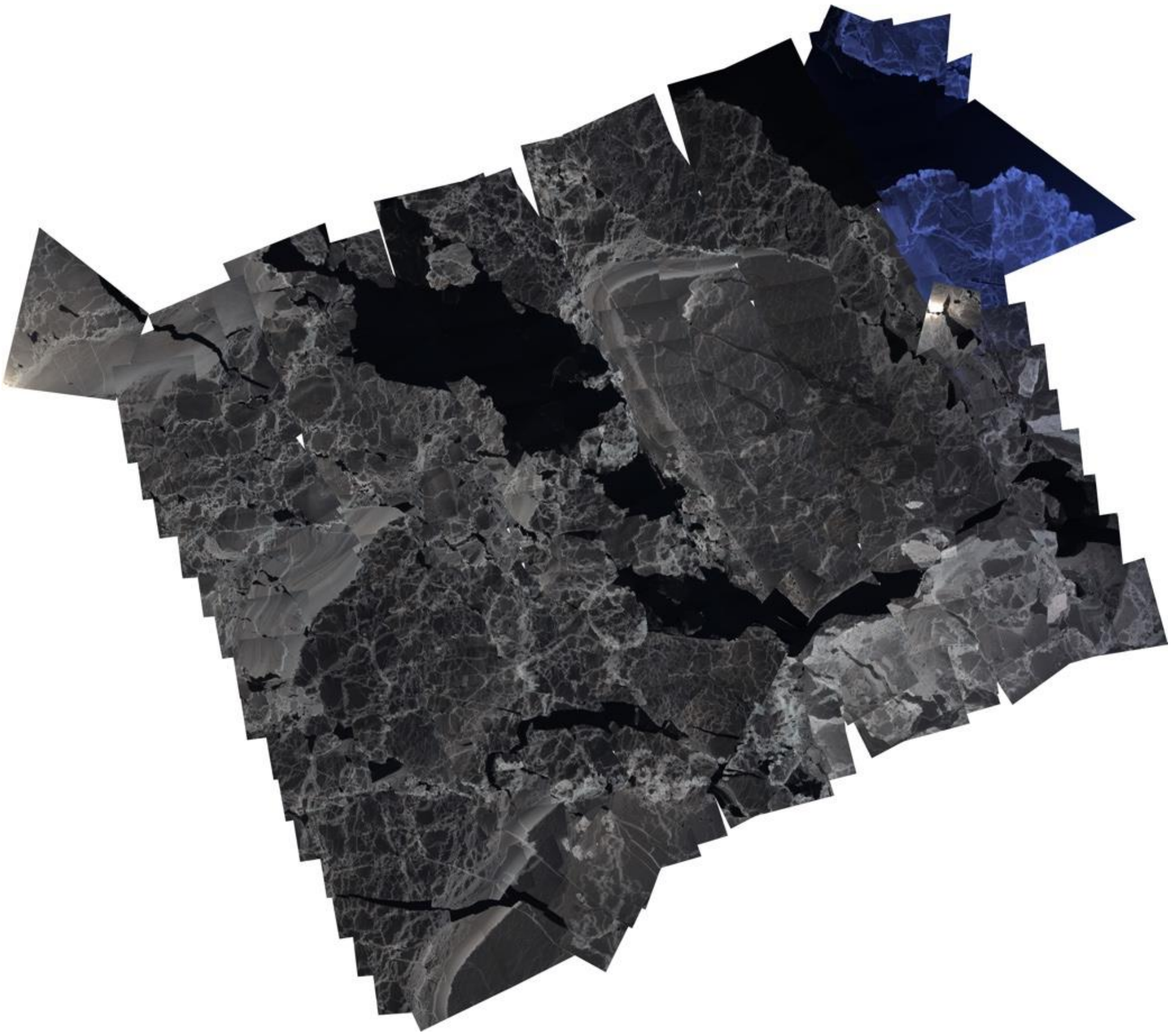

Figure 2.12.8 *Quick view mosaic of images taken on the second flight of 05/05/2022. The area is approximately 8 km x 6 km.*

DJI Matrice 210 RTK multirotor drifter deployment

Multiple buoys were deployed on icebergs using the modified DJI Matrice drone. Videos of each deployment were recorded.

GPRI Ku-band radar observations

The GPRI Ku-band radar system was installed on the starboard side on the helicopter deck, see Figure 2.12.2. During the cruise, we operated the radar system under different vessel operating conditions:

- Stationary in ice;
- Under way open waters;
- Under way in ice infested waters.

Due to mechanical stresses, the radar is not capable of operation during heavy seas or when the vessel is breaking ice. During transits in ice, the radar antennas were secured on the bridge roof. The radar was operated with a temporal sampling between 2 and 5 minutes, covering a sector of almost 180°. A short SAR experiment was also carried out. Table 2.12.2 shows an overview of the GPRI data collected.

Table 2.12.4 *Overview of GPRI data collected during CIRFA cruise.*

Station	Date dd/mm/yyyy	Number of images	Time (UTC)	Notes
	30/04/2022	38	08:53–13:35	Iceberg, travelling
CIRFA22-034A	01/05/2022	69	08:22–14:30	2 icebergs, travelling, 5 min sampling
CIRFA22-046	04/05/2022	60	14:43–16:52	2 min sampling
CIRFA22-047	05/05/2022	91	07:32–18:57	SAR experiment
CIRFA22-054	07/05/2022	15	07:05–08:20	

Parrot Disco fixed-wing drone operations

The fixed-wing drone was operated at two ice stations. The drone was operated in a controlled pattern, and all the acquired images have been combined by using structure-from-motion (SfM) to produce orthomosaics with high resolution, see figures 2.12.5 and 2.12.6.

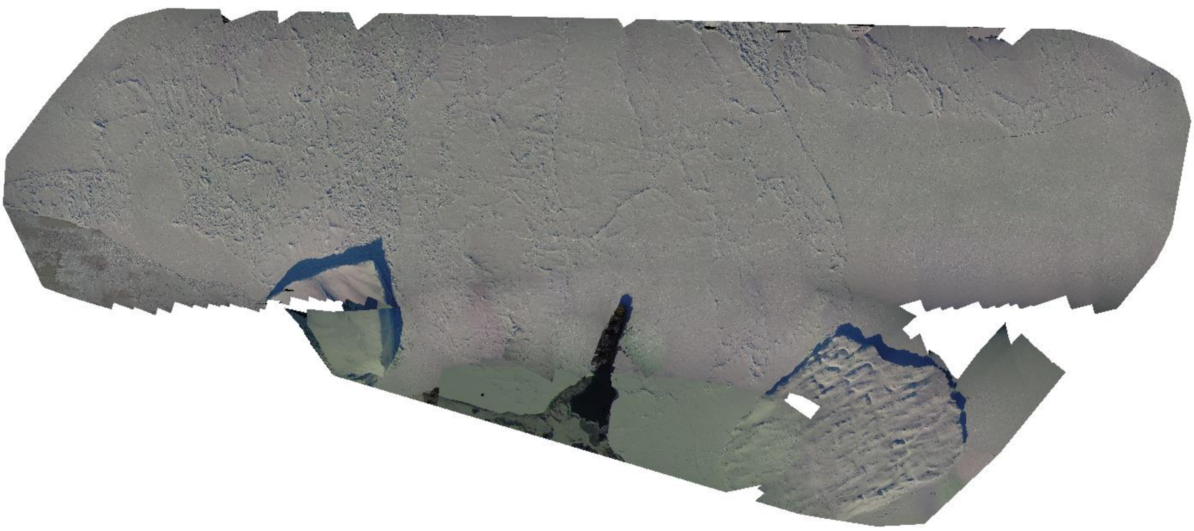

Figure 2.12.9 *Orthomosaic produced by Parrot Disco from the ice station on 01/05/2022.*

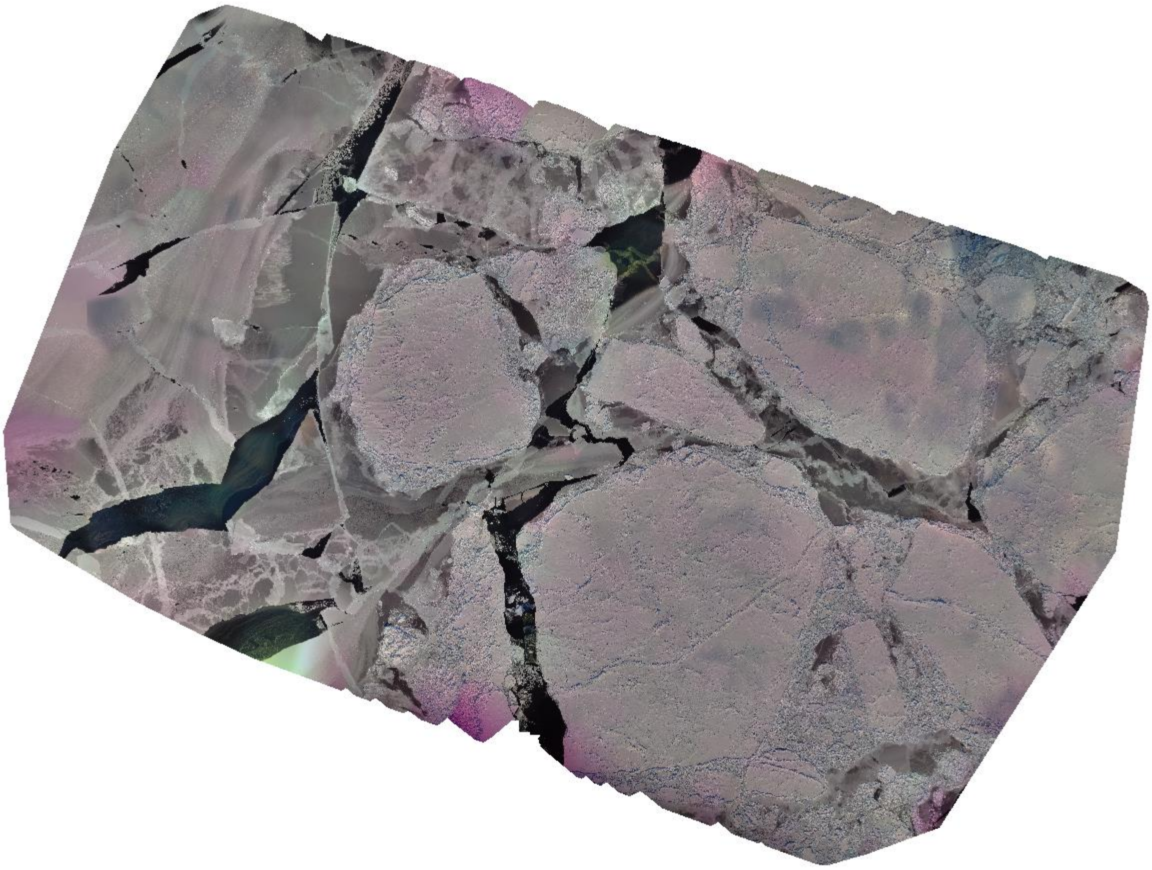

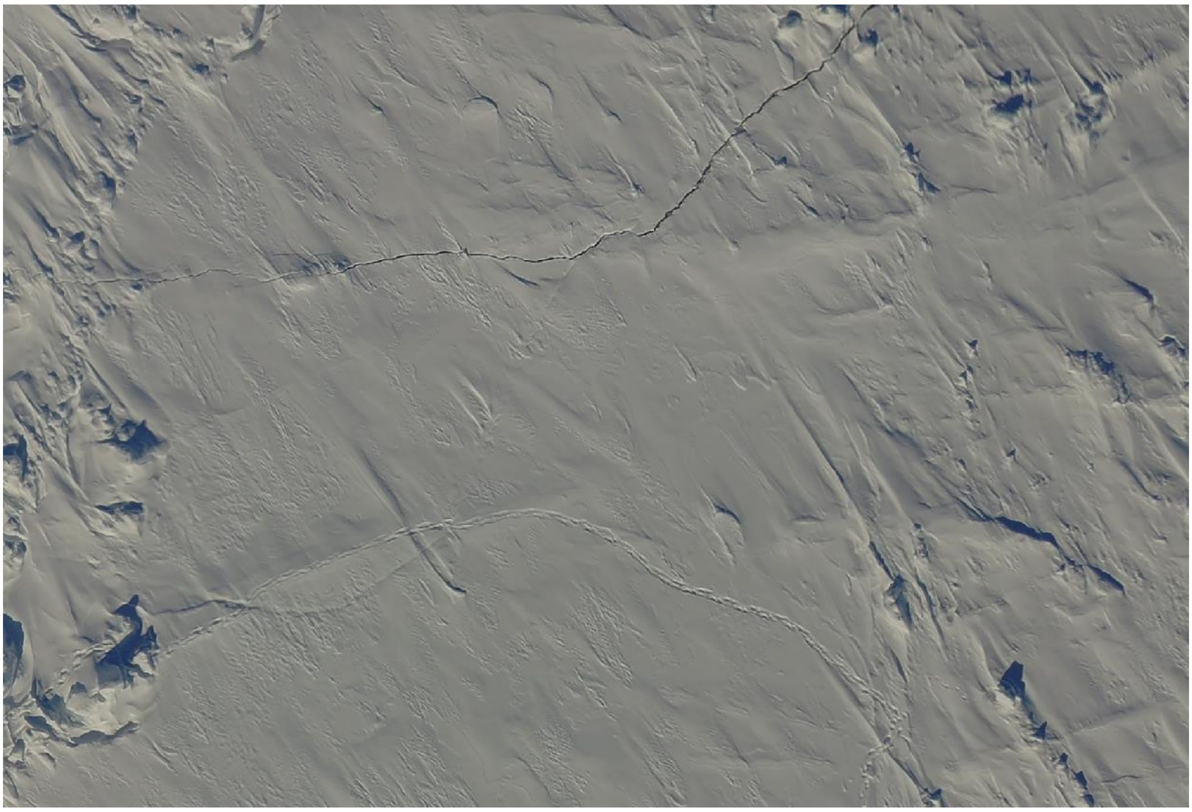

Figure 2.12.10 *Orthomosaic produced using the Parrot Disco from the ice station 05/05/2022. The image on the right shows polar bear tracks and a crack in the ice, demonstrating the 5 cm spatial resolution of the mosaic.*

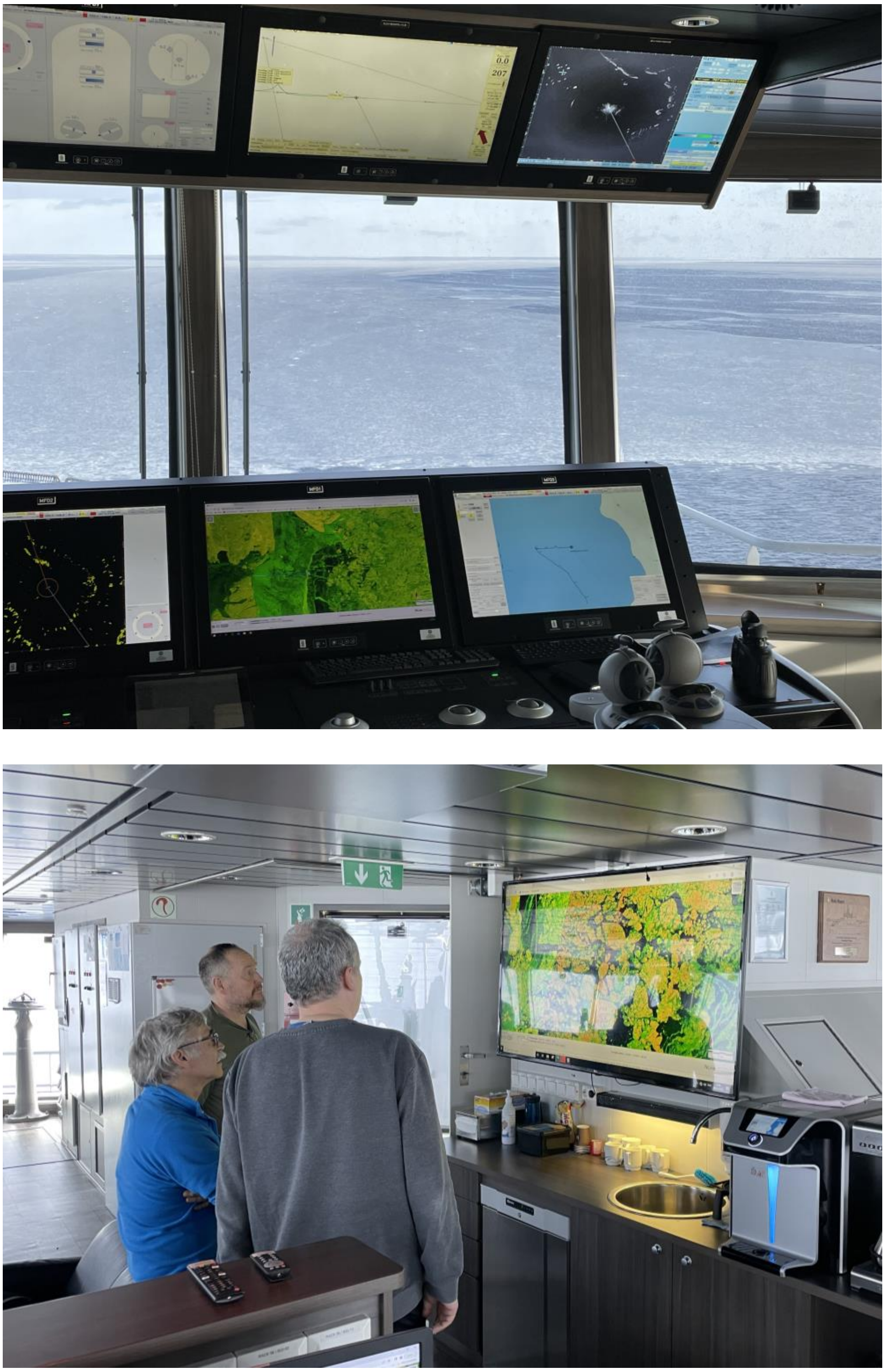

Figure 2.12.11 *During the cruise, the NORCE developed NLive visualisation and operational support system, was used extensively for operational support and for planning and observation of ongoing drone operations.*

Maritime Robotics' Drone Operations

Team: Danilo Petrocelli (Maritime Robotics) and Morten Einarsve (Maritime Robotics)

Maritime Robotics has performed several drone operations as part of the CIRFA cruise 2022 with the main goal to collect EO/IR imagery of areas of interest located up to 2 km from *RV Kronprins Haakon*.

The data has been acquired by using in-house developed camera rig, which consist of Electro-Optical/Infra-Red cameras, IMU system and RTK GNSS receivers. The camera rig was mounted as payload on the DJI Matrice 600 multicopter. Specification of EO/IR cameras can be found in the following Table 2.12.5:

***Table 2.12.5** EO/IR Camera specifications*

Camera Type	Brand	Model	Resolution	hFoV	Footprint [100m altitude]			Avg area x Pixel
					Width	Height	Area	
EO	Teledyne Dalsa	Genie Nano C4040	4112x3008	85.7°	164 m	134 m	21861 m^2	17.65 cm^2
IR	Teledyne Dalsa	Calibir GXM	640x480	73.2°	134 m	103 m	13781 m^2	448.58 cm^2

Figure 2.12.12 *Maritime Robotics multicopter with camera rig. Photos: William Copeland (MET).*

Figure 2.12.13 *Danilo Petrocelli and Morten Einarsve (Maritime Robotics) operating the drone during the CIRFA 2022 cruise. Photo: William Copeland (MET).*

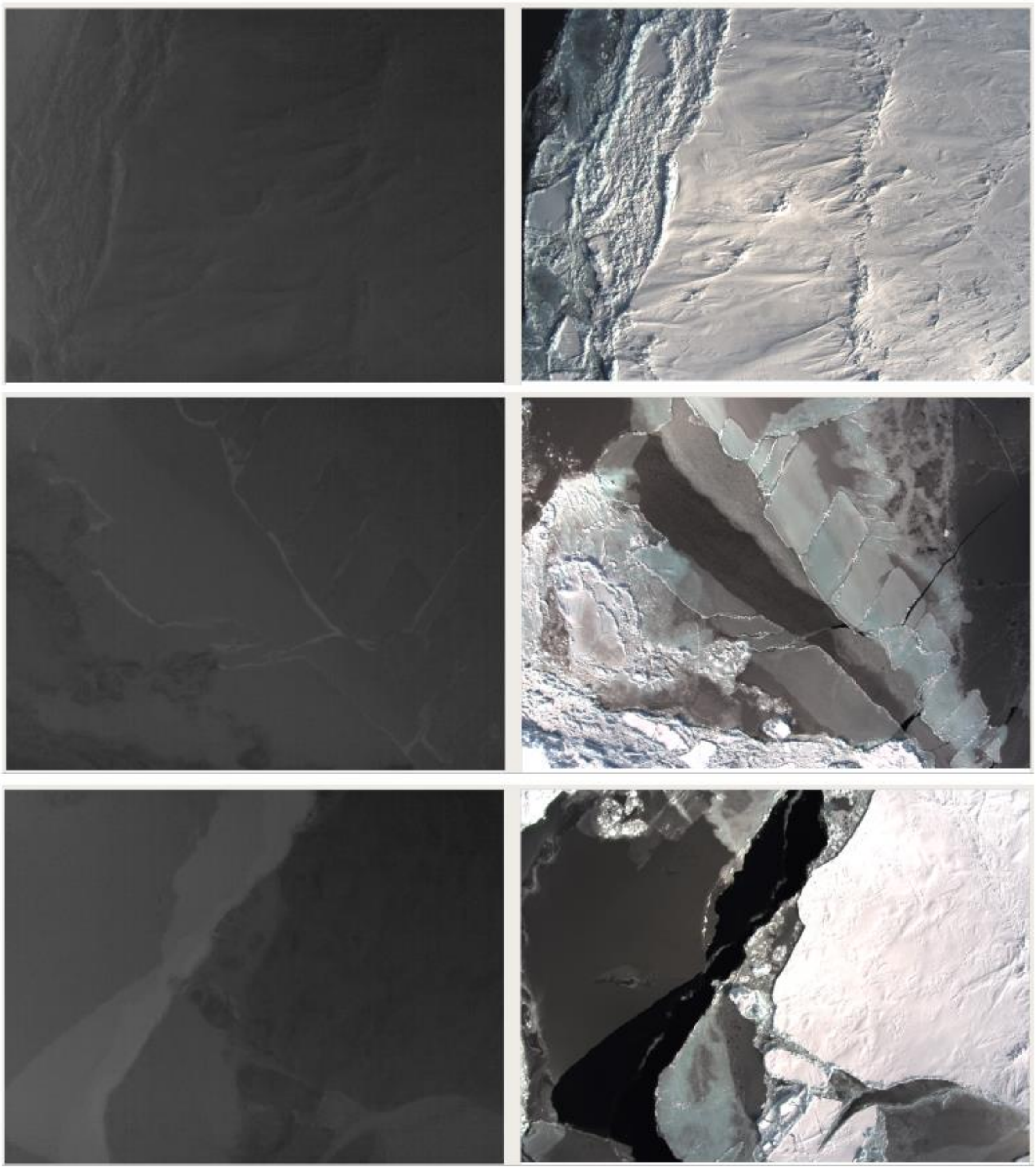

Figure 2.12.14 *Sample of EO/IR pair of images collected during the CIRFA22 cruise.*

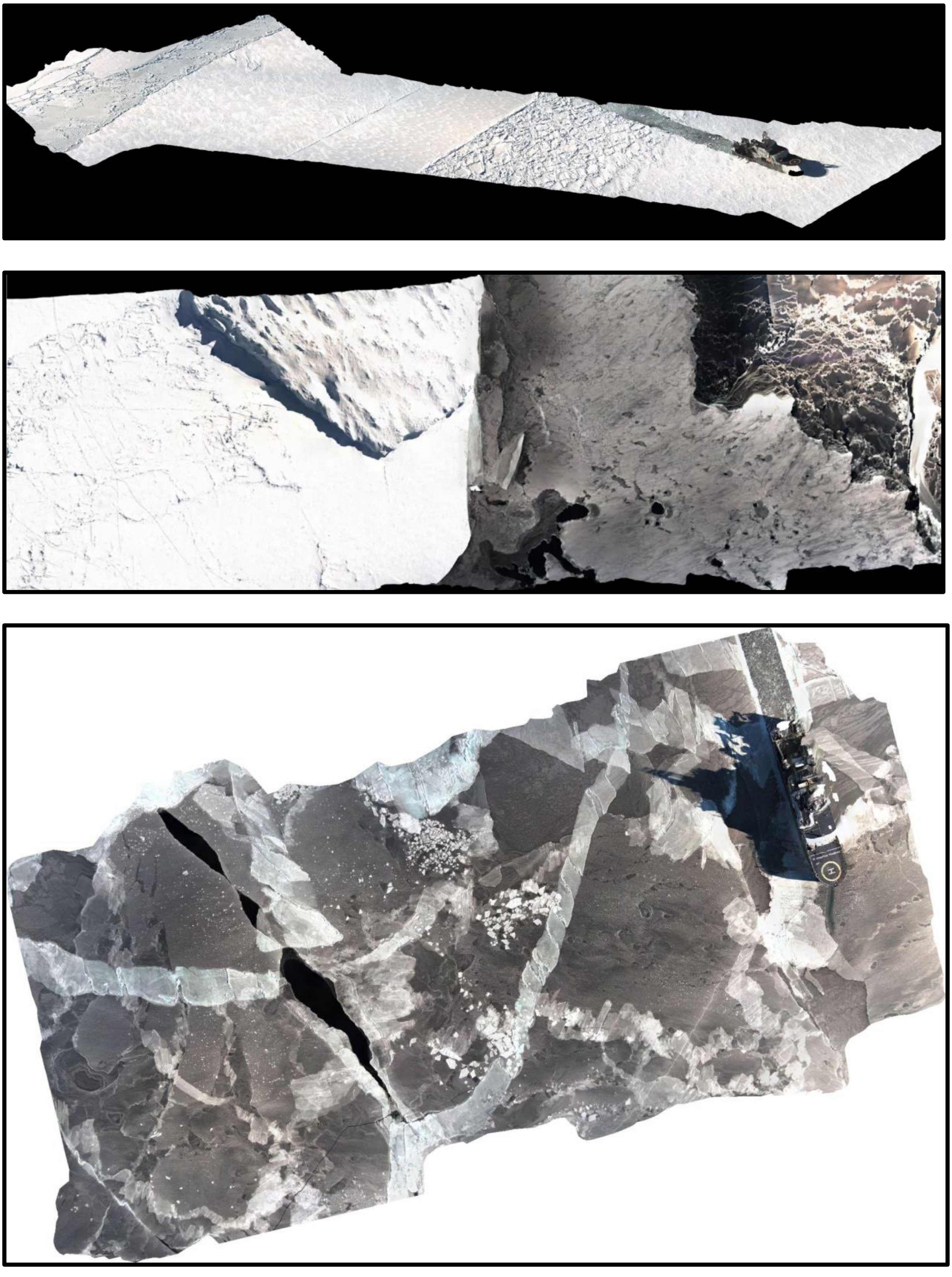

Figure 2.12.15 *Samples of Orthomosaic created during the CIRFA22 cruise.*

A total of 38 flights (32 flights with DJI Matrice 600 multicopter and 6 flights with Mavic2 pro drone) have been performed during the CIRFA 2022 cruise. All the drone operations performed with the DJI Matrice 600 multicopter are listed in the following Table 2.13.6:

Table 2.12.6 *DJI Matrice 600 drone operations.*

Station	Date	Number of Flights	Start Time (UTC)
CIRFA22_010	24/04/2022	01	17:42:00
CIRFA22_024A	27/04/2022	05	09:00:00
			10:17:00
			11:21:00
			14:13:00
CIRFA22_024B	28/04/2022	06	07:57:00
			10:08:49
			11:55:24
			12:19:43
			14:37:52
CIRFA22_031	30/04/2022	01	07:50:37
CIRFA22_034A	01/05/2022	06	07:33:14
			08:22:07
			10:19:41
			10:44:53
			13:50:27
			14:16:54
CIRFA22_038B	03/05/2022	05	12:11:53
			12:36:28
			13:54:41
			14:29:46

			15:00:00
CIRFA22_046	04/05/2022	03	14:53:00
			16:28:00
			16:57:00
CIRFA22_047	05/05/2022	03	08:21:00
			08:45:00
			11:34:00
CIRFA22_053	06/05/2022	01	14:51:00
CIRFA22_054	07/05/2022	01	07:21:00

Maritime Robotics has also performed 6 flights with the DJI Mavic2 pro drone to create social media material and/or help the ice operations by looking for potential polar bears in areas not easily accessible.

Table 2.12.7 *DJI Mavic2 pro drone operations.*

Station	**Date**	**Number of Flights**	**Start Time (UTC)**
CIRFA22_018	26/04/2022	01	13:23:00
CIRFA22_034A	01/05/2022	03	12:15:00
			16:32:00
			16:51:00
CIRFA22_024B	30/04/2022	02	08:21:00
			13:33:00

The data collected during the CIRFA cruise 2022 will be used to create a sea-ice dataset to train Deep Learning models to automatically detect and classify different types of sea-ice in real time.

2.13. Ice Watch – Sea ice and meteorology observations

Team: William Copeland (MET Norway) Trond Robertsen (MET Norway), Marina Duran Moro (MET Norway), Martina Idžanović (MET Norway), Edel Rikardsen (MET Norway), Jozef Jan Rusin (MET Norway/UiT), Anthony Paul Dougleris (UiT) Wolfgang Dierking (UiT) and Eduard Khachatrian (UiT)

Shore-based Support: Alistair Everett and Nick Hughes (MET Norway)

General information

Ice Watch is a web-based platform which allows the recording and archiving of visual shipboard sea ice observations. The system was originally developed by the Geographic Information Network of Alaska (GINA) at the University of Alaska Fairbanks (UAF) in 2012, but has been hosted by the Norwegian Meteorological Institute since 2019. Ice Watch is still jointly coordinated with MET Norway, and the International Arctic Research Centre (IARC) and GINA at UAF. The overall aim of the Ice Watch system is to create in-situ datasets that can be used to validate and improve derived information products such as ice charts, automatic classifications of satellite data, and sea ice forecast models.

Ice Watch uses the Arctic Shipborne Sea Ice Standardisation Tool (ASSIST) software to collect and archive data. This platform has been designed for scientists and sea ice analysts with expertise in sea ice observation sheets, codes and observation protocols. Observations are taken on an hourly basis while the vessel is in transit and include total ice concentration, the top three most common ice types and their concentrations / properties, photography and any practical information such as time, and longitude and latitude. All recorded data is stored and made publicly accessible on the Ice Watch web page https://icewatch.met.no. The ship, route, location markers and observation logs can be viewed either as quick looks or downloaded as JSON, Sigrid 3 or CSV files. The Ice Watch web page contains an archive of past cruises extending back to 2006.

In total, 204 sea ice and meteorological observations were made from the bridge and observation deck of *RV Kronprins Haakon* during transit time between 14:00 UTC on 23rd April and 13:00 UTC on the 8th May 2022 (Figure 2.13.1). Observations were carried out in accordance with the Ice Watch guidelines, with emphasis put on sea ice concentration which is an important aspect of present day ice charting. Ice type and the associated features such as topography, snow cover and floe size were also collected. All data for this cruise can be accessed and downloaded via the IceWatch website.

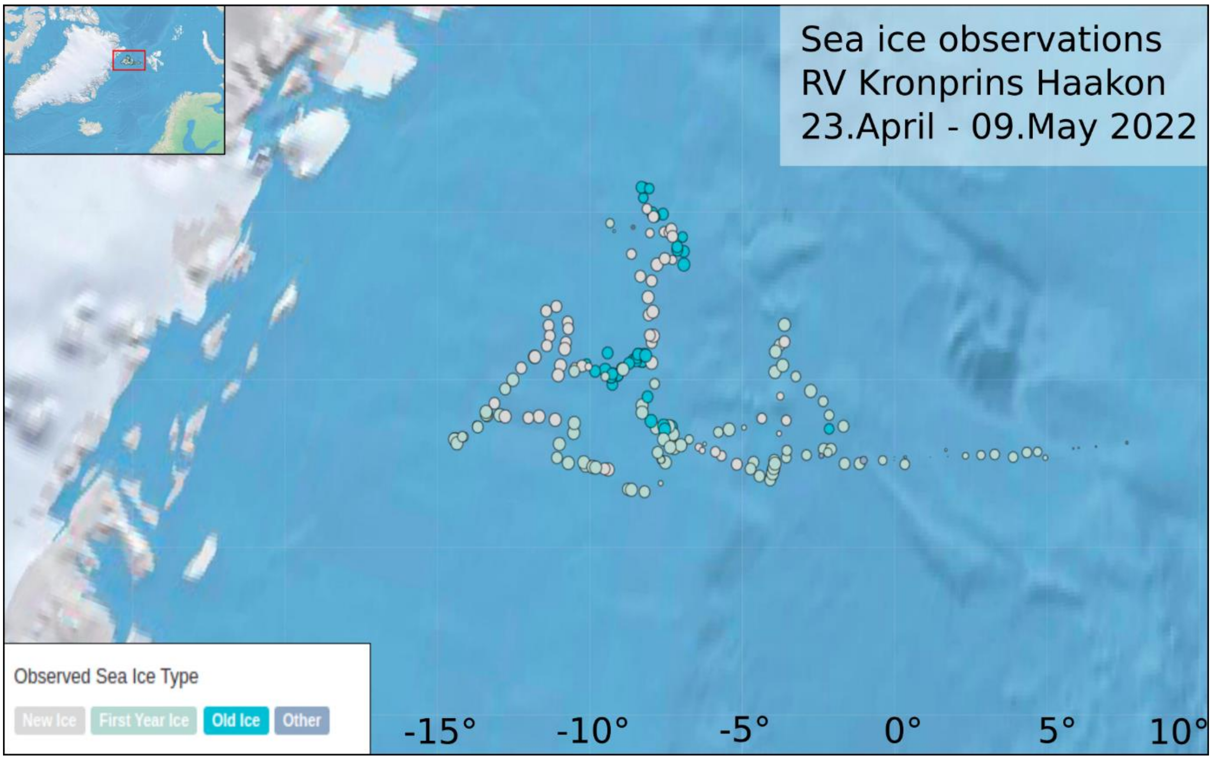

Figure 2.13.1 *Map showing the locations of ice observations taken during the CIRFA 2022 cruise and their corresponding sea ice type.*

Figure 2.13.2 *The observation deck became the centrepoint for observations and training for new observers. Photos by Trond Robertsen (MET, left) and William Copeland (MET, right).*

Meteorological and general observations

Time (UTC), date, longitude and latitude were recorded as obligatory fields in the ASSIST software, along with the name of the primary observer. Meteorological observations were collected using a combination of ship data and observation by trained eye of surroundings from the observation deck of the ship. The following information was recorded, complementing each sea ice observation and providing a dataset for those working with modelling and weather model verification:

- Air Temperature (ºC)
- Water Temperature (ºC)
- Wind speed (knots) and direction (degrees)
- Cloud (Oktas)
- Visibility (m-km)
- Weather (Meteorology codes 1-90)
- Comments; e.g. rapidly changing visibility, shifting from 1-10km

The lowest temperature recorded during the cruise was -25.7℃ at 04:00 UTC on 27th April, while the highest temperature was recorded multiple times on 25th and 26th April and again on 4th and 6th of May at -2℃. The strongest mean wind speed recorded occurred at 10:00 UTC on the 25th April at 30 knots (15m/s), while the lowest mean wind speed was 0 knots on the morning of 6th May. However, it must be noted that these figures are from observation over the 10 minute period, and it is not known if there were any dramatic changes during the 50 minute blind spot. For a full overview of meteorological conditions please see the Tokt Log.

Figure 2.13.3 shows the meteorological codes used to define weather conditions over a 10 minute period of observation and visibility. While tables 2.13a, are the raw meteorological data with date and time/ long and lat included.

3.6 Meteorological Observation Codes

3.6.1 Cloud Development During Past Hour Codes (00-03)

00:	Cloud development not observed or not observable
01:	Clouds dissolving or becoming less developed
02:	State of sky on the whole unchanged
03:	Clouds forming or developing

3.6.2 Fog/Precipitation During Past Hour But Not At Time Of Obs (20-28)

20:	Drizzle not freezing or snow grains
21:	Rain not freezing or snow grains
22:	Snow not freezing or snow grains
23:	Rain and snow, or ice pellets
24:	Drizzle or rain, freezing
25:	Showers of rain
26:	Showers or snow or of rain and snow
27:	Showers of hail or of hail and rain
28:	Fog in the past hour, not at present

3.6.3 Blowing or Drifting Snow (36-39)

36:	Drifting snow, below eye level, slight/moderate
37:	Drifting snow, below eye level, heavy
38:	Blowing snow, above eye level, slight/moderate
39:	Blowing snow, above eye level, heavy

3.6.4 Fog/ Mist (41-49)

41:	Fog in patches, visibility < 1000m
42:	Fog thinning in last hour, sky discernible, visibility < 1000m
43:	Fog thinning in last hour, sky not discernible, visibility < 1000m
44:	Fog unchanged in last hour, sky discernible, visibility < 1000m
45:	Fog unchanged in last hour, sky not discernible, visibility < 1000m
46:	Fog beginning/thickening in last hour, sky discernible, visibility < 1000m
47:	Fog beginning/thickening in last hour, sky not discernible, visibility < 1000m
48:	Fog depositing rime, sky discernible, visibility < 1000m
49:	Fog depositing rime, sky not discernible, visibility < 1000m

3.6.5 Precipitation As Drizzle (50-59)

50:	Slight drizzle, intermittent
51:	Slight drizzle, continuous
52:	Moderate drizzle, intermittent
53:	Moderate drizzle, continuous
54:	Dense drizzle, intermittent
55:	Dense drizzle, continuous
56:	Freezing drizzle, slight
57:	Freezing drizzle, moderate or dense
58:	Drizzle and rain, slight
59:	Drizzle and rain, moderate or dense

3.6.6 Precipitation As Rain, Not Showers (60-69)

60:	Slight rain, intermittent
61:	Slight rain, continuous
62:	Moderate rain, intermittent
63:	Moderate rain, continuous
64:	Heavy rain, intermittent
65:	Heavy rain, continuous
66:	Freezing rain, slight
67:	Freezing rain, moderate or heavy
68:	Rain or drizzle and snow, slight
69:	Rain or drizzle and snow, moderate/heavy

3.6.7 Frozen Precipitation, Not Showers (70-79)

70:	Slight fall of snow flakes, intermittent
71:	Slight fall of snow flakes, continuous
72:	Moderate fall of snow flakes, intermittent
73:	Moderate fall of snow flakes, continuous
74:	Heavy fall of snow flakes, intermittent
75:	Heavy fall of snow flakes, continuous
76:	Ice prisms, with/without fog
77:	Snow grains, with/without fog
78:	Isolated starlike snow crystals
79:	Ice pellets

3.6.8 Precipitation As Showers (80-90)

80:	Slight rain showers
81:	Moderate or heavy rain showers
82:	Violent rain showers
83:	Slight showers of rain and snow
84:	Moderate/heavy showers of rain and snow
85:	Slight snow showers
86:	Moderate or heavy snow showers
87:	Slight showers of soft or small hail
88:	Moderate/heavy showers of soft/small hail
89:	Slight showers of hail
90:	Moderate or heavy showers of hail

3.6.9 Visibility Codes

90:	< 50 m
91:	50–200 m
92:	200–500 m
93:	500–1000 m
94:	1–2 km
95:	2–4 km
96:	4–10 km
97:	> 10 km
-1:	Not available

Figure 2.13.3 *Meteorological codes used to define weather over a 10 minute observation period.*

Table 2.13a *M code (meteorological code), Vis (Visibility, TCC (Total cloud cover in oktas), WS (true wind speed in knots), WD (Wind Direction in degrees), A.Temp (Air temperature in Celsius) and W.Temp (Surface water temperature in Celsius).*

Date and time	LAT	LON	M. code	Vis	TCC	WS (Knots)	WD (Degrees)	A.Temp ºC	W.Temp ºC
2022-05-08 13:00:00 UTC	78.8333	6.5	85	93	8	25	318	-8	0
2022-05-08 10:30:00 UTC	78.8333	5.6333	85	93	8	25	328	-8	2
2022-05-08 10:00:00 UTC	78.8333	5.15	85	94	8	23	329	-8	2
2022-05-08 08:59:00 UTC	78.8333	5	85	95	7	24	327	-9	1
2022-05-08 08:03:00 UTC	78.8	4.2	85	94	8	22	332	-9	1
2022-05-08 07:00:00 UTC	78.8333	4	85	94	8	25	321	-9	1
2022-05-08 05:57:00 UTC	78.8333	3.7	38	93	8	24	330	-9	-1
2022-05-08 05:01:00 UTC	78.8167	3.3	38	94	8	20	331	-10	-2
2022-05-08 03:03:00 UTC	78.8333	2.8	2	95	8	/	/	-10	-2
2022-05-08 02:01:00 UTC	78.8333	2.4167	3	97	8	23	314	-9	-1
2022-05-08 01:02:00 UTC	78.8333	1.9833	2	96	4	24	314	-9	-2
2022-05-08 00:11:00 UTC	78.8667	1.4333	3	96	4	25	307	-8	-1
2022-05-07 23:00:00 UTC	78.8333	0.3017	86	95	8	18	291	-11	-2
2022-05-07 22:04:00 UTC	78.8	0.2833	3	97	5	16	296	-9	-2
2022-05-07 20:54:00 UTC	78.8167	0.3333	2	96	2	19	293	-9	-2
2022-05-07 19:53:00 UTC	78.8	0.9833	1	96	2	12	301	-12	-2
2022-05-07 18:51:00 UTC	70.8	-1.4	3	97	7	13	312	-11	-2
2022-05-07 18:00:00 UTC	78.85	-1.8667	3	96	7	15	305	-9	-2
2022-05-07 17:00:00 UTC	78.9667	-1.85	2	97	5	10	294	-11	-2
2022-05-07 16:00:00 UTC	79.0333	-1.8667	1	97	3	12	290	-12	-2
2022-05-07 15:00:00 UTC	79.1	-2.05	1	97	5	10	287	-10	-2
2022-05-07 13:59:00 UTC	79.15	-2.4167	2	97	7	9	292	-9	-2
2022-05-07 13:01:00 UTC	79.2167	-2.8667	70	96	6	7	304	-11	-2
2022-05-07 12:10:00 UTC	79.2667	-3.25	2	97	6	9	301	-14	-2
2022-05-07 11:15:00 UTC	79.3667	-3.3667	2	97	6	7	324	-11	-2
2022-05-07 05:00:00 UTC	79.4667	-3.2667	85	96	7	14	34	-15	-2
2022-05-07 04:00:00 UTC	79.3833	-3.2333	85	96	7	20	30	-15	-2
2022-05-07 03:00:00 UTC	79.3333	-3.4833	85	96	7	18	36	-15	-2
2022-05-07 01:55:00 UTC	79.2333	-3.4667	77	93	8	14	/	-15	-2
2022-05-07 00:59:00 UTC	79.1167	-3.2833	3	97	2	20	34	-14	-2
2022-05-06 23:52:00 UTC	79	-3.0667	1	97	5	21	38	-13	-2
2022-05-06 23:03:00 UTC	78.9333	-3.25	1	96	7	20	41	-12	-2
2022-05-06 21:53:00 UTC	79	-3.7667	42	93	7	20	41	-11	-2
2022-05-06 20:53:00 UTC	78.95	-4.25	43	93	8	20	37	-10	-2
2022-05-06 20:01:00 UTC	78.9333	-4.6667	44	93	8	21	35	-9	-2
2022-05-06 18:50:00 UTC	78.9167	-4.9667	47	93	8	18	32	-2	/
2022-05-06 17:53:00 UTC	78.85	-5.3167	47	93	8	13	42	-7	-2
2022-05-06 17:06:00 UTC	78.8667	-5.7667	77	93	8	12	32	-7	-2
2022-05-06 16:06:00 UTC	78.8833	-6.2167	77	93	8	11	9	-6	-2
2022-05-06 15:15:00 UTC	78.9167	-6.3667	41	95	4	1	333	-7	-2
2022-05-06 14:16:00 UTC	78.9	-6.4167	42	94	1	3	10	-8	-2
2022-05-06 13:00:00 UTC	78.9	-6.4667	45	92		1	34	-7	-2
2022-05-06 10:08:00 UTC	78.9167	-6.5167	/	92		0	269	-8	-2
2022-05-06 08:58:00 UTC	78.9167	6.3	43	93	0	3	250	-10	-2
2022-05-06 06:00:00 UTC	78.85	-6.4667	47	90	0	5	231	-10	-2
2022-05-06 05:00:00 UTC	78.9	-6.7167	46	91	1	5	236	-11	-2
2022-05-06 04:00:00 UTC	78.9333	-6.8833	40	96	1	5	236	-10	-2
2022-05-06 03:00:00 UTC	78.9667	-7.15	40	97	1	6	259	-11	-2
2022-05-06 02:02:00 UTC	79.0022	-7.1833	2	97	1	7	235	-10	-2
2022-05-06 01:00:00 UTC	79.05	-7.05	0	97	0	7	221	-10	-2

Date and time	LAT	LON	M. code	Vis	TCC	WS (Knots)	WD (Degrees)	A.Temp ºC	W.Temp ºC
2022-05-06 00:05:00 UTC	79.1167	-6.9	0	97	0	7	219	-8	-2
2022-05-05 23:05:00 UTC	79.2167	-7.05	1	97	5	7	228	-8	-2
2022-05-05 22:00:00 UTC	79.35	-7.0833	2	97	7	7	219	-7	-2
2022-05-05 21:08:00 UTC	79.4667	-7.1833	3	97	7	7	224	-7	-2
2022-05-05 20:01:00 UTC	79.6167	7.3167	2	97	2	8	228	-7	-2
2022-05-05 19:00:00 UTC	79.7	-7.21	2	97	3	2	245	-7	-2
2022-05-05 17:00:00 UTC	79.7333	-7	2	97	1	4	243	-7	-2
2022-05-05 16:00:00 UTC	79.7333	-6.7667	2	97	2	11	241	-7	-2
2022-05-05 15:00:00 UTC	79.7167	-6.4	2	97	3	9	244	-7	-2
2022-05-04 18:00:00 UTC	79.7833	-6.45	2	97	2	2	186	-5	-1
2022-05-04 16:00:00 UTC	79.7833	-6.65	2	97	2	1	200	-2	-1
2022-05-04 14:00:00 UTC	79.8	-6.6667	2	97	5	2	207	-7	-2
2022-05-04 13:00:00 UTC	79.8833	-6.9	3	97	4	2	283	-6	-2
2022-05-04 12:02:00 UTC	79.95	-7.2	2	97	1	0	243	-7	-1
2022-05-04 10:58:00 UTC	79.9667	-7.7167	0	97	0	7	250	-6	-1
2022-05-04 10:06:00 UTC	80.0667	-7.8833	0	97	0	3	288	-11	-2
2022-05-04 06:02:00 UTC	80.0667	-7.7333	2	97	1	5	241	-11	-2
2022-05-04 04:00:00 UTC	80.0667	-7.9667	2	97	2	2	262	-11	-2
2022-05-04 03:00:00 UTC	80.0167	-7.8833	2	97	2	2	312	-11	-2
2022-05-04 02:00:00 UTC	79.95	-7.55	2	97	3	2	314	-8	-2
2022-05-04 01:00:00 UTC	79.9333	-7.5	2	97	3	3	310	-8	-2
2022-05-04 00:00:00 UTC	79.9333	-7.4333	2	97	3	4	305	-8	-2
2022-05-03 23:00:00 UTC	79.8667	-6.95	2	97	4	5	318	-8	-2
2022-05-03 21:56:00 UTC	79.8517	-6.5333	2	97	6	11	322	-7	-1
2022-05-03 21:02:00 UTC	79.85	-6.8333	2	97	6	12	328	-7	-2
2022-05-03 19:56:00 UTC	79.8667	-7.1167	2	97	6	12	322	-7	-2
2022-05-03 18:55:00 UTC	79.85	-7.55	2	97	6	12	316	-7	-2
2022-05-03 18:29:00 UTC	79.8667	-8.0667	2	97	4	12	332	-8	-2
2022-05-03 17:21:00 UTC	79.8667	-8.0667	2	97	4	12	332	-8	-2
2022-05-03 16:03:00 UTC	79.8667	-8.7833	1	97	5	17	298	-9	-2
2022-05-03 11:00:00 UTC	79.8667	-8.8	2	97	5	6	322	-9	-2
2022-05-03 10:00:00 UTC	79.8333	-8.6333	1	97	6	6	318	-9	-2
2022-05-03 09:00:00 UTC	79.7333	-8.0167	1	97	7	8	326	-9	-2
2022-05-03 08:00:00 UTC	79.6333	-7.6667	2	97	8	9	343	-8	-2
2022-05-03 07:00:00 UTC	79.5333	-7.3667	1	97	8	16	323	-8	-2
2022-05-03 06:00:00 UTC	79.45	-7.2833	2	96	8	8	312	-9	-2
2022-05-03 04:57:00 UTC	79.35	-7.1833	1	96	8	26	314	-9	-2
2022-05-03 04:01:00 UTC	79.3167	-7.1167	77	94	8	29	332	-10	-2
2022-05-03 03:05:00 UTC	79.25	-7.2333	77	94	8	20	334	-9	-2
2022-05-03 02:05:00 UTC	79.25	-7.2667	3	96	8	14	307	-11	-2
2022-05-03 01:05:00 UTC	79.25	-7.2833	/	96		28	345	-9	-2
2022-05-02 23:58:00 UTC	79.2333	-8.35	2	96	7	20	344	-9	-2
2022-05-02 23:00:00 UTC	79.2167	-7.3167	/	97	5	6	319	-11	-2
2022-05-02 22:00:00 UTC	79.2167	-7.3167	85	97	4	7	322	-9	-2
2022-05-02 21:00:00 UTC	79.2167	-7.5	2	97	3	5	322	-10	-2
2022-05-02 20:00:00 UTC	79.2333	-7.4833	2	97	3	5	324	-10	-2
2022-05-02 19:00:00 UTC	79.25	-7.45	1	96	3	7	329	-9	-2
2022-05-02 18:00:00 UTC	79.25	-7.4667	85	96	7	4	340	-8	-2
2022-05-02 17:07:00 UTC	79.2167	-7.5833	2	97	6	11	307	-8	-2
2022-05-02 16:00:00 UTC	79.2	-7.6833	2	97		4	285	-7	-2
2022-05-02 15:09:00 UTC	79.1667	-7.8333	2	96	7	8	284	-7	-2

Date and time	LAT	LON	M. code	Vis	TCC	WS (Knots)	WD (Degrees)	A.Temp ºC	W.Temp ºC
2022-05-02 14:06:00 UTC	79.1667	-7.8834	3	96	7	7	275	-6	-2
2022-05-02 12:00:00 UTC	79.1333	-7.9667	11	93	7	6	270	-3	-2
2022-05-02 11:00:00 UTC	79.1333	-7.9667	2	97	3	5	286	-7	-2
2022-05-02 10:00:00 UTC	79.0833	-8.0833	1	97	3	6	282	-4	-2
2022-05-02 09:00:00 UTC	79.1167	-8.15	2	97	4	4	270	-8	-2
2022-05-02 08:00:00 UTC	79.1167	-8.15	3	97	4	4	300	-8	2
2022-05-02 07:00:00 UTC	78.1333	-8.1333	1	97	2	7	310	-9	-2
2022-05-02 05:59:00 UTC	79.1333	-8.1167	1	97	3	10	122	-7	-2
2022-05-02 05:02:00 UTC	79.1167	-8.3167	1	97	6	14	341	-6	-2
2022-05-02 04:08:00 UTC	79.15	-8.35	1	96	5	13	316	-11	-2
2022-05-02 03:04:00 UTC	79.1333	-8.6333	77	94	8	14	338	-8	-2
2022-05-02 02:00:00 UTC	79.15	-8.8333	77	94	8	22	343	-7	-2
2022-04-30 16:00:00 UTC	79.1667	-8.9	2	97	2	4	353	-16	-2
2022-04-30 15:00:00 UTC	79.15	-9.0167	2	97	2	5	19	-15	-2
2022-04-30 14:00:00 UTC	79.1333	-9.2167	2	97		4	26	-14	-2
2022-04-30 13:00:00 UTC	79.1167	-9.2167	2	97		3	35	-11	-2
2022-04-30 11:56:00 UTC	79.0833	-9.65	2	97	2	5	69	-11	-2
2022-04-30 10:51:00 UTC	79.1333	-9.6333	3	96	3	1	188	-11	-2
2022-04-30 10:07:00 UTC	79.2167	-9.5833	2	97	2	3	181	-11	-2
2022-04-30 08:06:00 UTC	79.25	-9.5833	2	97	1	3	173	-10	-2
2022-04-30 06:56:00 UTC	79.3167	-9.5667	2	97	1	5	182	-13	-2
2022-04-30 06:00:00 UTC	79.35	-9.6167	2	97	0	2	43	-14	-2
2022-04-30 05:00:00 UTC	79.4167	-10.0167	2	97		1	10	-19	-2
2022-04-30 04:00:00 UTC	79.3833	-10.2833	2	97	0	3	11	-17	-2
2022-04-30 03:00:00 UTC	79.3167	-10.15	2	97	0	2	350	/	-2
2022-04-30 02:00:00 UTC	79.2667	-10.0667	2	97	1	2	340	-15	-2
2022-04-30 01:00:00 UTC	79.2167	-10.1	2	97	1	2	360	-15	-2
2022-04-30 00:04:00 UTC	79.15	-10.4	2	97	2	8	47	-14	-2
2022-04-29 23:14:00 UTC	79.15	-10.4167	2	97	2	11	50	-15	-2
2022-04-29 21:59:00 UTC	79.0833	-10.7333	2	97	1	11	27	-15	-2
2022-04-29 21:10:00 UTC	79.0167	-10.9	2	97	1	9	6	-15	-2
2022-04-29 20:09:00 UTC	78.9667	-11.0667	2	97	1	8	311	-18	-2
2022-04-29 19:05:00 UTC	78.8833	-11.295	2	97	0	7	332	-17	-2
2022-04-29 18:01:00 UTC	78.8192	-11.4694	2	97	0	6	353	-16	-2
2022-04-29 17:02:00 UTC	78.7558	-11.6594	2	97	0	7	5	-16	-2
2022-04-29 16:10:00 UTC	78.6872	-11.9992	1	97	1	6	17	-16	-2
2022-04-29 06:11:00 UTC	78.6667	-12.1833	/	90		6	13	-19	-2
2022-04-27 09:13:00 UTC	78.6667	-12.2	2	97	1	7	266	-22	-2
2022-04-27 06:57:00 UTC	78.65	-12.1167	0	97	0	10	28	-18	-2
2022-04-27 06:01:00 UTC	78.69	-11.9544	0	97	0	13	24	-17	-2
2022-04-27 04:52:00 UTC	78.7514	-11.6333	2	97	1	11	329	-20	-2
2022-04-27 04:04:00 UTC	78.8347	-11.4875	2	97	1	8	348	-26	-2
2022-04-27 03:01:00 UTC	48.8167	-11.4333	2	97	2	15	331	-22	-2
2022-04-27 02:00:00 UTC	78.8333	-11.0833	2	97	2	5	333	-20	-2
2022-04-27 01:00:00 UTC	78.8333	-10.9333	2	97	1	4	16	-17	-2
2022-04-27 00:00:00 UTC	78.85	-10.3	2	97	1	9	30	-16	-2
2022-04-26 23:00:00 UTC	78.8667	-10	2	97		14	360	-14	-2
2022-04-26 21:59:00 UTC	78.8642	-9.55	2	96	1	16	2	-14	-2
2022-04-26 21:00:00 UTC	78.8667	-9.0167	2	96	2	19	8	-13	-2
2022-04-26 19:03:00 UTC	78.8167	-8.9833	2	97	1	5	1	-15	-2
2022-04-26 17:59:00 UTC	78.75	-9.3333	3	96	3	13	39	-15	-2

Date and time	LAT	LON	M. code	Vis	TCC	WS (Knots)	WD (Degrees)	A.Temp ºC	W.Temp ºC
2022-04-26 16:59:00 UTC	78.6833	-9.35	0	97	0	NA	NA	-13	-2
2022-04-26 16:08:00 UTC	78.6667	-9.0167	1	97	1	13	53	-12	-2
2022-04-26 15:07:00 UTC	78.6833	-8.6	3	95		13	25	-13	-2
2022-04-26 14:04:00 UTC	78.6667	-8.5333	3	96		7	323	-14	-2
2022-04-26 12:00:00 UTC	78.6667	-8.3333	3	96	1	8	246	-15	-2
2022-04-26 11:06:00 UTC	78.6667	-8.25	0	97	0	16	227	-15	-2
2022-04-26 09:20:00 UTC	78.6667	-8	0	97	0	12	252	-15	-2
2022-04-26 07:57:00 UTC	78.6667	-7.9	1	96	4	11	209	-20	-2
2022-04-26 06:58:00 UTC	78.5833	-7.23	1	96	6	11	209	-19	-2
2022-04-26 05:02:00 UTC	78.5833	-7.3	2	97	1	8	229	-19	-2
2022-04-26 04:00:00 UTC	78.5833	-7.2	0	96	0	7	243	-20	-2
2022-04-26 03:09:00 UTC	78.5833	-6.85	2	97	1	8	217	-20	-2
2022-04-26 02:05:00 UTC	78.6333	-6.4333	2	96	2	9	271	-20	-2
2022-04-26 01:09:00 UTC	78.75	-6.45	3	96	3	3	357	-19	-2
2022-04-26 00:04:00 UTC	78.75	-6.4833	2	96	2	6	333	-19	-2
2022-04-25 23:07:00 UTC	78.75	6.4833	2	96	3	9	331	-19	-2
2022-04-25 22:12:00 UTC	78.46	-6.36	2	97	4	11	345	-20	-2
2022-04-25 21:00:00 UTC	78.7833	-6.6	2	97	5	13	341	-20	-2
2022-04-25 20:00:00 UTC	78.8167	-6.2667	2	97	4	11	351	-20	-2
2022-04-25 19:00:00 UTC	78.8333	-6.2667	1	97		12	355	-20	-2
2022-04-25 18:01:00 UTC	78.8167	-6.15	3	96	7	14	338	-19	-2
2022-04-25 16:05:00 UTC	78.8333	-5.9833	1	97	1	16	352	-19	-2
2022-04-25 14:53:00 UTC	78.8333	-5.4833	3	96	6	24	353	-20	-2
2022-04-25 14:00:00 UTC	78.8167	-5.3667	1	96	3	23	343	-19	-2
2022-04-25 12:03:00 UTC	78.8167	-5	2	96		20	246	-18	-2
2022-04-25 11:04:00 UTC	78.8	-4.8333	2	96	6	28	337	-18	-2
2022-04-25 10:09:00 UTC	78.7667	-4.3833	3	96	7	30	351	-17	-2
2022-04-25 09:22:00 UTC	78.75	-4	3	97	1	10	342	-16	-2
2022-04-25 05:00:00 UTC	78.7833	-3.9333	2	97	0	19	292	-15	-2
2022-04-25 04:00:00 UTC	78.7167	-3.7333	0	97		16	295	-2	-2
2022-04-25 03:09:00 UTC	78.7	3.4333	2	97	0	12	306	/	-2
2022-04-25 02:06:00 UTC	78.7167	-3.4	0	97	0	14	212	-17	-2
2022-04-25 01:00:00 UTC	78.7333	3.3833	0	97	0	16	337	-15	-2
2022-04-25 00:00:00 UTC	78.75	-3.3667	0	97	0	16	337	-15	-2
2022-04-24 23:00:00 UTC	78.46	3.35	0	97	0	18	241	-17	-2
2022-04-24 22:00:00 UTC	78.7833	3.3333	0	97	0	18	200	-17	-2
2022-04-24 21:00:00 UTC	78.8	3.35	/	97		13	210	-17	-2
2022-04-24 20:00:00 UTC	78.8167	-3.0167	3	97	3	25	192	-15	-2
2022-04-24 17:00:00 UTC	78.85	3.0167	2	97	1	20	346	-12	-2
2022-04-24 12:00:00 UTC	78.8333	2.4667	2	97	2	14	240	-13	-2
2022-04-24 11:00:00 UTC	78.8667	1.9833	2	97	2	8	173	-12	-2
2022-04-24 07:00:00 UTC	78.8667	1.7833	2	97	1	8	250	-16	-1
2022-04-24 06:00:00 UTC	78.9833	-1.45	2	97	1	5	284	-16	-1
2022-04-24 05:00:00 UTC	78.8333	-2.05	0	97	0	12	340	-13	-1
2022-04-24 02:00:00 UTC	78.8167	-0.8667	0	97	0	10	340	-13	-1
2022-04-24 01:00:00 UTC	78.8167	-0.8667	0	95	1	22	340	-13	0
2022-04-24 00:00:00 UTC	78.8167	0.0167	1	95	2	24	340	-14	-1
2022-04-23 21:00:00 UTC	78.8333	0	3	97	6	24	341	-13	-1
2022-04-23 19:00:00 UTC	78.8333	0.25	3	97	6	27	341	-13	-1
2022-04-23 16:00:00 UTC	78.8333	1	/	97	6	22	347	-12	2
2022-04-23 15:00:00 UTC	78.8333	1.4833	11	97	5	22	353	-11	2
2022-04-23 14:00:00 UTC	78.8333	2	71	97	5	20	334	-11	-1

Sea ice observations

Hourly observations of the sea ice were carried out during transit times along the entire cruise route. The observation deck became the centre point for observations as it provided 360º views of the surrounding ice. However, for thicknesses, the observer moved down to the bridge on deck 8 to observe ice moving through a window facing directly down to the overturning ice where a one metre marker had been drawn onto the glass. If ridge height were difficult to ascertain from the upper decks, the observer moved down to deck 3 to see the ice from near sea level. All observations were first noted as a paper copy using the ASPeCt observation forms, and then transferred to the ASSIST software using the ASSIST defined observation criteria. This was done not only to have a physical copy of the observations, but also due to the need for manoeuvrability during observation taking. Figure 2.13.4 shows some of the observation techniques used.

Figure 2.13.4 *The left-hand image shows the downward facing window on the bridge with one metre marker, allowing the observer to estimate ice thicknesses as the ice overturns alongside the vessel. The top right image shows a fantastic example of pancake ice from deck 3 where it was easier to make the distinction as to whether the pancakes were cemented or rafter or not. The bottom right image shows how snow thicknesses were estimated after the ship had broken through the ice. There is a clear distinction between the snow layer and ice layer. All photos: William Copeland (MET).*

The parameters used to characterise the ice are shown in figure 2.13.5. It is important to remember that due to the dynamic nature of sea ice, not every characteristic is possible to identify in the 10 minute observation period, but a best estimate is given. If a significant change in sea ice occurred during the 50 minute observation blind spot, it was noted in the notes section of the next observation with time and location or a new observation was taken.

ICE TYPE (ty)

10	Frazil
11	Shuga
12	Grease
20	Nilas
30	Pancakes
40	Young grey ice, 0.1-0.15 m
50	Young grey-white ice, 0.15-0.3 m
60	First year, 0.3-0.7 m
70	First year, 0.7-1.2 m
80	First year, >1.2 m
85	Multiyear floes
90	Brash
95	Fast ice

ICE CONC^n (c)
to be expressed in tenths

SEA ICE (z) AND SNOW THICKNESS (sz)
to be expressed in centimetres

FLOE SIZE (f)

100	Pancakes
200	New sheet ice
300	Brash/broken ice
400	Cake ice, <20 m
500	Small floes, 20-100 m
600	Medium floes, 100-500 m
700	Large floes, 500-2000 m
800	Vast floes, >2000 m

TOPOGRAPHY (t)

100	Level ice
200	Rafted pancakes
300	Cemented pancakes
400	Finger rafting
5xy	New, unconsolidated ridges (no snow)
6xy	New ridges filled with snow or a snow cover
7xy	Consolidated ridges (no weathering)
8xy	Older, weathered ridges

x values:

0	0-10% areal coverage
1	10-20%
2	20-30%
3	30-40%
4	40-50%
5	50-60%
6	60-70%
7	70-80%
8	80-90%
9	90-100%

y values:

1	0.5 m av. sail height
2	1.0 m
3	1.5 m
4	2.0 m
5	3.0 m
6	4.0 m
7	5.0 m

SNOW TYPE (s)

0	No snow observation
1	No snow, no ice or brash
2	Cold new snow, <1 day old
3	Cold old snow
4	Cold wind-packed snow
5	New melting snow (wet new snow)
6	Old melting snow
7	Glaze
8	Melt slush
9	Melt puddles
10	Saturated snow (waves)
11	Sastrugi

OPEN WATER

0	No openings
1	Small cracks
2	Very narrow breaks, <50m
3	Narrow breaks, 50-200 m
4	Wide breaks, 200-500 m
5	Very wide breaks, >500 m
6	Lead/coastal lead
7	Polynya/coastal polynya
8	Water broken only by small scattered floes
9	Open sea

Figure 2.13.5 ASPeCt Codes used to record ice observations manually before converting the data into the ASSIST software.

Sea ice observations are very much a subjective analysis of the ice. This is why all new observers spent time with an experienced member of the team to gain both the knowledge needed and to train their eyes to identify concentration, ice types (with corresponding characteristics) and snow characteristics. During 'on station' days, all data was reviewed and double checked for continuity, error and follow up if needed.
Due to the sheer amount of data collected from sea ice observations, only the total concentration (TC), primary ice type (P, ice type) and primary (largest thickness) are included in table 2.13b. For the secondary and tertiary data and more, please see the full dataset at the IceWatch website (https://icewatch.met.no/cruises/130).

Table 2.13b *Sea ice observation data showing Total Concentration (TC), Primary ice type (P. Ice type) and the corresponding greatest thicknesses (GT).*

Date and time	LAT	LON	TC (Tenths)	P. Ice type	PT (cm)
2022-05-08 13:00:00 UTC	78.8333	6.5	2	90	140
2022-05-08 10:30:00 UTC	78.8333	5.6333	1	90	50
2022-05-08 10:00:00 UTC	78.8333	5.15	1	50	20
2022-05-08 08:59:00 UTC	78.8333	5	1	50	20
2022-05-08 08:03:00 UTC	78.8	4.2	4	60	30
2022-05-08 07:00:00 UTC	78.8333	4	7	70	70
2022-05-08 05:57:00 UTC	78.8333	3.7	8	60	30
2022-05-08 05:01:00 UTC	78.8167	3.3	8	60	30
2022-05-08 03:03:00 UTC	78.8333	2.8	8	60	30
2022-05-08 02:01:00 UTC	78.8333	2.4167	7	70	70
2022-05-08 01:02:00 UTC	78.8333	1.9833	5	70	100
2022-05-08 00:11:00 UTC	78.8667	1.4333	2	80	200
2022-05-07 23:00:00 UTC	78.8333	0.3017	2	60	50
2022-05-07 22:04:00 UTC	78.8	0.2833	8	70	70
2022-05-07 20:54:00 UTC	78.8167	-0.3333	7	60	40
2022-05-07 19:53:00 UTC	78.8	-0.9833	9	60	30
2022-05-07 18:51:00 UTC	70.8	-1.4	9	70	100
2022-05-07 18:00:00 UTC	78.85	-1.8667	7	70	70
2022-05-07 17:00:00 UTC	78.9667	-1.85	8	85	210
2022-05-07 16:00:00 UTC	79.0333	-1.8667	8	80	180
2022-05-07 15:00:00 UTC	79.1	-2.05	8	80	180
2022-05-07 13:59:00 UTC	79.15	-2.4167	10	60	50
2022-05-07 13:01:00 UTC	79.2167	-2.8667	8	80	200
2022-05-07 12:10:00 UTC	79.2667	-3.25	10	80	200
2022-05-07 11:15:00 UTC	79.3667	-3.3667	9	60	70
2022-05-07 05:00:00 UTC	79.4667	-3.2667	10	70	80
2022-05-07 04:00:00 UTC	79.3833	-3.2333	9	40	8
2022-05-07 03:00:00 UTC	79.3333	-3.4833	10	60	40
2022-05-07 01:55:00 UTC	79.2333	-3.4667	10	60	40
2022-05-07 00:59:00 UTC	79.1167	-3.2833	6	30	5
2022-05-06 23:52:00 UTC	79	-3.0667	8	50	15
2022-05-06 23:03:00 UTC	78.9333	-3.25	4	30	5
2022-05-06 21:53:00 UTC	79	-3.7667	8	50	15
2022-05-06 20:53:00 UTC	78.95	-4.25	4	60	30
2022-05-06 20:01:00 UTC	78.9333	-4.6667	10	60	30
2022-05-06 18:50:00 UTC	78.9167	-4.9667	8	60	30
2022-05-06 17:53:00 UTC	78.85	-5.3167	3	60	50
2022-05-06 17:06:00 UTC	78.8667	-5.7667	7	60	30
2022-05-06 16:06:00 UTC	78.8833	-6.2167	10	60	50
2022-05-06 15:15:00 UTC	78.9167	-6.3667	10	70	150
2022-05-06 14:16:00 UTC	78.9	-6.4167	9	70	80
2022-05-06 13:00:00 UTC	78.9	-6.4667	10	75	200
2022-05-06 10:08:00 UTC	78.9167	-6.5167	10	85	350
2022-05-06 08:58:00 UTC	78.9167	-6.3	10	85	200
2022-05-06 06:00:00 UTC	78.85	-6.4667	10	70	100
2022-05-06 05:00:00 UTC	78.9	-6.7167	9	70	100
2022-05-06 04:00:00 UTC	78.9333	-6.8833	10	85	200
2022-05-06 03:00:00 UTC	78.9667	-7.15	10	80	130
2022-05-06 02:02:00 UTC	79.0022	-7.1833	10	80	120

Date and time	LAT	LON	TC (Tenths)	P. Ice type	GT (cm)
2022-05-06 01:00:00 UTC	79.05	-7.05	9	85	200
2022-05-06 00:05:00 UTC	79.1167	-6.9	8	60	50
2022-05-05 23:05:00 UTC	79.2167	-7.05	10	50	25
2022-05-05 22:00:00 UTC	79.35	-7.0833	10	50	20
2022-05-05 21:08:00 UTC	79.4667	-7.1833	10	40	20
2022-05-05 20:01:00 UTC	79.6167	7.3167	9	40	15
2022-05-05 19:00:00 UTC	79.7	-7.21	10	50	30
2022-05-05 17:00:00 UTC	79.7333	-7	9	50	30
2022-05-05 16:00:00 UTC	79.7333	-6.7667	7	50	30
2022-05-05 15:00:00 UTC	79.7167	-6.4	10	85	500
2022-05-04 18:00:00 UTC	79.7833	-6.45	9	85	500
2022-05-04 16:00:00 UTC	79.7833	-6.65	9	85	530
2022-05-04 14:00:00 UTC	79.8	-6.6667	9	85	500
2022-05-04 13:00:00 UTC	79.8833	-6.9	9	30	30
2022-05-04 12:02:00 UTC	79.95	-7.2	9	85	250
2022-05-04 10:58:00 UTC	79.9667	-7.7167	8	20	5
2022-05-04 10:06:00 UTC	80.0667	-7.8833	8	85	250
2022-05-04 06:02:00 UTC	80.0667	-7.7333	8	85	300
2022-05-04 04:00:00 UTC	80.0667	-7.9667	9	85	400
2022-05-04 03:00:00 UTC	80.0167	-7.8833	8	85	350
2022-05-04 02:00:00 UTC	79.95	-7.55	9	85	400
2022-05-04 01:00:00 UTC	79.9333	-7.5	9	30	10
2022-05-04 00:00:00 UTC	79.9333	-7.4333	8	85	400
2022-05-03 23:00:00 UTC	79.8667	-6.95	9	40	12
2022-05-03 21:56:00 UTC	79.8517	-6.5333	8	85	300
2022-05-03 21:02:00 UTC	79.85	-6.8333	9	40	10
2022-05-03 19:56:00 UTC	79.8667	-7.1167	8	40	10
2022-05-03 18:55:00 UTC	79.85	-7.55	7	30	5
2022-05-03 18:29:00 UTC	79.8667	-8.0667	3	30	5
2022-05-03 17:21:00 UTC	79.8667	-8.0667	1	12	3
2022-05-03 16:03:00 UTC	79.8667	-8.7833	5	70	90
2022-05-03 11:00:00 UTC	79.8667	-8.8	7	70	90
2022-05-03 10:00:00 UTC	79.8333	-8.6333	2	11	1
2022-05-03 09:00:00 UTC	79.7333	-8.0167	8	30	25
2022-05-03 08:00:00 UTC	79.6333	-7.6667	9	50	25
2022-05-03 07:00:00 UTC	79.5333	-7.3667	10	50	30
2022-05-03 06:00:00 UTC	79.45	-7.2833	9	50	30
2022-05-03 04:57:00 UTC	79.35	-7.1833	9	50	20
2022-05-03 04:01:00 UTC	79.3167	-7.1167	9	50	30
2022-05-03 03:05:00 UTC	79.25	-7.2333	10	85	220
2022-05-03 02:05:00 UTC	79.25	-7.2667	10	85	250
2022-05-03 01:05:00 UTC	79.25	-7.2833	8	85	200
2022-05-02 23:58:00 UTC	79.2333	-8.35	9	85	300
2022-05-02 23:00:00 UTC	79.2167	-7.3167	9	85	300
2022-05-02 22:00:00 UTC	79.2167	-7.3167	9	85	310
2022-05-02 21:00:00 UTC	79.2167	-7.5	9	85	300
2022-05-02 20:00:00 UTC	79.2333	-7.4833	9	85	300
2022-05-02 19:00:00 UTC	79.25	-7.45	9	85	300
2022-05-02 18:00:00 UTC	79.25	-7.4667	9	85	300
2022-05-02 17:07:00 UTC	79.2167	-7.5833	9	85	250
2022-05-02 16:00:00 UTC	79.2	-7.6833	9	85	310

Date and time	LAT	LON	TC (Tenths)	P. Ice type	GT (cm)
2022-05-02 15:09:00 UTC	79.1667	-7.8333	10	80	120
2022-05-02 14:06:00 UTC	79.1667	-7.8834	9	85	250
2022-05-02 12:00:00 UTC	79.1333	-7.9667	9	85	340
2022-05-02 11:00:00 UTC	79.1333	-7.9667	9	85	340
2022-05-02 10:00:00 UTC	79.0833	-8.0833	9	85	230
2022-05-02 09:00:00 UTC	79.1167	-8.15	9	/	230
2022-05-02 08:00:00 UTC	79.1167	-8.15	9	85	250
2022-05-02 07:00:00 UTC	78.1333	-8.1333	9	85	210
2022-05-02 05:59:00 UTC	79.1333	-8.1167	10	85	135
2022-05-02 05:02:00 UTC	79.1167	-8.3167	7	60	55
2022-05-02 04:08:00 UTC	79.15	-8.35	10	85	120
2022-05-02 03:04:00 UTC	79.1333	-8.6333	9	85	180
2022-05-02 02:00:00 UTC	79.15	-8.8333	6	30	5
2022-04-30 16:00:00 UTC	79.1667	-8.9	7	85	200
2022-04-30 15:00:00 UTC	79.15	-9.0167	9	40	10
2022-04-30 14:00:00 UTC	79.1333	-9.2167	8	50	60
2022-04-30 13:00:00 UTC	79.1167	-9.2167	9	60	60
2022-04-30 11:56:00 UTC	79.0833	-9.65	10	40	8
2022-04-30 10:51:00 UTC	79.1333	-9.6333	10	40	8
2022-04-30 10:07:00 UTC	79.2167	-9.5833	10	30	8
2022-04-30 08:06:00 UTC	79.25	-9.5833	9	50	20
2022-04-30 06:56:00 UTC	79.3167	-9.5667	9	50	15
2022-04-30 06:00:00 UTC	79.35	-9.6167	9	50	15
2022-04-30 05:00:00 UTC	79.4167	-10.0167	9	50	15
2022-04-30 04:00:00 UTC	79.3833	-10.2833	9	40	10
2022-04-30 03:00:00 UTC	79.3167	-10.15	9	20	7
2022-04-30 02:00:00 UTC	79.2667	-10.0667	9	50	15
2022-04-30 01:00:00 UTC	79.2167	-10.1	9	50	15
2022-04-30 00:04:00 UTC	79.15	-10.4	10	50	15
2022-04-29 23:14:00 UTC	79.15	-10.4167	10	50	15
2022-04-29 21:59:00 UTC	79.0833	-10.7333	9	50	15
2022-04-29 21:10:00 UTC	79.0167	-10.9	10	80	90
2022-04-29 20:09:00 UTC	78.9667	-11.0667	9	70	80
2022-04-29 19:05:00 UTC	78.8833	-11.295	9	50	15
2022-04-29 18:01:00 UTC	78.8192	-11.4694	9	60	70
2022-04-29 17:02:00 UTC	78.7558	-11.6594	8	60	70
2022-04-29 16:10:00 UTC	78.6872	-11.9992	8	60	40
2022-04-29 06:11:00 UTC	78.6667	-12.1833	10	60	45
2022-04-27 09:13:00 UTC	78.6667	-12.2	10	60	60
2022-04-27 06:57:00 UTC	78.65	-12.1167	10	60	35
2022-04-27 06:01:00 UTC	78.69	-11.9544	7	50	30
2022-04-27 04:52:00 UTC	78.7514	-11.6333	9	60	40
2022-04-27 04:04:00 UTC	78.8347	-11.4875	10	60	40
2022-04-27 03:01:00 UTC	48.8167	-11.4333	9	60	50
2022-04-27 02:00:00 UTC	78.8333	-11.0833	10	60	50
2022-04-27 01:00:00 UTC	78.8333	-10.9333	10	50	30
2022-04-27 00:00:00 UTC	78.85	-10.3	9	50	20
2022-04-26 23:00:00 UTC	78.8667	-10	10	50	17
2022-04-26 21:59:00 UTC	78.8642	-9.55	10	50	15
2022-04-26 21:00:00 UTC	78.8667	-9.0167	10	70	110
2022-04-26 19:03:00 UTC	78.8167	-8.9833	10	70	100

Date and time	LAT	LON	TC (Tenths)	P. Ice type	GT (cm)
2022-04-26 17:59:00 UTC	78.75	-9.3333	10	60	30
2022-04-26 16:59:00 UTC	78.6833	-9.35	9	70	70
2022-04-26 16:08:00 UTC	78.6667	-9.0167	10	60	20
2022-04-26 15:07:00 UTC	78.6833	-8.6	10	60	20
2022-04-26 14:04:00 UTC	78.6667	-8.5333	10	60	20
2022-04-26 12:00:00 UTC	78.6667	-8.3333	10	70	150
2022-04-26 11:06:00 UTC	78.6667	-8.25	10	60	50
2022-04-26 09:20:00 UTC	78.6667	-8	9	50	15
2022-04-26 07:57:00 UTC	78.6667	-7.9	10	50	15
2022-04-26 06:58:00 UTC	78.5833	-7.23	9	50	15
2022-04-26 05:02:00 UTC	78.5833	-7.3	9	80	190
2022-04-26 04:00:00 UTC	78.5833	-7.2	10	60	30
2022-04-26 03:09:00 UTC	78.5833	-6.85	9	60	30
2022-04-26 02:05:00 UTC	78.6333	-6.4333	4	60	30
2022-04-26 01:09:00 UTC	78.75	-6.45	5	60	40
2022-04-26 00:04:00 UTC	78.75	-6.4833	6	70	120
2022-04-25 23:07:00 UTC	78.75	6.4833	7	70	120
2022-04-25 22:12:00 UTC	78.46	-6.36	10	70	100
2022-04-25 21:00:00 UTC	78.7833	-6.6	9	70	100
2022-04-25 20:00:00 UTC	78.8167	-6.2667	10	70	90
2022-04-25 19:00:00 UTC	78.8333	-6.2667	10	60	50
2022-04-25 18:01:00 UTC	78.8167	-6.15	10	60	50
2022-04-25 16:05:00 UTC	78.8333	-5.9833	10	80	120
2022-04-25 14:53:00 UTC	78.8333	-5.4833	6	30	5
2022-04-25 14:00:00 UTC	78.8167	-5.3667	5	40	5
2022-04-25 12:03:00 UTC	78.8167	-5	8	40	5
2022-04-25 11:04:00 UTC	78.8	-4.8333	8	40	15
2022-04-25 10:09:00 UTC	78.7667	-4.3833	9	50	10
2022-04-25 09:22:00 UTC	78.75	-4	9	80	150
2022-04-25 05:00:00 UTC	78.7833	-3.9333	9	70	80
2022-04-25 04:00:00 UTC	78.7167	-3.7333	9	60	40
2022-04-25 03:09:00 UTC	78.7	-3.4333	9	80	150
2022-04-25 02:06:00 UTC	78.7167	-3.4	9	80	150
2022-04-25 01:00:00 UTC	78.7333	-3.3833	10	80	120
2022-04-25 00:00:00 UTC	78.75	-3.3667	10	80	120
2022-04-24 23:00:00 UTC	78.46	-3.35	10	80	150
2022-04-24 22:00:00 UTC	78.7833	-3.3333	10	80	150
2022-04-24 21:00:00 UTC	78.8	-3.35	9	80	150
2022-04-24 20:00:00 UTC	78.8167	-3.0167	8	80	120
2022-04-24 17:00:00 UTC	78.85	-3.0167	8	80	200
2022-04-24 12:00:00 UTC	78.8333	-2.4667	8	70	100
2022-04-24 11:00:00 UTC	78.8667	-1.9833	9	70	100
2022-04-24 07:00:00 UTC	78.8667	-1.7833	9	70	120
2022-04-24 06:00:00 UTC	78.9833	-1.45	9	70	120
2022-04-24 05:00:00 UTC	78.8333	-2.05	4	90	200
2022-04-24 02:00:00 UTC	78.8167	-0.8667	6	90	150
2022-04-24 01:00:00 UTC	78.8167	-0.8667	2	60	150
2022-04-24 00:00:00 UTC	78.8167	-0.0167	0	/	/
2022-04-23 21:00:00 UTC	78.8333	0	0	/	/
2022-04-23 19:00:00 UTC	78.8333	0.25	0	/	/
2022-04-23 16:00:00 UTC	78.8333	1	0	80	120
2022-04-23 15:00:00 UTC	78.8333	1.4833	0	90	50
2022-04-23 14:00:00 UTC	78.8333	2	2	80	120

Photography

Each observation is complemented with three photos, one from the port, front and starboard side of the vessel (Figure 2.13.6). Photos are later used for validation checks, testing of algorithms aiming to decipher ice concentration from photography and simply to provide a visual representation of ice conditions at each location. In total, over 600 photos were taken during the cruise.

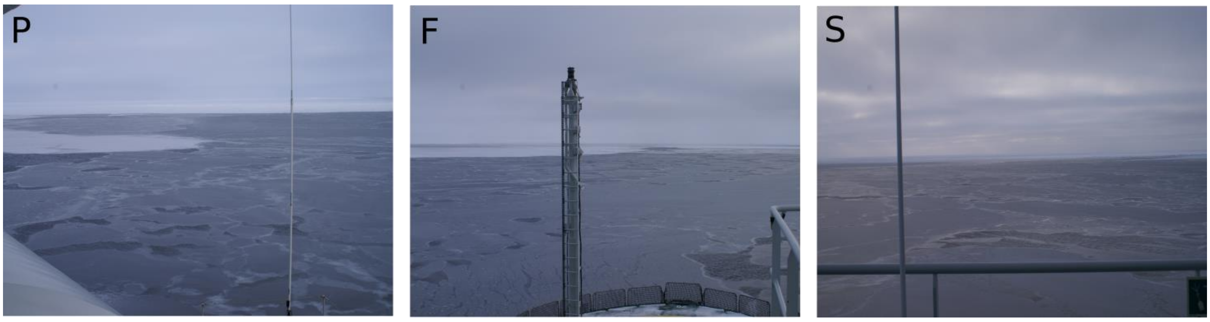

Figure 2.13.6 *Three photos taken as part of sea ice observation. One from port (P), forward (F) and starboard (S) side of the vessel. Photos are not taken towards the aft due to the effect of the ship movement on the ice. All photos: William Copeland (MET).*

Ice Watch App

Due to the advanced requirements of the ASSIST software, the Polar Citizen Science Collective (PCSC) group and MET Norway created the Ice Watch APP. The app is a simplified version of the ASSIST software, and allows for citizen scientists to contribute data to the Ice Watch system using their mobile phones and without the need for long-term experience of sea ice observations. Within the app, location and time data are recorded automatically, meanwhile the user can create and manage datasets and take photos, all on their own mobile device.

During the CIRFA 2022 cruise, the app was trialled for ease of use. This was the first time the app was used on a regular basis for observations over such a long time period. The experience and feedback gained from using the app will be transferred to the developers and discussed in terms of successes, future improvements and recommendations.

Future use of the ice observation data

Ice Watch data is open source and available for anyone to download and use as they wish. The dataset from this cruise will join thousands of observations that are part of the Ice Watch catalogue. The data store provides a means of validation and calibration of data from the Copernicus Sentinel satellites and other Earth Observation missions, where the lack of routine spatially and temporally coincident data from the Polar Regions hinders the development of automatic classification products, which are becoming increasingly sought after by both operational services and end users alike. At MET Norway, in-situ data will also be incorporated into the ice charting systems to improve products we generate for our end users.

2.14. Meteorological forecasts

Team: William Copeland (MET Norway) and Trond Robertsen (MET Norway)

Weather forecasts provide an important tool for planning and navigation during any type of expedition, especially in areas where there is a lack of internet connection. Weather updates were provided by MET Norway and assessed by the team to provide a detailed forecast for the days ahead.

Forecasts from MET Norway and additional resources

Daily text forecasts for the Belgica Bank area were provided via email from the Meteorological Institute in Tromsø. The forecast format can be seen below in figure 2.14.1.

Issued by MET Norway, Forecasting Division in Northern Norway: Sunday, May 1 at 12:00 .

Low 1001 hPa 72 N 05 W, moving SE and expected 989 hPa at 69 N 21 E Monday 06 utc.
High 1045 hPa 78 N 48 W, moving SE and expected 1038 hPa at 75 N 32 W Monday 06 utc.

Forecast valid until Sunday at 24
Belgica Bank N
West and northwest force 2 to 4, in the afternoon and evening in the north and northeasternmost part force 5 to 6. Dry and good, some clouds in the evening.
Temperature: -10 to -16.

Forecast valid Monday
Belgica Bank N
Northwest force 3 to 5, in the afternoon and evening force 6 in the north and eastern part.
Light snow in the northernmost part with moderate, else dry and mainly good.
Some clouds, mainly in the north and east.
Temperature: -9 to -15.

Forecast valid Tuesday
Belgica Bank N
Northwest force 3 to 5, in eastern part force 6 until afternoon.
Light snow in the northernmost part with moderate until forenoon, else dry and good.
Some clouds, less in the afternoon.
Temperature: -9 to -15.

Figure 2.14.1 *Example of text forecast sent by MET Norway. Using this information, forecasts were created alongside low-resolution MODIS satellite imagery and synoptic charts. The baseline model for forecasts was the AROME-Arctic model, which is one of the Norwegian Meteorological Institute's own products. Other models used to create forecasts while onboard included the ECMWF, ICON Global and GFS. The reason for using these additional* *models was due to the area in which the ship was navigating. The Belgica Bank area has only one automatic meteorological station nearby (Henrik Krøyer Holme, 80°38'N 13°43'W, run by the Danish Meteorological Institute) for in-situ data for model verification. Hence, it was useful to get a second or third opinion on the forecasts we were receiving from MET Norway in Tromsø to analyse which model was handling the local conditions as reliably as possible within the normal margin of error. And to indicate the full range of possibilities for any given day.*

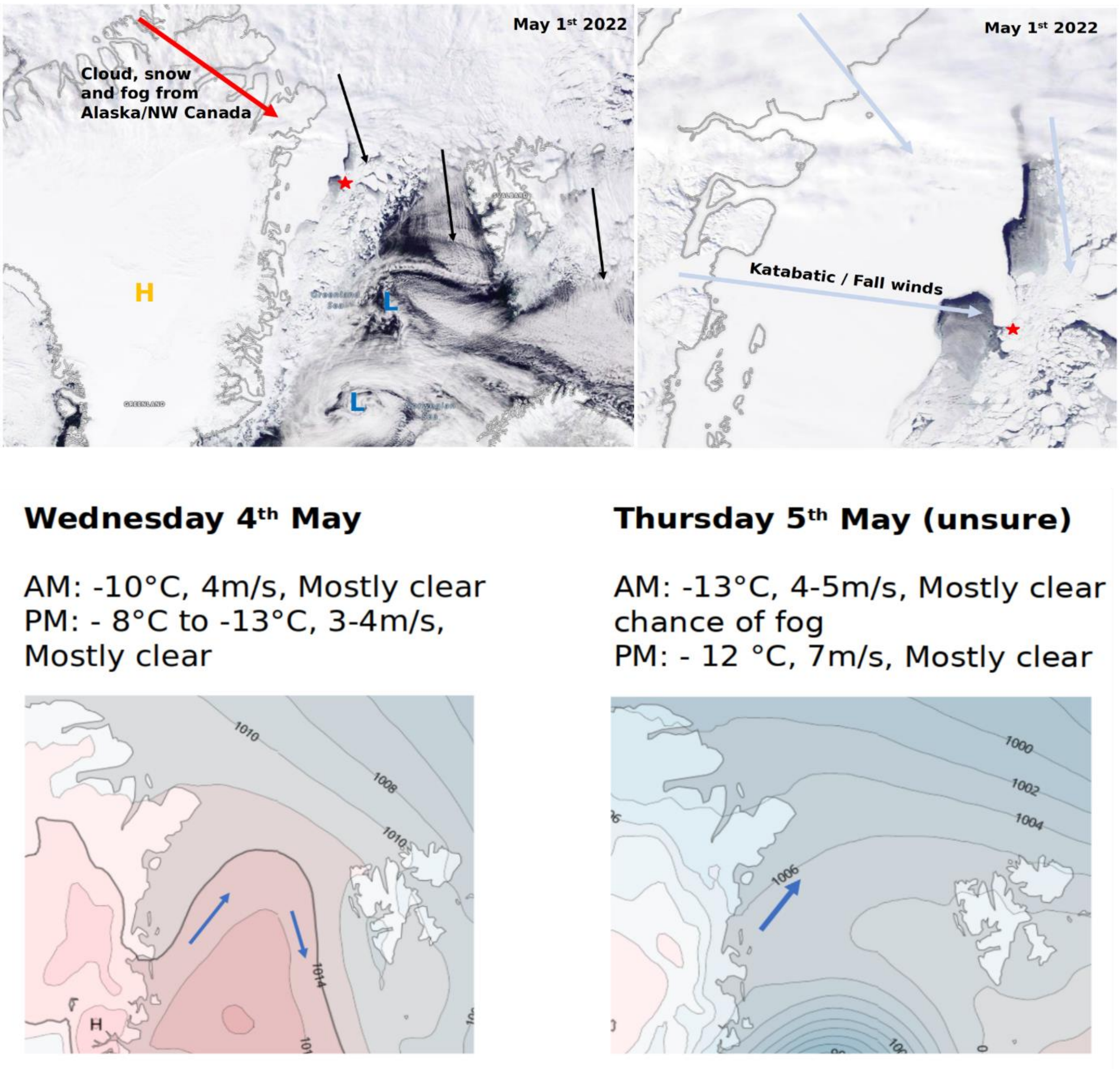

***Fig 2.14.2** Examples of slides shown during evening meetings onboard, created during the day to show the overall weather pattern and why we experienced the conditions we did. Satellite imagery, adapted NASA-Terra MODIS accessed 01/05/2022 and Synoptic charts, adapted ECMWF model projection from meteoblue.com.*

Weather setup over the cruise track 22nd April to 8th May, 2022

Weather conditions were mainly reliant on ship location rather than the overall weather set up over the region. The entire period was characterised by a large high-pressure system over Greenland with low pressure systems moving from north to south east across the Svalbard region, with the polar vortex anchored to the north east of Svalbard. This meant that when the ship was at its most westerly location (Ice Station 1), the weather was controlled by the high-pressure system and clear skies with cold temperatures were observed. While any deviation to the east opened up the risk of increased wind from the north west, moisture (fog) and cloud amounts. During the first days of May, a pulse of warm air around the high-pressure system from north west Canada resulted in higher cloud amounts, a moderate fall wind from the north west and some snowfall in the early hours of the 2nd May. The final shift came between 4-5th May, when a small high-pressure core moved out into the southern Fram Strait, meaning weak south westerly winds affected the Belgica Bank region. On the 6th May there was a standstill, with light winds throughout the morning caused by an incoming shift to north westerly winds. This resulted in a bank of thick fog across the southern Belgica Bank region which caused significantly reduced visibility for a time. Between the 7th - 9th May we were in transit between the Greenland shelf and Svalbard where we encountered steadily strengthening northerly winds. A low-pressure system centred to the east of Svalbard was dragging these northerly winds along the western Svalbard coast bringing snow showers and high cloud amounts

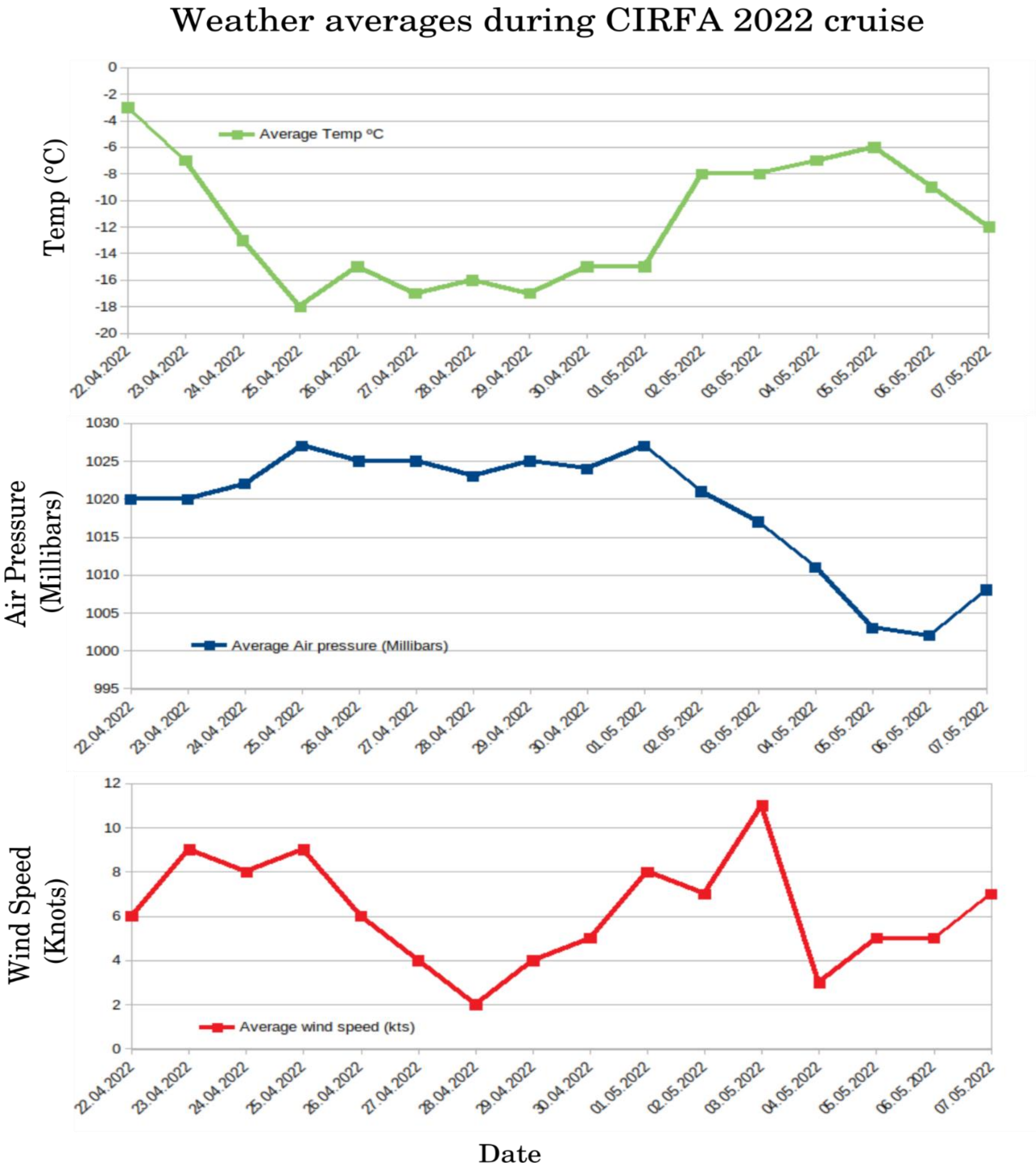

Figure 2.14.3 *Daily averages of temperature, air pressure and wind up to the 7th May, 2022.*

A photographic representation of weather conditions is given in figure 2.14.4. Days with multiple photos represent shifts in weather patterns throughout the day or specifically interesting phenomena. For example, on the 27th April, a mirage caused by a temperature inversion under the high-pressure system resulted in distant icebergs being mirrored into the sky. And then on the 6th May, thick fog was present for much of the day, however by the evening the fog had dispersed. The 8th May is not included because conditions were the same as on 7th May with heavy snow showers and a gusty northerly wind, this was also a date where few observations were taking place and therefore photography was sparse.

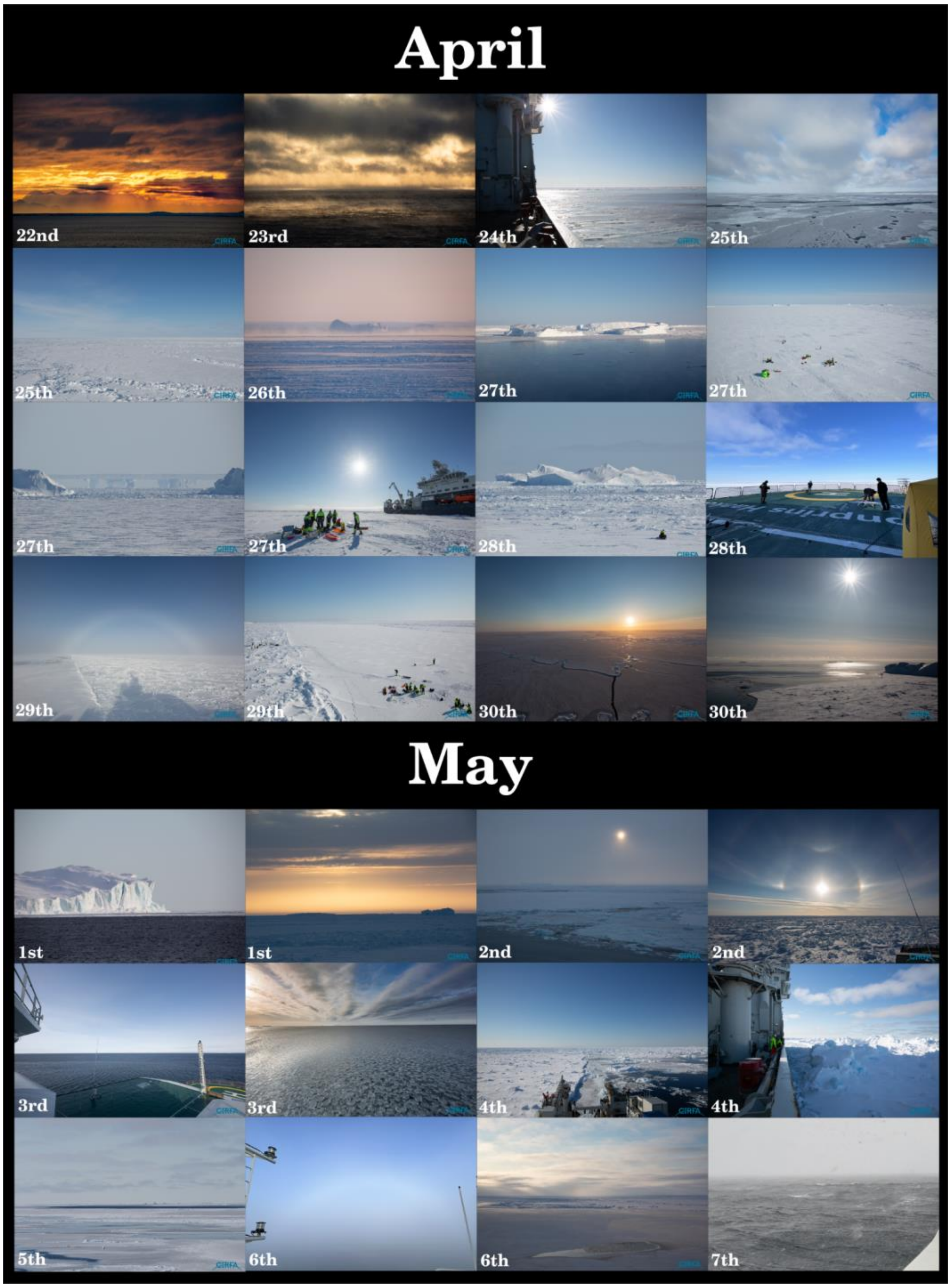

Figure 2.14.4 *A photographic calendar style representation of weather conditions for each day of the cruise. All photos: William Copeland (MET).*

3 Safety aspects

Team: Christian Zoelly (NPI) and Sebastian Gerland (NPI)

In advance of the expedition and while at sea/on the ice, we followed the safety routines listed below, and adjusted to the respective conditions.

In advance:

- Risk assessments for all activities with potential of accidents were written and gone through by the respective teams.
- Training of sea ice work and use of potentially dangerous equipment (e.g. drills, rotating tools) in February on fjord sea ice near Tromsø.
- First aid courses and refresher first aid training on the mainland and during transit,
- Survival suit course ("draktkurs") for all participants,
- Theoretical and practical polar bear safety training in Longyearbyen for those who were supposed to handle firearms for polar bear guarding,
- UiT participants completed compulsory online safety courses (HMS 501; 502; 503),
- Covid-19: Our cruise occurred during a time with eased covid restrictions without quarantine and testing requirements. However, we agreed on our own measures: We encouraged all participants to be careful and test themselves ahead of the cruise, and we used facemasks during travel to Svalbard ahead of the cruise.

During the expedition:

- IceWatch personnel from MET Norway supplied valuable weather updates with focus on air temperature, wind speed and direction, and fog/visibility.
- During the expedition, we had daily evening meetings to summarise the day, plan the next day(s), have detailed weather updates, and discuss potential adjustments in work and/or safety routines.
- When people were working on the ice, we had at least 3 people with binoculars on the bridge looking for polar bears in the area, plus one coordinator to communicate the status with crew and teams on the ice. We kept a list of people accessing the ice and returning to the ship with names and times.
- Each group on the sea ice had at least one dedicated polar bear guard with firearm (rifle) and flare gun nearby. Only guards with the respective course training and permit from Tromsø police were actually guarding.
- Before accessing any sea ice, the thickness was checked and cracks observed closely.
- For longer ice work with several groups on the ice, we placed flags in 100 m intervals to better estimate distances, had one or more polar bear guards on the ice, and 3 bridge watches. All groups that worked on the ice carried a VHF radio, first aid kit, extra clothes, a thermos bottle with hot drinks, and snacks.

- The choice of required clothing on an ice station was made after the ice was assessed. Buoyant clothing was always required (respective survival suit, regatta suit, or other warm clothing with additional life vest).
- On the only foggy day, we waited for visibility to improve, allowed work only by a limited team and close to the ship, and doubled the number of bear watch people on board. Three additional people were placed outside and a bit lower than bridge level outside on deck (at the helideck and searchlights at the stern of the ship) equipped with binoculars and VHF radios.
- In areas with less good overview to spot potential polar bears, drone flights were used to check for bears before accessing the ice. In addition, we used 2 skidoos to patrol larger areas.
- When working on landfast sea ice, the ship was usually moved a short distance to the ice to be in a stable position. When working on drifting sea ice, the ship was moored to the ice.
- Any other activities (e.g. IMB deployments by skidoo, sea ice sampling using the basket) had their own beforehand risk assessments, with increased levels of communication, updates and safety equipment to be taken along.
- Work on deck and in the working areas at the CTD hangar and moonpool area required to wear helmets and safety shoes. A rescue buoy and a ladder were moved close to the moonpool. Special instructions were given in connection with loading/unloading activity at ice stations, and during a mooring operation, when access to areas close to the main activity were limited.

4 Outreach activities during the expedition

Team: Andrea Schneider (UiT), Anca Cristea (NPI, shore-based support) and Kamilla Josefine Rudberg (MET, shore-based support)

During the expedition, the main research activities and insights to daily life on the vessel and when working on the ice were introduced in the form of a journal with selected photos, and published via social media to reach an audience beyond science. Articles and short stories were published daily except during weekdays on Facebook and Twitter, and were shared to other social media platforms by expedition participants, colleagues and friends. The Norwegian Polar Institute`s Oceanography and Sea Ice social media channel posted four additional posts about the CIRFA cruise, and the Norwegian Weather Forecast Service Yr has summarised our daily posts in Norwegian and shared the summaries on Facebook and Instagram. A printout of the posts was shared on board during the expedition.
To ensure that the outreach on social media is directly associated with CIRFA, the project logo was added to each published photograph along with the name of the photographer. Imagery from our partners is branded with the partner logo in addition.

Table 4.1 *Summary of the main Facebook posts from CIRFA and Yr. The numbers are as of May 18, 2022.*

Post title	**Date**	**Reach** Number of people that have seen a post.	**Engagements** Number of interactions made with a post (views, clicks, comments, likes, shares).
CIRFA Cruise Diary 1 – Here we go!	21 April	381	130
CIRFA Cruise Diary 2 – "It actually floats!"	25 April	413	99
CIRFA Cruise Diary 3 – On Ice Watch	26 April	108	93
CIRFA Cruise Diary 4 – Moon landings on Arctic sea ice	27 April	1185	189
CIRFA Cruise Diary 5 – A treasure box	29 April	277	47
CIRFA Cruise Diary 6 – Sleeping on board an icebreaker	2 May	160	34
CIRFA Cruise Diary 7 – On the ice	3 May	234	69

CIRFA Cruise Diary 8 – Grounded icebergs	4 May	1718	137
CIRFA Cruise Diary 9 – Expeditions inside an expedition	5 May	206	66
CIRFA Cruise Diary 10 – Drones at work	9 May	1985	192
CIRFA Cruise Diary 11 – New ways of looking ahead	12 May	95	103
CIRFA Cruise Diary 12 – This time it is about numbers!	13 May	197	86
YR Facebook summary posts in Norwegian, post 1	22 April 2022	17 196	151
YR Facebook summary posts in Norwegian, post 2	29 April 2022	13 264	40
Oceanography & Sea Ice NPI - CRUISE NEWS IN REAL TIME	27 April 2022	n/a	n/a
Oceanography & Sea Ice NPI - SLEEPING ONBOARD AN ICEBREAKER	29 April 2022	n/a	n/a
Oceanography & Sea Ice NPI - GROUNDED ICEBERGS	6 May 2022	n/a	n/a
Oceanography & Sea Ice NPI - DRAGON SCALES	13 May 2022	n/a	n/a

CIRFA Cruise Diary 1: Here we go!

On April 22, 33 researchers travel to the Eastern Fram Strait in the Atlantic Ocean. Our goal is to compare satellite data with real world observations of sea ice and snow, to collect data for oceanographic models, and to test new technology
We spent the past 3 months with refining our research plan, training how to use our instruments, safety training, packing and shipping our equipment, and endless paperwork. If we are lucky, we might now even meet the crown prince and princess of Norway, who have lend their name to our vessel *RV Kronprins Haakon*, and who are currently visiting Svalbard. To follow our adventures, keep an eye on the CIRFA cruise diary! ;)

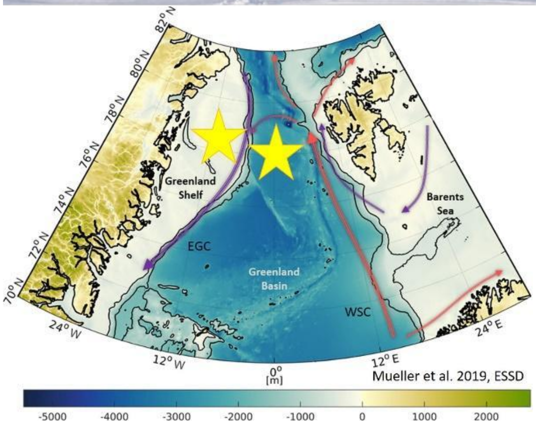

CIRFA Cruise Diary 2: It actually floats!

"It actually floats!" shouts Martina happily, tired after a long day but excited about her first data logger floating on the water surface while the ship slowly takes up speed.
In preparation of the cruise, Martina and her colleagues assembled 15 small boxes filled with a GPS antenna, a wave sensor, batteries, and satellite communication. After all the preparation, parts that help the drifters to stay afloat did not arrive before we left the harbor, with a sink being the only option to test if the instruments float by themselves. If they turn upside down or sink, they would not work.
A few hours after starting our cruise, the first instrument named "Isbjørn is" started its journey – proudly afloat in the vast ocean under the Arctic midnight sun on Friday night. On its journey, it will measure waves and surface currents, and send us its data. The new data tell researchers how good their ocean models are. The models can be used to calculate the movement of oil spills for clean ups, icebergs for navigation, man over board for search and rescue operations, plastic in the ocean, and many more practical applications. If "Isbjørn is" is lucky, it strands on a beach, eventually gets found and returned to Martina and her colleagues after its journey.
By now, six more instruments are successfully collecting data.



CIRFA Cruise Diary 3: On ice watch (Tuesday, 26 April)

There are news from the observation deck: We met the first ice about half a day earlier than what we had expected. It was first small and loose ice floes, but soon it became much denser, thicker, and very exciting with many different ice types, ridges, patterns in the snow from the wind, and polar bear tracks!

When observing the ice, we have to remind us constantly that what we see on the ocean surface is the "tip of the iceberg": Only one tenth of the thickness of the ice is visible. The majority of it is hidden below the water surface, and can harm ships and offshore installations.

Ice watch is a popular task on board that we do around the clock. MET Norway is even testing an app that can be used by tourists on cruise ships. Real world observations are important to compare with satellite images and automatically generated ice charts. This is the best way to improve remote and automated estimates, so that they can be used for navigation purposes.

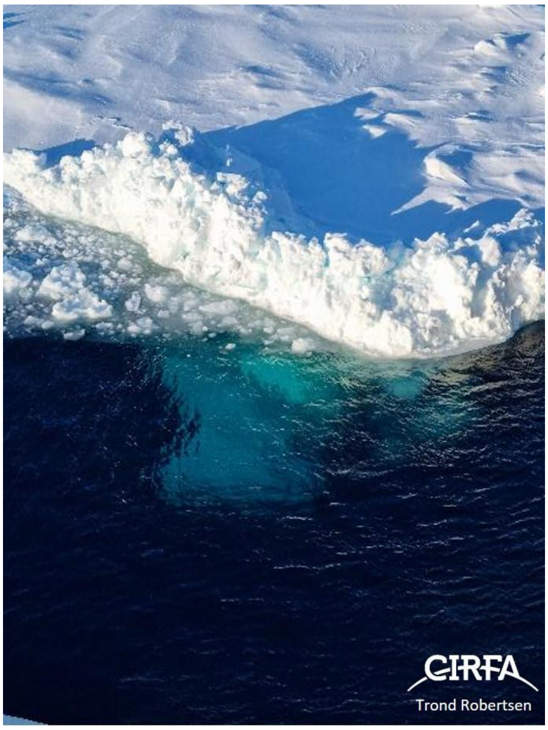

CIRFA Cruise Diary 4: Moon landings on Arctic sea ice (Wednesday, 27 April)

Have you ever witnessed a moon landing with your own eyes? As we are meeting thicker ice, researchers start working directly on the sea ice. Seen from the bridge, this reminds of a moon landing: Two researchers and a polar bear guard are lifted by a basket and a crane onto the ice. The first thing they do is to check if the ice is safe, before they walk ca. 100 m away, then do measurements, deploy a “drifter”, and return. The entire procedure takes about 30 minutes. While the people are on the ice, three people on the bridge watch out for polar bears all around the ship.
The tricky point is to park the icebreaker along the ice edge without making ever more cracks ;)
The drifter instruments that we deploy are tracking the movement of the ice and send the data to us via satellites. The instruments were assembled in the weeks leading up to the cruise with a data logger, batteries, a GPS and a satellite antenna inside. We expect them to send data for about 3 months. They are kept white to avoid attracting wildlife and heating up and melting into the snow, and they may also loose human smell after about two days. Comparing the sea ice situation around us with satellite images, and the data from the drifters help us getting a better understanding of sea ice dynamics.

CIRFA Cruise Diary 5: A treasure box

In research, data are valuable, especially from areas that are difficult to access. In addition to that, long-term data from such areas hold treasures!

NPI's Arctic Ocean Outflow Observatory in the Fram Strait was established over 30 years ago and is one of three long-term 'gateway' observatories that monitors the volumes of sea ice, freshwater, carbon and nutrients that enter or leave the Arctic Ocean through the Fram, Davis and Bering Straits.

Regular profiles of temperature and salinity, which are measured by lowering an instrument called a CTD from research vessels are a key part of the observatory. During the CIRFA cruise, *RV Kronprins Haakon* will cross the Fram Strait, stopping to collect a profile of temperature and salinity measurements every time it passes a degree of longitude. The CTD is lowered to the seafloor through a hole in the ship called a moonpool. At deep stations, the CTD takes ca. 1.5 hours to descend to the seafloor 2500 below the surface and another 1.5 hours to make the return trip.

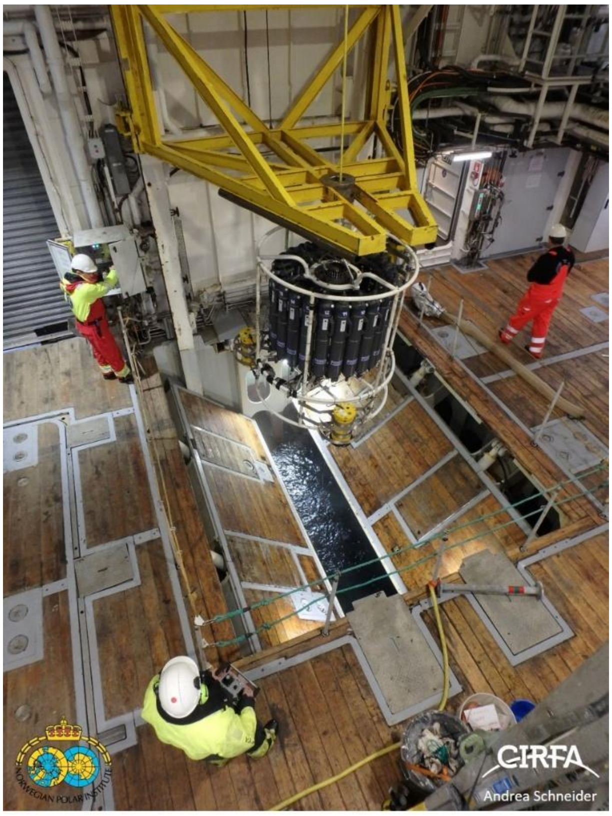

Annual CTD sections are usually made in late-summer around the sea ice minimum when ice conditions are more favourable. Opportunities to collect similar data around the sea ice maximum in spring are rare, but very valuable, as they allow us to put our summer measurements into an annual context.

The time series of data collected by moored instruments and CTD profiles is Fram Strait has revealed significant reductions in the thickness of sea ice passing out of the Arctic Ocean as well as variations in the amount of freshwater transported in the East Greenland Current that have the potential to affect deep water formation rates in the North Atlantic, which large-scale consequences for global climate.

CIRFA Cruise Diary 6: Sleeping on board an icebreaker

Now that *RV Kronprins Haakon* is breaking its way through the ice, the question "How did you sleep last night?" has an entirely new meaning. The else silent and stable sailing ship now sounds, rocks and rumbles when we meet thick ice, interrupted by stretches of smooth sailing through thin ice.

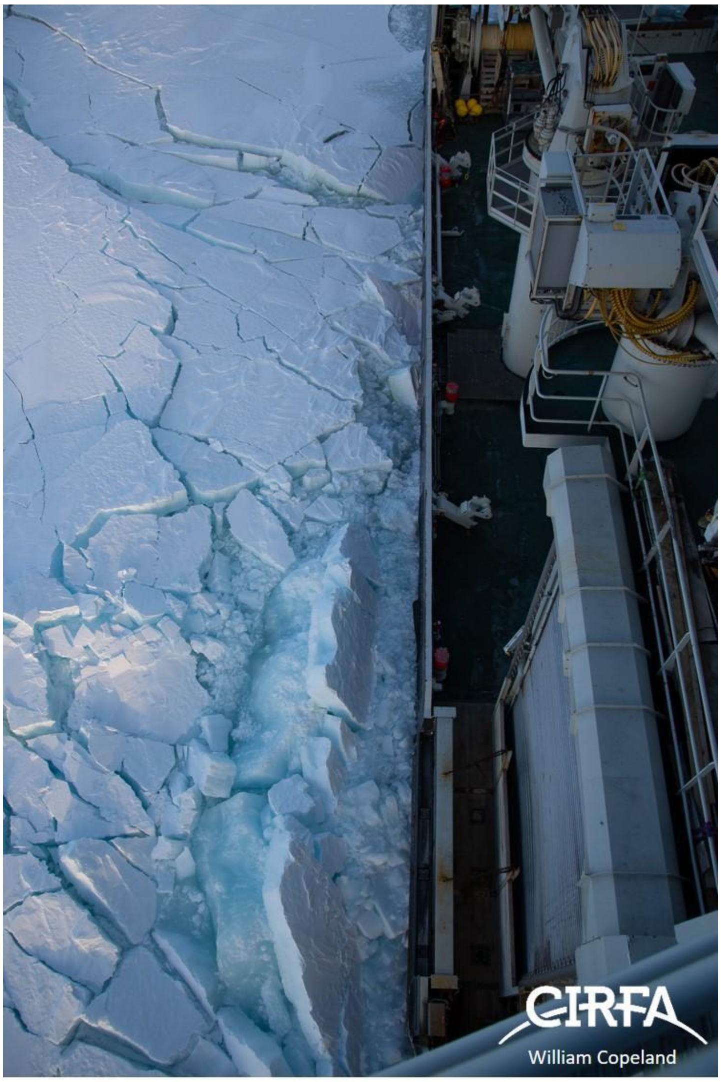

On the first night of icebreaking, some woke up, turned on the light, and kept checking how much water there might be on the floor in their cabin. Some felt like they were eaten by a whale and rumbled around in its stomach for hours, while others are discussing different types of earplugs in great detail.

The ship can navigate through quite thick ice. Through how thick ice can it go? This depends on how old (and thus how hard) the ice is and how much snow lies on it. However, more than once we had to turn around and find a new way.

Quite many of us are happy that the ship is parked now for a few days next to an ice floe where we will work on for longer – because we will sleep so peacefully ;)

And a video of the sound □

CIRFA Cruise Diary 7 – On the ice

After sailing through ice that is drifting southwards at any moment, we have now reached ice that nearly doesn't move. In addition, large icebergs that broke off from Greenland's glaciers are scattered around and touch the shallow seafloor at ca 150m water depth. These icebergs hold most of the sea ice in place and prevent it from drifting away. Our ship *RV Kronprins Haakon* is parked at a "dream beach" in between two of these icebergs. It is hard to imagine a more homey and scenic place on the sea ice-covered Ocean to spend the coming night and day :)

We are so excited to set our feet and instruments on the ice! All the time while being on the ice, we have several colleagues watching out for potential polar bears. On the ice, a safety team first conducts a reconnaissance trip to get familiar with the area and the terrain. They check how thick the ice is to work on it safely, and place flags to better estimate distances from the ship. This time, we also use snowmobiles to patrol the area in front of the ship since we observe very many polar bear tracks, and the two large icebergs around us reduce our field of vision.

Then, smaller teams go onto the ice. Team "snow" studies the snow with its layers, hardness and crystals, takes samples and photographs. Team "ice core" drills ice cores for determining properties of the sea ice, for example how many seasons it may have experienced. Team "surface" uses laser and radar to investigate the surface of the snow and the ice. In addition, two drone teams map the surrounding area from the air. We time our work with satellite overflights and compare real world measurements with the satellite images that our colleagues on the mainland send to us on the ship.

During research expeditions, time seems to pass twice as quickly as at home. After breakfast, we spend most of the day working outside on the ice. After the science work of the day, samples need to be stored, some samples need further treatment or measurements, equipment needs to get cleaned, dried, adjusted, and prepared for the following day. Every evening after dinner, we summarise the day, plan the next day, make adjustments of our work if necessary, and share preliminary research results and other updates. On many days during a research expedition, we work in shifts around the clock, with the early morning hours often being the quietest time.


MARITIME
ROBOTICS
CIRFA
Morten Einarsve


CIRFA
Wolfgang Dierking

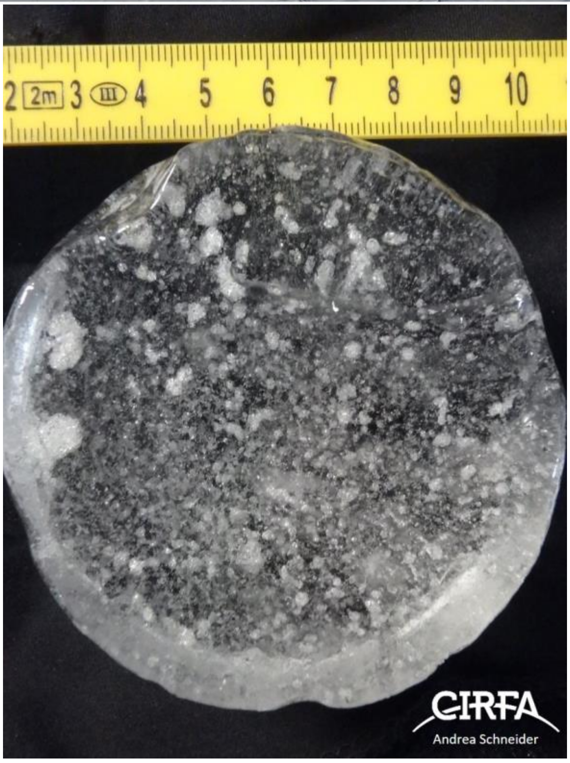
2 3 4 5 6 7 8 9 10
CIRFA
Andrea Schneider

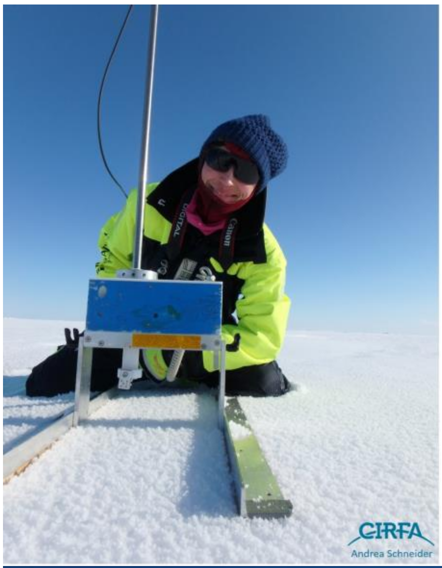
CIRFA
Andrea Schneider


CIRFA
William Copeland


CIRFA
Andrea Schneider

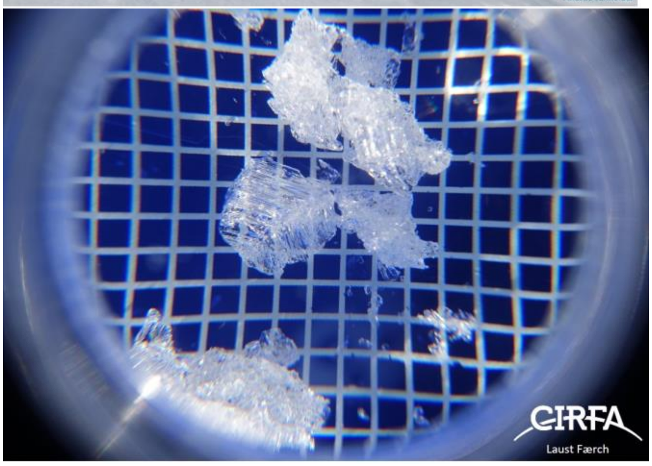
CIRFA
Laust Færch

CIRFA Cruise Diary 8 – Grounded icebergs

Floating icebergs may be harmful to ships and other offshore activities. Some Arctic countries have developed methods to identify and map icebergs in open water from satellite imagery to inform their fishing and shipping fleets. The methods reliably identify icebergs in open water thanks to a high contrast between the dark ocean surface and bright icebergs. However, with climate warming, shipping and other offshore activities may increase and advance into new locations with less well known ice situations.

Detecting icebergs surrounded by sea ice is challenging because of a lower contrast between the icebergs and the sea ice. Belgica Bank offshore north-eastern Greenland is a perfect location to develop and test new methods. Icebergs from nearby Greenland glaciers are lodged at the shallow seafloor and hold one of the world`s most extensive so-called landfast ice areas immobile over longer periods. This offers a unique opportunity to test different sensors carried by different satellites, and improve algorithms that automatically detect icebergs surrounded by sea ice.

Further to the East in the Fram Strait, a current carries drifting ice and occasionally icebergs southwards closer to areas with ship traffic. CIRFA and NORCE now address the challenge of mapping and forecasting the movement icebergs in drifting sea ice by experimentally setting out GPS trackers on some of them. A carefully designed frame keeps the tracker from sliding off the icebergs. We used fishing line to attach them below a drone from NORCE that places the trackers near the top of the icebergs. On our expedition, we have successfully set out three GPS trackers on icebergs.

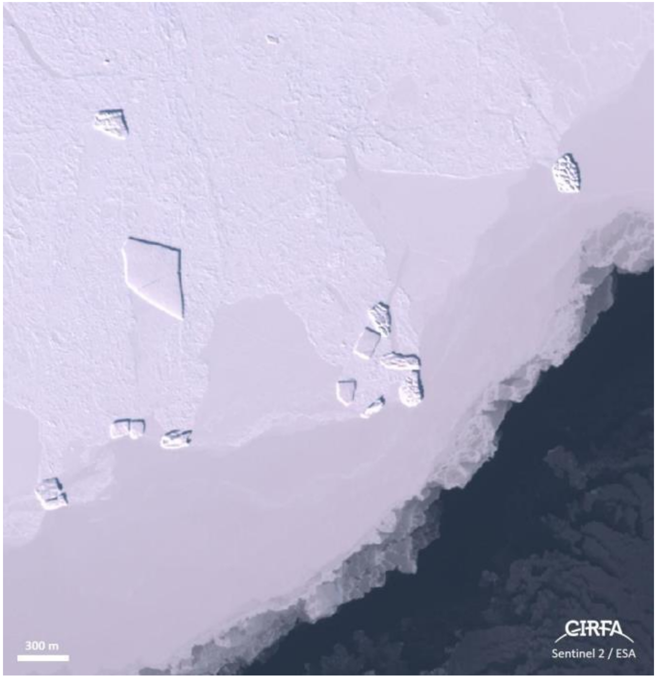
300 m
CIRFA
Sentinel 2 / ESA


CIRFA
William Copeland


CIRFA
Wenkai Guo

CIRFA Cruise Diary 9 – Expeditions inside an expedition

Long time after midnight, the eyes of us on the ship`s bridge are still glued to binoculars. We are watching three of our colleagues travelling with snowmobiles in the distance. The polar day makes it possible for us to work round the clock. Will their mission be successful? As part of our expedition, there were three such missions. We are setting out instruments - ice mass balance buoys - a few kilometres ahead of the ship and into the safe heavens of immobile sea ice in between grounded icebergs. Five of them have been set out away from open water to live as long as possible. Some small pieces of sea ice are regularly breaking off this dynamic wintertime coast of Greenland. In summer, all the ice will be adrift and travelling south into warmer waters.

We are leaving our instruments behind to get the data of air, snow, ice and upper ocean temperature over the summer. The instruments have a five metres long thermistor chain to measure a vertical temperature profile from air through snow and ice into the upper ocean. They have batteries and satellite communication to transmit their data. Back at home, when our expedition will be over, we will be able to observe how the sea ice over Belgica Bank melts and drifts away under this summer`s sun. Which of the buoys will survive the longest?

The low sun casts long shadows from the ridges of ice rubble and blocks that sometimes make the three researchers disappear for a moment. They stop on previously selected areas of flat ice to install the instruments, before scouting their way through the ridged terrain to the next area of their choice. We receive progress updates via VHF radio, and sleep better when we know that they have safely and successfully returned.

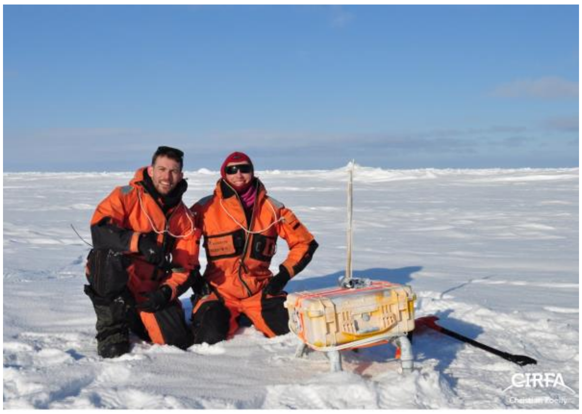

CIRFA Cruise Diary 10 – New ways of looking ahead

We are delighted that drone pilot Morten and machine learning engineer Danilo from Maritime Robotics join our expedition. With them, three drones travelled from Trondheim in mid-Norway to the Arctic to curiously take off from *RV Kronprins Haakon*`s helicopter deck and scan the unique icescape made of thick and thin sea ice, ridges, and icebergs with different camera setups.

Compared to humans being directly on the ground or satellite imagery from a great distance, drone footage offers a detailed view from low elevation. The drones operate up to 2 kilometres away from the ship when they are photographing the surface in a quest to make high-resolution orthomosaics and 3D topographic maps from the drone footage.

Morten and Danilo aim to develop drone camera setups and automatic image interpretation to optimise near-real time decision making for offshore navigation, among others for the Digital Arctic Shipping project (https://das.nersc.no/). In the near future, this may contribute to recognize easy or challenging ice conditions, or floating objects or obstacles, and guide a ship around or towards them. On our expedition, one of their drones went for a reconnaissance mission to look for potential polar bears behind icebergs that we cannot easily or safely access ourselves.

From Morten we learned about an interesting fact: Unlike during our teenage-years when we competed with our friends about having the latest joystick model for computer games, he much prefers programming the autopilot of his drone for the next flight ;)

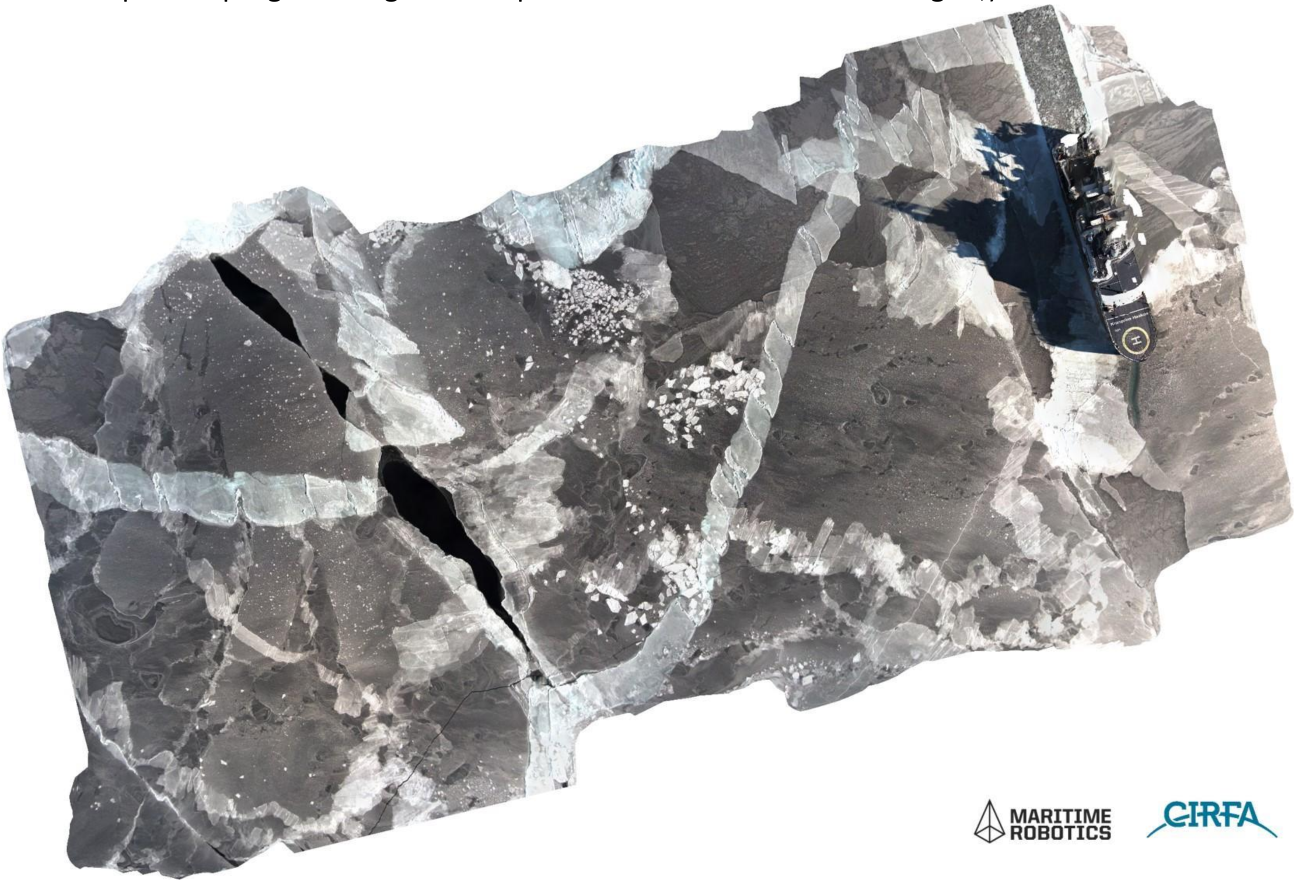

MARITIME ROBOTICS CIRFA

CIRFA Cruise Diary 11 – Drones at work

NORCE`s drone team has set up its headquarters inside the helicopter hangar of *RV Kronprins Haakon*. They have drones with different tasks with them; and the drones carry the names Shark and Fox, among others. On our expedition, drone flights enable us to gain better situational awareness of the ice that is surrounding us, contribute to route planning, and collect data to compare with satellite images. One of the drones, the Fox, is a snow expert. It carries a radar that measures snow thickness and snow layering over different sea ice types from low altitude. Since snow crystals on the ground constantly change, snow cover is challenging to interpret from satellite imagery. Therefore, many researchers perform numerous manual measurements. The snow measurements of the Fox drone cannot replace manual measurements, but its radar covers a larger area than researchers on the ice could do.

The Shark drone is a specialist in aerial photography. On its flights, it photographs the surface beneath itself and sends its images in near-real time back to its pilot. An online tool (called NLive) visualises photo-trails or photo-mosaics that were broadcasted on the ship and viewed even by people in mainland Norway.

The Shark needs about 20 minutes to scan an area of the size of a small village. On our expedition, the Shark and the NLive system helped to find suitable sea ice to work on, and discovered an interesting looking patch of ice that we were keen to visit. The ice turned out to look like dragon skin! The ice turned out to look like dragon skin! Possible future applications of the Shark and the NLive system may be smart ice navigation and travel route planning, for example through the [Digital Arctic Shipping] project. Since it can scout for thin ice areas when satellite images are unavailable, it may contribute to reducing fuel consumption and improving travel safety in icy waters.

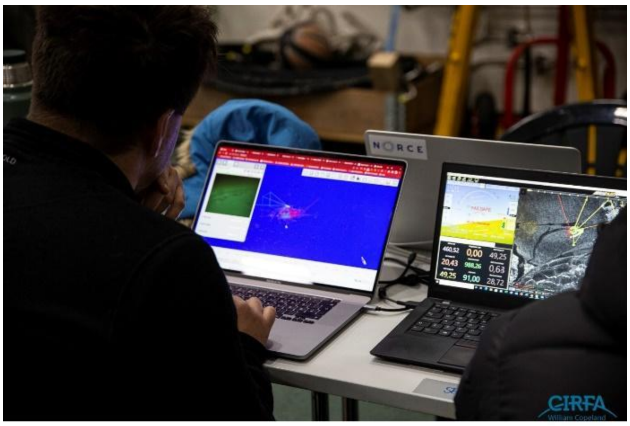

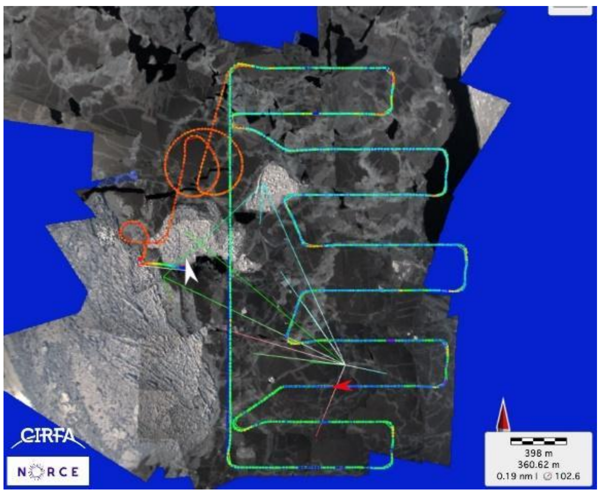

CIRFA Cruise Diary 12 – This time it is about numbers!

33 scientists from 17 nations. 19 crew members. 18 days at sea. -25.7C was the lowest recorded air temperature. 85 stairs from the lowest deck to the observation deck high up on *RV Kronprins Haakon*.

We reached beyond 80N and 12W, and observed and sampled countless different types of sea ice and icebergs. We visited 45 sites for CTD`s to investigate the water column, deployed more than 30 GPS trackers for sea ice, iceberg and ocean surface current records, visited 15 sites for sea ice and snow studies, we installed 3 long-term observation sites for sea ice mass balance and 1 long-term observation site to collect oceanographic data. Multiple drones took off from the ship for dozens of flights. We were spoiled with 15 days and nights with sunny and calm weather and had many unique and safe encounters with walruses, seals, polar bears and birds.

The CIRFA 2022 expedition came to a successful end, and we are now keen to start working on our samples and data to understand the snow and sea ice observed from the ground, from drones, and satellites better. We are not only returning with hard drives full of data, boxes full of samples, and experiences with new technology; we have also found new colleagues and friends to keep pushing the frontier of today`s knowledge and know-how.


CIRFA


CIRFA


CIRFA
William Copeland


CIRFA
William Copeland


KRONPRINS HAAKON
CIRFA
Wenkai Guo

5 List of participants

Below is a list of all expedition participants with affiliation, function, group, and contact information.
The participants were divided into five teams: 1) Cruise leaders, safety and outreach; 2) Sea ice and snow; 3) Oceanography; 4) Ground Remote Sensing (RS) and drones; 5) Modelling, ice drift, and ice observations. Group leaders are highlighted with their names in bold letters.

Members of the land-based support team are Anca Cristea (NPI), Saloua Claily (UiT), Kamilla Josefine Rudberg (MET), Johannes Röhrs (MET), Nick Hughes (MET) and Alistair Everett (MET).

	Affiliation	Person	Function(s)	Team	E-Mail
1	NPI	Sebastian Gerland	Cruise leader	Cruise leaders, safety, outreach	gerland@npolar.no
2	UiT	Torbjørn Eltoft	Cruise co-leader	Cruise leaders, safety, outreach	torbjorn.eltoft@uit.no
3	NPI	Christian Zoelly	Safety and logistics	Cruise leaders, safety, outreach	christian.zoelly@npolar.no
4	UiT	Andrea Schneider	Outreach	Cruise leaders, safety, outreach	andrea.schneider@uit.no
5	UiT	**Wolfgang Dierking**	Remote sensing specialist, group leader	Sea ice and snow	wolfgang.dierking@awi.de
6	UiT	Johannes Lohse	Remote sensing specialist	Sea ice and snow	johannes.p.lohse@uit.no
7	UiT	Malin Johansson	Remote sensing specialist	Sea ice and snow	malin.johansson@uit.no
8	UiT	Wenkai Guo	Trainee, sea ice classification specialist, photography	Sea ice and snow	wenkai.guo@uit.no

9	UiT	Eduard Khachatrian	Trainee, sea ice classification specialist	Sea ice and snow	eduard.khachatrian@uit.no
10	UiT	Jack Landy	Remote sensing specialist	Sea ice and snow	jack.c.landy@uit.no
11	UiT	Anna Telegina	Trainee, sea ice classification specialist	Sea ice and snow	anna.telegina@uit.no
12	UiT	Anthony Doulgeris	Remote sensing specialist	Sea ice and snow	anthony.p.doulgeris@uit.no
13	UiT	Catherine Taelman	Validation of satellite classification	Sea ice and snow	catherine.c.taelman@uit.no
14	UiT	Polona Itkin	Snow specialist	Sea ice and snow	polona.itkin@uit.no
15	MET	Jozef Rusin	Trainee, sea ice classification specialist	Sea ice and snow	jozef.rusin@uit.no
16	NPI	**Paul Dodd**	Ocean scientist, group leader	Oceanography/ Sea ice and snow	paul.dodd@npolar.no
17	NPI	Mats Granskog	Ocean and Sea ice scientist	Oceanography/ Sea ice and snow	mats.granskog@npolar.no
18	NPI	Yannick Kern	Ocean and Sea ice scientist	Oceanography/ Sea ice and snow	yannick.kern@npolar.no
19	NORCE	**Tom Rune Lauknes**	Remote sensing, group leader	Ground RS and drones	tlau@norceresearch.no
20	NORCE	Rolf Ole R. Jenssen	Remote sensing/Machine learning specialist	Ground RS and drones	roje@norceresearch.no

21	ISAE - SUPAERO	Laurent Ferro-Famil	Ground-based radar measurements	Ground RS and drones	Laurent.FERRO-FAMIL@isae-supaero.fr
22	ISAE - SUPAERO	Frédéric Boutet	Ground-based radar measurements	Ground RS and drones	frederic.boutet@univ-rennes1.fr
23	NORCE	Agnar H. Sivertsen	Drone specialist	Ground RS and drones	agsi@norceresearch.no
24	MR	Morten Einarsve	Drone specialist/pilot	Ground RS and drones	morten.einarsve@maritimerobotics.com
25	MR	Danilo Petrocelli	Machine learning engineer	Ground RS and drones	danilo@maritimerobotics.com
26	NORCE	Tore Riise	Drone specialist/pilot	Ground RS and drones	tore@norceresearch.no
27	MET	**Knut-Frode Dagestad**	Drift forecasts, outreach, group leader	Modelling, ice drift, ice observations	knutfd@met.no
28	MET	Martina Idzanovic	Drifter assembly/deployment specialist	Modelling, ice drift, ice observations	martinai@met.no
29	MET	Marina Duran Moro	Remote sensing and model assimilation	Modelling, ice drift, ice observations	marinadm@met.no
30	MET	Trond Robertsen	Ice navigation and weather forecast specialist	Modelling, ice drift, ice observations	trondr@met.no
31	MET	William Copeland	Ice navigation and weather forecast	Modelling, ice drift, ice observations	williamjp@met.no

			specialist, photography		
32	MET	Edel Rikardsen	Ocean and Ice Modelling specialist	Modelling, ice drift, ice observations.	edel.rikardsen@met.no
33	UiT	Laust Færch	Iceberg specialist	Modelling, ice drift, ice observations	laust.farch@uit.no

Thank you!